

Tehnički Glasnik

Technical Journal



ISSN 1846-6168 (Print)
ISSN 1848-5588 (Online)
Godište (Volume) 10
Broj (Number) 3-4
Stranica (Pages) 55-127
Varaždin, prosinac (December) 2016.

TEHNIČKI GLASNIK TECHNICAL JOURNAL

Znanstveno-stručni časopis Sveučilišta Sjever
Scientific professional journal of University North

Godište (Volume) 10
Varaždin, srpanj-prosinac (July-December) 2016.

Broj (Number) 3-4
Stranica (Pages) 55–127

Adresa uredništva (Address of Editorial Office):

Sveučilište Sjever – Tehnički glasnik
Sveučilišni centar Varaždin
104. brigade 3, 42000 Varaždin, Hrvatska;
Tel. ++385/ 42/ 493 328, Fax. ++385/ 42/ 493 333
e-mail: tehnickiglasnik@unin.hr
<http://tehnickiglasnik.unin.hr>
<http://www.unin.hr/djelatnost/izdavastvo/tehnicki-glasnik/>
<http://hrcak.srce.hr/tehnickiglasnik>

Osnivač i izdavač (Founder and Publisher):

Sveučilište Sjever

Savjet časopisa (Council of Journal):

Predsjednik Marin MILKOVIĆ, Goran KOZINA, Vladimir ŠIMOVIĆ, Mario TOMIŠA,
Vlado TROPŠA, Damir VUSIĆ (Sveučilište Sjever); Milan KLJAJIN (SF Slavonski Brod/ Sveučilište Sjever)

Urednički odbor (Editorial Board):

Predsjednik Damir VUSIĆ (Sveučilište Sjever), Milan KLJAJIN (SF Slavonski Brod/ Sveučilište Sjever),
Marin MILKOVIĆ, Krešimir BUNTAČ, Anica HUNJET, Živko KONDIĆ, Goran KOZINA, Ljudevit KRPAN, Marko STOJČIĆ,
Božo SOLDI, Mario TOMIŠA, Vlado TROPŠA, Vinko VIŠNJIĆ (Sveučilište Sjever); Duško PAVLETIĆ i Branimir PAVKOVIĆ (TF Rijeka);
Mile MATIJEVIĆ, Damir MODRIĆ, Nikola MRVAC, Kladio PAP i Ivana ŽILJAK STANIMIROVIĆ (GF Zagreb);
Krešimir GRILEC i Biserka RUNJE (SF Zagreb); Dražan KOZAK, Roberto LUJIĆ, Leon MAGLIĆ, Ivan SAMARDŽIĆ,
Ante STOJČIĆ i Katica ŠIMUNOVIĆ (SF Slavonski Brod); Ladislav LAZIĆ (MF Sisak); Ante ČIKIĆ (VTŠ Bjelovar);
Darko DUKIĆ (Sveučilište u Osijeku, Odjel za fiziku); Gordana DUKIĆ (Filozofski fakultet u Osijeku); Srđan MEDIĆ (VELK Karlovac);
Sanja KALAMBURA (Veleučilište Velika Gorica); Marko DUNĐER (FF Rijeka, Odsjek za politehniku); Goran ŠIMUNOVIĆ (SF Slavonski Brod);
Predrag ČOSIĆ (FSB Zagreb)

Međunarodni urednički savjet (International Editorial Council):

Boris TOVORNIK (UM FER Maribor); Milan KUHTA (University of Maribor, Faculty of Civil Engineering);
Nenad INJAC (KPH Wien/Krems); Džafer KUDUMOVIĆ (MF Tuzla); Marin PETROVIĆ (MF Sarajevo); Salim
IBRAHIMEFENDIĆ (KF Kiseljak); Zoran LOVREKOVIĆ (VTŠ Novi Sad); Igor BUDAK (Fakultet tehničkih nauka,
Univerzitet u Novom Sadu); Darko BAJIĆ (Mašinski fakultet Univerziteta Crne Gore); Tomáš HANÁK (Brno
University of Technology, Czech Republic); Aleksandr Viktorovich SHKOLA, Klimentko Evgenij VLADIMIROVIĆ,
Oleg Aleksandrovich POPOV (Odessa State Academy of Civil Engineering and Architecture, Ukraine)

Glavni urednik (Editor-in-Chief):

Milan KLJAJIN

Tehnički urednik (Technical Editor):

Goran KOZINA

Grafički urednik (Graphics Editor):

Snježana IVANČIĆ VALENKO

Lektori i prevoditelji (Linguistic Advisers and Translators):

Iva GRUBJEŠIĆ, (za engleski jezik); Mario KOLAR (za hrvatski jezik)

Informatička podrška (IT support):

Davor LEVANIĆ

Tisak:

Centar za digitalno nakladništvo, Sveučilište Sjever

Svi objavljeni članci u časopisu su recenzirani (All papers published in journal have been reviewed)
Časopis je besplatan i izlazi u četiri broja godišnje (The journal is free and published four issues per year)

Naklada (Circulation): 100 primjeraka (issues)

Časopis je referiran u (Journal is referred in):

EBSCOhost Academic Search Complete
Hrčak - Portal znanstvenih časopisa RH

Rukopisi se ne vraćaju (Manuscripts are not returned)

Registracija časopisa (Registration of journal):

Časopis "Tehnički glasnik" upisan je u Upisnik HGK o izdavanju i distribuciji tiska 18. listopada 2007. godine pod
rednim brojem 825.

Uređenje zaključeno (Preparation ended):

prosinac (December) 2016.

CONTENT
SADRŽAJ

<i>Hižak J., Logožar R.</i> AN OVERVIEW OF THE GENETIC ALGORITHM AND ITS USE FOR FINDING EXTREMA — WITH IMPLEMENTATIONS IN MATLAB PRIKAZ GENETIČKOG ALGORITMA I NJEGOVA UPORABA ZA NALAŽENJE EKSTREMA — S IMPLEMENTACIJAMA U MATLABU	55
<i>Prester J., Jung Erceg P., Kumić I.</i> BARRIERS TO THE IMPLEMENTATION OF KEY ENABLING TECHNOLOGIES IZAZOVI IMPLEMENTACIJE KLJUČNIH RAZVOJNIH TEHNOLOGIJA	71
<i>Aydin E. A., İkiiz T.</i> AN APPROXIMATE SOLUTION FOR THE PLANE WAVE DIFFRACTION BY AN IMPEDANCE STRIP: H-POLARIZATION CASE OKVIRNO RJEŠENJE ZA DIFRAKCIJU RAVNOG VALA IMPEDACIJSKOM TRAKOM: SLUČAJ H-POLARIZACIJE	79
<i>Vladimirovich Kovrov A., Vladimirovich Kovtunenko A, Konstantinovna Vysochan N.</i> THE EFFECT OF THE LOADING ORDER ON THE FORMATION OF THE STRESS-STRAIN STATE OF THE REINFORCED CONCRETE FRAME STRUCTURE UTJECAJ PORETKA OPTEREĆENJA NA FORMIRANJE STANJA NAPREZANJA I ISTEZANJA OKVIRNE STRUKTURE KONSTRUKCIJE OD ARMIRANOG BETONA	98
<i>Moskalova C., Popov O.</i> AN ANALYSIS OF THE TECHNOLOGICAL PROPERTIES OF FACILITATED PLASTER SOLUTIONS MADE FROM DRY BUILDING MIXES ANALIZA TEHNOLOŠKIH SVOJSTAVA OLAKŠANIH GIPSANIH RJEŠENJA IZ SUHIH GRAĐEVINSKIH MJEŠAVINA	102
<i>Hamioud S., Khalfallah S.</i> FREE-VIBRATION OF BERNOULLI-EULER BEAM USING THE SPECTRAL ELEMENT METHOD SLOBODNA VIBRACIJA BERNOULLI-EULEROVE ZRAKE KORIŠTENJEM METODE SPEKTRALNOG ELEMENTA	106
<i>Dovgan I., Kolesnikov A., Semenova S., Zaitseva O.</i> THE QUANTITATIVE CHARACTERISTICS OF THE MICROSTRUCTURE OF BUILDING COMPOSITES KVANTITATIVNE KARAKTERISTIKE MIKROSTRUKTURE GRAĐEVINSKIH KOMPOZITA	113
<i>Terzić B., Despalatović M., Majić G., Stergulc M., Kriletić A., Šormaz K.</i> THE DEVELOPMENT OF A FREQUENCY CONVERTER FOR HIGH SPEED PERMANENT MAGNET GENERATORS IN COGENERATION PLANTS RAZVOJ PRETVARAČA FREKVENCIJE ZA VISOKOBRZINSKE GENERATORE S PERMANENTNIM MAGNETIMA U KOGENERACIJSKIM POSTROJENJIMA	117
<i>Kostyuk A., Kovtunenko D.</i> AN EXPERIMENTAL RESEARCH OF THE COMBINED JOINTS OF WALL PANELS FROM THE NATURAL HARDENING FOAM CONCRETE EKSPERIMENTALNA ISTRAŽIVANJA KOMBINIRANIH SPOJEVA ZIDNIH PLOČA OD PRIRODNO OTVRDNUTE BETONSKE PJENE	124
Upute autorima Instructions for authors	IV

UVODNA RIJEČ

Poštovani suradnici, autori i čitatelji,

Časopis "Tehnički glasnik" ulazi s novom 2017. godinom u drugo desetljeće svoga izlaženja. Lijepa je to obljetnica, na kojoj valja zahvaliti svima koji su na bilo koji način doprinijeli da se kontinuitet objavljivanja ne prekine. Očito je da je časopis tijekom proteklih deset godina imao svojih uspona i padova. Trenutačno se nalazi na svojevrsnoj prekretnici, u sadržajnom i formalnom smislu. S obzirom na intenzivan razvoj, rast i transformaciju izdavača časopisa - Sveučilišta Sjever, želja je uredništva da se časopis na konkretniji način identificira interdisciplinarno u STE(A)M području. Provest će se ciljane aktivnosti u smislu akcijskog plana kojima će se, uz određene zahvate u redizajnu vizualnog identiteta časopisa, stvoriti preduvjeti za privlačenje i objavu većeg broja kvalitetnih radova. Na svima nama zajedno je da uložimo dodatne napore u narednom razdoblju kako bi se kvaliteta objavljenih radova te samog časopisa podigla na višu razinu. Viši rejting časopisa implicirat će i viši rejting znanstvene prepoznatljivosti Sveučilišta Sjever, i to ne samo na nacionalnoj, već i na međunarodnoj razini.

Na izmaku još jedne uspješne godine, uredništvo časopisa zahvaljuje svima koji daju svoj doprinos u objavljivanju časopisa "Tehnički glasnik". Posebno zahvaljujemo vrijednim autorima radova koji nam ukazuju povjerenje objavom svojih radova, upravo u našem časopisu.

Uredništvo časopisa "Tehnički glasnik" želi mnogo lijepih, uspješnih i produktivnih trenutaka u novoj 2017. godini svim dosadašnjim i budućim autorima, čitateljima i suradnicima.

Srdačan pozdrav,

Izv. prof. dr. sc. Damir Vusić
Predsjednik uredničkog odbora

INTRODUCTORY COMMENT

Dear associates, authors and readers,

With the new year of 2017, Technical Journal enters the second decade of its publication. That is a wonderful anniversary, for which it is necessary to thank everyone who in any way contributed to the continuity of the publication. It is obvious that the journal had its ups and downs in the past ten years. It is currently at a turning point, both in the terms of content and form. Due to the intense development, growth and transformation of its publisher, University North, the desire of the editorial board is that the journal finds its identity in a more concrete interdisciplinary way in the STE(A)M area. Targeted activities in terms of an action plan will be carried out, and with certain procedures in the redesigning of the visual identity of the journal, they will create the preconditions needed to attract and publish a larger number of quality papers. It is on all of us to make further efforts in the coming period to raise the bar when it comes to the quality of the published papers and the journal. A higher rating of the journal will imply a higher rating of scientific recognition. Moreover, a higher rating

of the journal will imply a higher rating of the scientific recognition of the University North, not only at the national level, but also at the international level.

At the end of another successful year, the editorial board of the journal would like to thank all those who contribute to the publication of the Technical Journal. We would especially like to thank the diligent authors who show us their confidence by publishing their papers in our journal.

The editorial board of the Technical Journal wishes a lot of beautiful, successful and productive moments in the new year of 2017 to all its current and future authors, readers and associates.

Best regards,

*Associate Professor Damir Vusić, PhD
President of the editorial board*

AN OVERVIEW OF THE GENETIC ALGORITHM AND ITS USE FOR FINDING EXTREMA — WITH IMPLEMENTATIONS IN MATLAB

PRIKAZ GENETIČKOG ALGORITMA I NJEGOVA UPORABA ZA NALAŽENJE EKSTREMA — S IMPLEMENTACIJAMA U MATLABU

Jurica Hižak, Robert Logožar

Original scientific paper

Abstract: *The paper outlines the main concepts of the genetic algorithm (GA) in a combined, educational-scientific style. Every step of the GA is first motivated by its biological paragon, then mathematically formalized and explained on simple examples, and finally supported by implementations in MATLAB. Two programs that use GA for the illustrative cases of finding functions' extrema are shown. The authors conclude the paper by presenting the original use of GA in the Stochastic Iterated Prisoner Dilemma, which gave a new insight into this problem.*

Keywords: *genetic algorithm, fitness function, function extrema, stochastic iterative prisoner dilemma.*

Izvoran znanstveni rad

Sažetak: *Ovaj rad predstavlja glavne koncepte genetičkog algoritma (GA) u kombiniranom, edukativno-znanstvenom stilu. Svaki je korak GA isprva motiviran svojim biološkim uzorom, potom matematički formaliziran i objašnjen na jednostavnim primjerima te konačno potkrijepljen primjerima u MATLABU. Predstavljena su dva programa koja koriste GA za ilustrativne slučajeve nalaženja ekstrema funkcija. Autori zaključuju članak prikazom izvorne uporabe GA u stohastičkoj iterativnoj dilemi zatvorenika, što je dalo novi pogled na ovaj problem.*

Ključne riječi: *genetički algoritam, funkcija podobnosti, ekstremi funkcija, stohastička iterativna dilema zatvorenika.*

1. INTRODUCTION

The concept of evolution is omnipresent not only in nature and natural sciences, but can be also found in all other human activities. A good general definition of this notion, with explication in biology is found in [1]: “Evolution is, in effect, a method of searching among an enormous number of possibilities for ‘solutions’. In biology, an enormous set of possibilities is the set of possible genetic sequences, and the desired ‘solutions’ are highly fit organisms—organisms which are capable of surviving and reproducing in their environments.”

1.1. Genetics in computation

In computing (computer science), an *evolutionary algorithm* investigates the space of feasible solutions of some quantitative problem and—according to some prescribed criteria—finds the best among the selected ones. This process is then iterated until one of the obtained solutions is “good enough.” Therefore, a computational procedure in an evolutionary algorithm is a process analogous to what is happening to live organisms in the natural evolution. The evolutionary algorithms are studied within the field of *evolutionary computing*.

Nowadays the evolutionary computing comprehends three big scientific fields: genetic algorithms, evolutionary strategies, and genetic programming. There are many different evolutionary algorithms, as well as several variations of each of them. However, the underlying idea

of all of them is the same: given a *population* of solutions, high-quality solutions are more likely to be selected during the process of selection and reproduction. [2]

Thus, the basic idea and even the terminology of evolutionary algorithms follow the actions of the natural evolution. Of course, one might expect that there are also several technical differences between the two, which may depend on the particular field of the evolutionary computing. Nevertheless, the fundamental functioning of all evolutionary algorithms can be grasped through the following brief insight into the genetic algorithm.

For a given problem, the reduced set of potential solutions is generated in a random fashion. Every solution, or individual—also called (artificial) chromosome—contains artificial genes. Unlike the real chromosomes, which consists of the DNAs built of series of pairs of the four nucleotide bases (A-T, C-G, T-A, G-C), the artificial chromosomes are simple sequences of zeros and ones.¹

¹ Since the nature is the inspiration for this whole area of computing, here we give a short explication of how the coding is done in the DNA. It should be stressed that this coding is not nearly as straightforward as for the artificial chromosomes. Furthermore, it is highly adjusted to the concrete function it has — to store the information on how ribosomes will form proteins from amino-acids. That information is translated by the messenger RNA. The RNA is a copy of the DNA structure, with the only difference that it has the T (Thymine) base replaced with the U (Uracil) base. Of the two helices, only one—the coding strand—is enough to define the information held in the RNA (the other is determined by the pairwise complements, as in the

From every generation of chromosomes, the best ones are chosen. And while the best individuals in biological populations are selected by complex biological and environmental mechanisms, the selection process in genetic algorithms is governed by the evaluation of the observed population by a fitness function. It assigns a fitness value to every individual in the population. Then, the selection of the best individuals (chromosomes) is done in a stochastic process, in which the probability of selection of an individual is proportional to its fitness value. So, although better individuals have a greater chance of being selected, their selection is not guaranteed. Even the worst individuals have a slight chance for survival. [2]

The stochasticity of the procedure is further enhanced by the processes of recombination and mutation. Their action ensures the variability of solutions, and thus contributes to the exploration of the **whole** search or state space (the set of all possible solutions). This is essential for avoiding the traps of local extrema, in which traditional algorithms get stuck quite often.

Altogether, the combined action of the variation and selection operators results in a very efficient method for improving every next generation of solutions and relatively fast convergence to the desired optimal solution. That is why the evolutionary algorithms are very popular in solving a great variety of problems in both applied and fundamental sciences, such as finding extrema of complex functions, discovering the best game strategies, solving transport problems and modeling complex shape objects.² Among those are also the hardest computational problems, which belong to the so-called NP complexity class.³ Despite some limitations and deficiencies, the evolutionary algorithms tackle all these tough tasks very successfully, thanks to their changed paradigm of operation and the loosened aim. That is, if the accurate solution is so hard-to-find, why not search for a solution that is just “good enough.”

1.2. The purpose and the plan of the paper

In this paper, we shall focus our attention to the genetic algorithm (GA). We shall describe the GA in comparison to the corresponding biological processes and give the formalization of its basic steps. Then we shall implement these steps in the widely used mathematical and engineering programming environment MATLAB[®].⁴ The

DNA). In the coding strand, the minimal complete biochemical information is stored in the three-letter words called codons, formed by the letters A, U, C, G. There are $4^3 = 64$ such words. The sequences of these words convey the information necessary for the formation of proteins, which is the basis for the existence and reproduction of all living organisms. [11]

² The shape of NASA ST5 spacecraft antenna was modeled by using GA to create the best radiation pattern. [12]

³ NP stands for *nondeterministic, polynomial time*, meaning that the solution of the NP problem class can be found by the nondeterministic Turing machine (NTM) in the polynomial (favorable) time. The NTM is a theoretical machine that can guess the answers of the hard problems in the polynomial time, even though they require exponential time on normal, deterministic machines (algorithms). A simple comment and a connection of the NP problems to the GA can be found in [9].

⁴ MATLAB[®] is a trademark of the MathWorks Inc.

theoretical presentation is made in an educational, easy-to-follow approach, but mathematically corroborated where needed. For the readers who are already familiar with the field of evolutionary computation on a general level, a few illustrative examples written in MATLAB can make this article interesting as a step further toward the practical use of genetic algorithms—possibly also for their own problems. On the other hand, for the huge group of MATLAB users who are novices to the field, this could be a motivation to learn the topic that was mostly being connected to computer science. The final aim of this endeavor was to show that the genetic algorithm could be effectively programmed in MATLAB, and to describe how this was done in another authors' work, within the field of the game theory.

After the broader outline of the concepts used in evolutionary computation and the genetic algorithm was already given in this introduction, in section 2 we give the basic ideas that underlie the GA more precisely.

In section 3 we deal with the creation of individuals for the initial population. We spend some time to formalize the problem mathematically in a precise and complete manner. However, to keep the reading simple and interesting for the broader audience, we provide several simple examples. And along with them, the formalized steps are immediately implemented in MATLAB.

Section 4 formalizes and then exemplifies the process of selection of individuals for the new population (generation) and discusses the fitness function. The roulette wheel parent selection was illustrated on a simple example and implemented in MATLAB. In section 5 we explain the recombination and mutation, and, as always, cover the theoretical part with examples and the MATLAB code. Then, in section 6 we discuss the behavior of the GA in finding extrema for two illustrative functions. The full MATLAB codes for these programs are given in Appendix A.

In section 7, we discuss the use of GA in the iterated prisoner dilemma problem and show how it can discover unexpected aspects of such nontrivial systems. It should be—as we see it—the main scientific novelty of this work. Finally, section 8 concludes this paper.

2. OUTLINE OF THE GENETIC ALGORITHM

The genetic algorithm was invented by John Holland in 1975. [3] In order to find the function extrema, Holland presented each potential solution (extremum) as a sequence of bits, called the *artificial chromosome*. The bits, containing zeros and ones, or groups of several bits, can be considered as artificial, *binary genes* (Figure 1, confer also footnote number 1).

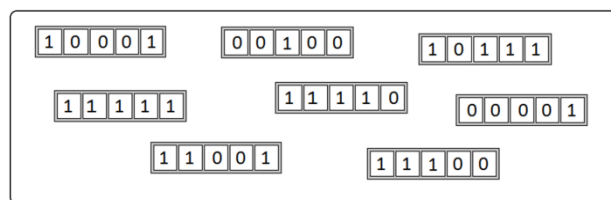


Figure 1. The population of artificial chromosomes, with genes presented by bits.

Obviously, an artificial chromosome can be any form of data that properly describes the features of individuals within some population. Some of the individuals, i.e. chromosomes—as we shall simply call them in the further text—would eventually appear as the solution of the given problem.

2.1. Genetic algorithm

A pseudocode of a common version of the GA is given in Algorithm 1. The input is clear from the previous text. The optional input enables the calculation of the satisfying fitness value that can serve as one of the termination criteria (discussed more in the next subsection).

In step 1, the initial population of solutions (or individuals, or chromosomes) is created by random selection from the whole search space. This is elaborated in more details in section 3. In step 2, the initial population is evaluated by the fitness function, i.e. each chromosome of the population is assigned its fitness value (more on the fitness function is given in §4.1 and §4.2).

The iterative process that follows is presented by the two nested while loops. The condition of the outer loop is the negation of the termination criteria, which are explained in §2.2. For now, we assume that the criteria are not met so that the algorithm enters the outer loop.

Within the outer loop, in step 3.1, the GA enters another while-loop, which governs the selection of individuals for the next population. Within the nested loop, in step 3.1.1, a pair of chromosomes is selected randomly from the previous population (generation). The probability for this reselection is proportional to the relative fitness values of the chromosomes (see §4.3), i.e. the more probable chromosomes will be reselected more likely. In general, some of them can be selected more than once, and some of them will not survive the selection process and will not appear in the next generation. In step 3.1.2, the chromosomes from the selected parent pair are subjected to the recombination operator, which first splits them, and then mix the split parts in a specified way. Normally, every pair of parents will produce two descendants, so that every new generation of offspring contains the same number of individuals as the previous generation. In step 3.1.3, the two new children are enlisted as the new chromosomes of the next population. The process is iterated until the new population is filled with the desired number of chromosomes. When this is done, the while-loop 3.1 is completed.

In step 3.2, the descendant chromosomes are exposed to mutation. Depending on the chosen mutation rate, the mutation changes a certain number of genes in the population's gene pool (for further explanations see §5.4).

The processes of mutation and recombination are usually described by the action of the *recombination and mutation operator*, respectively, commonly known as the *variation operators* (more about them in section 5).

In step 3.3, the old population is replaced with the new one and the list of children is deleted. In step 3.4, the new population is evaluated by the fitness function, which is the same action as in step 2 (the duplication of these steps is a sacrifice to achieve the structured, while loop). Now the first iteration of the outer loop is finished, and the termination criteria are checked again.

Algorithm 1. A version of the genetic algorithm (GA).

Input: original function, search space (the set of all individual solutions, or chromosomes), fitness function.

Optional input: good enough solution, from which the good enough fitness value is calculated.

1. **Create initial population** by randomly selecting a certain number of chromosomes from the search space;
2. **Evaluate** the fitness of the current population by calculating every chromosome's fitness value.
3. **While the termination criteria are not met, do:**
[Terminat. criteria: the best fitness value is good enough or the specified number of iterations is done, or ...]
 - 3.1 **While the new population is not completed, do:**
 - 3.1.1 **Select** two parent chromosomes by random selection from the previous population;
 - 3.1.2 **Recombine** the parent chromosomes to obtain two children;
 - 3.1.3 **Enlist** the two children in the new population;
 - 3.2 **Mutate** the chromosomes in the new population;
 - 3.3 **Replace** the previous population with the new one;
 - 3.4 **Evaluate** the fitness of the current population (0.2).

Output: the best chromosome found (the one with the highest fitness value).

2.2. Termination criteria

If the fitness value of at least one chromosome satisfies some “prescribed criterion,” the algorithm is finished. If not, the algorithm enters the next iteration.

A careful reader will probably note that finding and specifying such a criterion pose a fundamental problem not only for GA but also for all other evolutionary algorithms. Namely, GA does not investigate the search space thoroughly, methodologically, or in any “systematic” way. So, there are no sure indicators of when the computation is over. For instance, if the GA is searching for the unknown global extrema of some function, it cannot possibly know how far it is from them. Also, if we didn't search the whole search space, we cannot be sure that somewhere there isn't a more extremal value.

Obviously, in the spirit of our unsystematic and stochastically governed algorithm, we need a similar kind of termination criteria, i.e. (i) something loose but practical, or (ii) something heuristically based.

As for (i), sometimes we might be given a hint of what would be a “desired” or “good enough” solution (e.g. from the knowledge about the observed problem gathered by other means, or by the specifications given by a client or by a boss). By knowing it, the good enough fitness value could be calculated (opt. input) and this would be our first criterion. However, although our client or boss could be satisfied, we as scientists may still wonder how good our solution is and if it can be made better. This will be discussed a bit more in a moment.

And if the good enough solution is not known, then the “heuristic criterion” (ii) boils down to: “stop the iteration after a certain number of iterations,” or “check the trends of certain *indicators* and decide about the termination.” The indicator most used is the population average

fitness. By tracking it in each iteration, one can draw some conclusions on how the GA is progressing. If the indicator is stalling in its “extremal plateau” for several iterations, the algorithm can be halted. However, this is by no means a sure decision. Namely, although one can expect that with every new iteration of the GA the populations “evolve,” i.e. that their average fitness values improve and get closer to a desired extremum, this cannot be taken for granted. The GA’s method of searching is stochastic and it often results in unpredictable behavior of the chosen indicators. For instance, the average fitness value of the subsequent populations may stagnate for many iterations, making us believe that it is stable and without a chance for improvements. But after such intervals of stability, GAs can suddenly show the solutions that are worse than previous, or they can surprise us with sudden improvements. This will be illustrated in §6.

Further discussion of the possible indicators for the termination of the GA and their behavior are beyond the scope of this paper. We can simply say that the GA can be run for several times with a different number of iterations or, alternatively, started with different initial populations. Then the obtained results can be compared.

2.3. Use of genetic algorithms

As was already hinted at the end of §1.1, the power of GA is in the great diversification of the intermediary solutions, which ensure that the most of the search space will be properly investigated. This is essential for the functions with several extrema, the so-called *multi-modal functions*, whose search space is *multi-modal search space*. For such functions GA does excel. On the other hand, the classical methods—based on the analytical approach—will very often fail on them. They will tend to go straight toward the nearest local extremum. Another advantage is that the GA does not impose any restrictions on the functions that they investigate. The functions need not be continuous or analytic (derivable).

3. SEARCH SPACE AND INITIAL POPULATION

In the outline of the genetic algorithm in §2, we have already discussed the notion of the artificial chromosome. From there, it is clear that the chromosomes are a suitable representation of individual solutions within the search space of some problem.

3.1. Search space and individual solutions — their presentations and values

In order to illustrate the functioning of GA and the creation of its initial population, we define a common task of this field:

Find the global extremum (minimum or maximum) of the function $f(x)$ of discrete equidistant values x .

To formalize the problem a bit more, we specify that x belongs to the discrete set X ,

$$x \in X = \{x_l, x_l + \Delta x, x_l + 2\Delta x, \dots, x_h\}, \quad (1)$$

where x_l is the set’s low and x_h its high limit, and Δx is the measure of the set’s resolution, $x_l, x_h, \Delta x \in \mathbb{R}$. Obviously, X is the set of all possible solutions, i.e. the *search space* of the problem. The extrema of $f(x)$ on this discrete set must be achieved for one of its N_x elements, $= x_{extr}$, where:

$$N_x = \text{card}(X) = \frac{x_h - x_l}{\Delta x} + 1. \quad (2)$$

Effectively, we have provided a discrete representation of some closed real interval $[x_l, x_h]$, as is always the case when numerical methods are used on digital computers. This is valid regardless of the details of the number presentation, i.e. it does not matter if they are coded as integers or floating point numbers.⁵ So, taking into account the eq. (2), we can choose the b -bit unsigned integer arithmetic without essential loss of generality. For it, the (whole) numbers span from 0 to $2^b - 1$. Thus, the achieved resolution Δx is

$$\Delta x = \frac{x_h - x_l}{2^b - 1}, \quad (3a)$$

and an arbitrary x from the search space X can be presented as the b -bit number n :

$$n = n(b) = \Delta x^{-1}(x - x_l) = \frac{2^b - 1}{x_h - x_l}(x - x_l). \quad (3b)$$

Vice-versa, the b -bit number $n(b) = n$ represents

$$x = x_l + \Delta x \times n = x_l + \Delta x \frac{x_h - x_l}{2^b - 1} n. \quad (3c)$$

The binary presentation $n(b)$ can be regarded as a vector,⁶ which comes as a nice formal point in the further treatment of chromosomes as individual solutions, and in performing operations on them.

Now, having established the general transformation between the individual solution (x) and its presentation $n(b)$ in some b -bit arithmetic, the elaboration can be simplified even further. By taking $\Delta x = 1$, the search space becomes a subset of integers. Furthermore, by taking $x_l = 0$, the lowest individual coincides with the low limit of the unsigned arithmetic and the highest individual coincides with the maximal number of the unsigned arithmetic, $x_h = 2^b - 1$, so that eq. (3c) gives

$$x = n = n(b). \quad (3d)$$

In an undersized example (for the sake of keeping the things simple), let us choose the 8-bit integer arithmetic. It has the search space of $2^8 = 256$ individuals x_i , in the range $0 \leq x_i \leq 255$. These solutions can be indexed in an appropriate manner. Instead of the programming-style indexing, starting from 0, here we use the mathematical indexation to comply with the notation in the rest of the paper. So the indices i are for 1 greater than values, and the search space is $X = \{x_1, x_2, \dots, x_{256}\}$. Further indexations of the individuals within the populations derived from X will be changed according to the total number of the individuals in those populations (see §3.2).

⁵ For instance, let us suppose that the interval of positive numbers $[0, 1]$ is covered by the single precision floating point numbers. The maximal resolution achieved by this arithmetic is given by the minimal Δx accurate across the whole interval. For $x_h = 1$, it is the relative precision of this data type, $\Delta x \approx 10^{-7}$. For the double precision arithmetic, $\Delta x \approx 10^{-14}$.

⁶ The chromosomes $x_i = n_i(b)$ are vectors in the vector space above the Galois field $\text{GF}(2^b)$.

It turns out that the presentation of individuals x_i in the binary system is both illustrative and practical for their further evaluation and manipulation in the form of artificial chromosomes in GAs. In our example, the binary presentation of the i -th individual is given as:

$$x_i = n_i\langle 8 \rangle = \langle d_7 d_6 \dots d_1 d_0 \rangle_{i, bin}, \quad (4a)$$

where d_j are binary digits, $j = 0, 1, \dots, b - 1 = 7$, $d_j \in \{0, 1\}$. The case of $x = x_{27}$ (where we use the above, “shifted” indexation),

$$x_{27} = n_{27}\langle 8 \rangle = 00011010_{bin},$$

is shown in Figure 2 (the subscript *bin* will be omitted further on where the use of binary numerals is obvious).

Since our simplified choice implies that $x = n\langle b \rangle$ [confer eq. (3c)], we do not need to differentiate between an individual solution (chromosome) and its binary presentation. And of course, if the value V is attributed to every such binary presentation (vector), our simplified case leads back to the initial value of the solution in the search space:

$$V(n_i\langle b \rangle) = \sum_{j=0}^{b-1} d_j \times 2^j = x_i. \quad (5a)$$

This is so because the mapping between $n_i\langle b \rangle$ and $V(n_i\langle b \rangle)$ is a bijective function.

The (mathematical) indexation of individuals in the 8-bit search space chosen above, gives $V(n_i\langle b \rangle) = i - 1$.

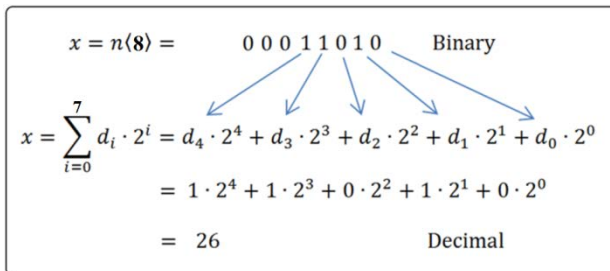


Figure 2. Summary of the notation via an example: individual solution, or chromosome $x_i = x$, its binary presentation $n\langle 8 \rangle$ in 8 bits, and the value, $V(n\langle 8 \rangle)$.

In the case of finding extrema of a function, the appropriate choice of the fitness function would be either the absolute value as defined above or some simple, linear function of it (see §4).

To generalize the above deliberation, for the function of two variables, $f(x, y)$, the chromosome is defined by the ordered pair (x_i, y_j) . In the binary presentation, it would be written as:

$$(x_i, y_j) = (\langle d_{b-1} \dots d_1 d_0 \rangle_i, \langle d_{b-1} \dots d_1 d_0 \rangle_j). \quad (6)$$

If the problem is of different nature, the search space and its presentation should be changed appropriately. E.g., if the task is to find the shortest path between the given points in a plane or some higher order space, then the chromosomes should be presented as sequences of points in that space. For k points T_l , $l = 1, 2, \dots, k$, and the initial (final) point $T_{l_{init}}$ ($T_{l_{fin}}$), the search space X would be the set of all sequences x_i ,

$$x_i = \langle T_{l_{init}}, T_{l_1}, T_{l_2}, \dots, T_{l_{fin}} \rangle, \quad (7)$$

such that the following obvious restrictions would imply: (i) there are no repetitions of the same points in the sequence, (ii) the total number of points in the sequence is $\leq k$.

We end this formal part with a few notes on the actual sizes of the search spaces in the practical use of GAs. E.g., if the space of 32-bit integers is used as the search space, the total of $4Gi \approx 4 \times 10^9$ individual solutions (chromosomes) exist. For modern computers, searching over such search space by the “brute force” would be no problem at all. With the computer performance of the order of 100 GIPS, and supposing that the function f can be calculated with about 10^2 instructions, it would be done in the order of a second (here we assume that the program code is written and compiled optimally, and is running much faster than the MATLAB code). However, for a two-variable function with the squared search space [amounting to $(2^{32})^2 = 16 \text{ Ei} \approx 2 \times 10^{19}$], the situation is drastically changed, and computing time would rise to the order of 10^9 s. This and similar examples clearly show why the computer science ought to rely on efficient algorithms and not on the sheer power of computers.

In practical applications, the GA can be used for the very large, exponentially growing search spaces, for which the exhaustive searches are inefficient. If the fitness function is not too complex for evaluation, it is now commonly accepted that the GA will produce satisfactory results in acceptable time for most of such problems.

3.2. Creation of the initial population

From the defined search space X , the initial population $X_l = X_0$ is created by choosing a relatively small portion of the possible solutions from the search space,

$$X_0 = \{x_{0,1}, x_{0,2}, \dots, x_{0,N_0}\} \in X. \quad (8a)$$

As we have concluded in the previous subsection, the GA is in practice normally used on very large search spaces. Then the cardinality of the initial population is reduced from the cardinality of the whole search space for many orders of magnitude, which we write as

$$\text{card}(X_0) = N_0 \ll \text{card}(X) = N_X. \quad (8b)$$

It turns out that the efficiency of GA and the quality of its results do not improve much with enlargement of its population. A typical N_0 for 1-D problems is of the order of magnitude 10^1 to 10^2 . For the b -bit chromosome presentations it is often suggested to take $N_0 = b$ (for more details see [9]). Once chosen—as it was already stated in §2—the number $N_l = N_0$ of individuals is normally kept throughout the iterations of the GA.

The selected number of N_0 individuals of the initial population will be chosen randomly from the total of N_X possible solutions of the search space. One way how to do it is described in the next subsection.

3.3. Definition of the search space and creation of the initial population in MATLAB

Example 1. Let the first, simple task be to find the maximum of the function $f(x) = 36x - x^2$. For the sake of making the example as simple as possible, we observe the interval of integers from 0 up to and including 31,

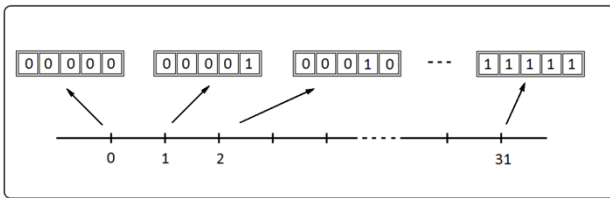


Figure 3. Binary presentation of the set of integers from 0 to 31 — which form the search space of Example 1.

Code Listing 1. Creation of the population of eight (8) 5-bit chromosomes in the MATLAB command prompt. The default orientation of binary numbers in MATLAB is reversed, with the most significant bit to the right.

```
>>popul=round(rand(8,5))
popul=
      0      0      0      1      0
      0      1      1      1      1
      1      1      0      0      1
      1      0      0      0      0
      0      1      0      1      1
      1      0      1      0      0
      1      0      0      0      1
      1      0      1      0      1
```

which implies that $x_l = 0, x_h = 31, \Delta x = 1$. The minimal number of bits that will allow the coding of the corresponding chromosomes is $b = 5$ (see Figure 3), leading to the search space

$$X = \{00000, 00001, \dots, 11110, 11111\}.$$

If we want to create the initial population of $N_0 = 8$ chromosomes from X , this can be done very easily in MATLAB. The simplest way is to create the 8×5 matrix of random numbers in the range $[0, 1)$ by using the function `rand`, and then to round them to 0s and 1s with the `round` function (Code Listing 1).

Getting back—from the binary numbers to their decimal values—is done by the MATLAB function `bi2de`. Thus, the binary presentation of the chromosome $n \langle b \rangle$ ($= n$) is translated to its decimal value x ($= x$) by the following statement (see also Code Listing 2):

$$x = \text{bi2de}(n) \tag{M1}$$

As a more general case, let us suppose that a search space in the interval $[0, 1]$ must be covered with a resolution of at least 0.05. From eq. (3a) it follows that

$$b \geq \log_2 \left(\frac{x_h - x_l}{\Delta x} + 1 \right), \tag{9}$$

leading to $b \geq 4.392$, and the minimal $b = 5$. With 5 bits, a slightly better Δx is achieved, $\Delta x = 1/31 = 0.3226$. This is shown in Figure 4.

For this case, the scaling from eq. (3c) gives the following MATLAB statement for conversion of the binary presentation of the chromosome $n \langle b \rangle$ ($= n$) to its decimal value x ($= x$),

$$x = x_l + \text{bi2de}(n) * (x_h - x_l) / (2^{\text{nbits}} - 1) \tag{M2}$$

Here the rest of the variables are: $x_l = x_l, x_h = x_h, \text{nbits} = b$.

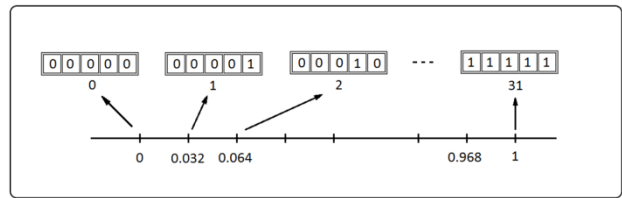


Figure 4. Another example of the 5-bit search space, organized in the real interval $[0,1]$, with $\Delta x = 1/31$.

Code Listing 2. Conversion of the binary presented chromosomes to their decimal values in MATLAB.

```
>>popul_dec= bi2de(popul)
popul_dec=
      8
     30
     10
      1
     26
      5
     17
     21
```

The MATLAB works with matrices, so that it can find the decimal value of the whole set of chromosomes by a single command:

$$\text{popul_dec} = x_l + \text{bi2de}(\text{popul}) * (x_h - x_l) / (2^{\text{nbits}} - 1) \tag{M3}$$

4. SELECTION

After the creation of the initial population of solutions, the individual solutions in it must be evaluated to get the estimation of how fit they are for reproduction. As was already mentioned in §1 and §2, the evaluation is done by the fitness function, in literature also known as *quality*, *capability*, *goodness*, or *objective* function.

4.1. Choice of the fitness function

The fitness function F maps the search space to the set of real (rational) or integer nonnegative values, i.e. it assigns the nonnegative *goodness* or *fitness value* $F(x_i)$ to each individual solution, or chromosome x_i ,⁷

$$F: X \rightarrow \mathbb{R}_0^+ (\mathbb{Z}_0^+), F: x_i \mapsto F(x_i) \geq 0. \tag{10}$$

The bigger is the value $F(x_i)$ the better will be the x_i 's chance for survival and crossbreeding.

In some cases, the fitness function can be the same as the function whose extrema are being found. However, this is so only if the fitness values are of the same, positive sign or zero for all the individual solutions. That is the case of our first example, in §3.3, where the maximum of $f(x) = 36x - x^2$ is being sought. There, the greater fitness value belongs to the chromosome that is closer to the parabola maximum, so that one can put simply $(x_i) = f(x_i)$.

⁷ The reason for non-negativity will become clear soon.

Otherwise, if the negative or both signs of the fitness values appear when finding some function's maximum, a problem arises when the probabilities proportional to the fitness values are to be assigned to the chromosomes. To shift the fitness values to the positive side, a positive constant should be added, so that in general $F(x_i) = f(x_i) + c$, $c \geq 0$.

The similar problem arises when the minimum is being sought for predominantly positive values of the original function $f(x_i)$. Now the chromosomes closer to the minimal value of $f(x_i)$ should be favored, meaning that $F(x_i)$ must be proportional to $-f(x_i)$. Again, if $-f(x_i)$ produces some negative values, a constant must be added, so that $F(x_i) = -f(x_i) + c$, $c \geq 0$.

Altogether, this leads to the following criterion for the fitness function:

The fitness function must be such that its higher values—to which the higher probabilities are to be assigned—are given to the chromosomes closer to the extremum that is being sought.

The general form of the fitness functions for finding extrema can now be summarized as follows:

$$\text{Finding max. of } f(x_i): F(x_i) = f(x_i) + c. \quad (11a)$$

$$\text{Finding min. of } f(x_i): F(x_i) = -f(x_i) + c. \quad (11b)$$

The choice of the constant c will be discussed in the next subsection.

For the travelling salesman problem, mentioned at the end of the §3.1, the appropriate value attributed to the x_i and its presentation $\langle T_{l_{init}}, T_{l_1}, T_{l_2}, \dots, T_{l_{nit}} \rangle$ would be the total length (λ) of the path defined by that presentation. Then one seeks the solution $x_{i_{min}}$, for which λ is minimal:

$$\text{Finding min. of } \lambda(x_i): F(x_i) = -\lambda(x_i) + c. \quad (12)$$

Further comments and an example of the application of GA to this problem can be found e.g. in [9, 10].

Generally, the fitness function should be picked appropriately to the problem. Furthermore, if the system's quality is described by a very complex function, the use of the GA could be questionable. In that case, the corresponding fitness function could impose too high a burden on the algorithm performance.

4.2. The choice of c (the problem of negative fitness values)

The role of the constant c is to shift the original function $f(x_i)$ to the nonnegative values. In the case of finding extrema of $f(x_i)$ that has negative values for some x_i , the ideal choice for c would be:

$$\text{Fnd. max. of } f(x_i): c = |\min\{f(x_i)\}|, f(x_i) < 0; \quad (13a)$$

$$\text{Fnd. min. of } f(x_i): c = |\max\{f(x_i)\}|, f(x_i) > 0. \quad (13b)$$

However, the $\min\{f(x_i)\}$ and $\max\{f(x_i)\}$ are generally not known. They pose the optimization problem that is just the opposite of the given one.

Another possibility to dissolve the problem of negative fitness values would be to make c so big that it surely lifts the $f(x_i)$ into the first quadrant for all $x_i \in X$. However, quite often this will cause another problem—the loss of details in the original function. That is, a great

global shift up can make the chromosomes' fitness values very large positive numbers, and cause a compression of their relative differences. This will in turn make the assigned probabilities less distinct.

The solution is to stick to the first idea but to reduce the pool from which the minimal or maximal value of $f(x_i)$ is being found. In the l -th iteration of the GA, the natural choice is to find these values only among the chromosomes of the previous population, which will be shortly designated as l' , $l' = l - 1$, for $l = 1, 2, \dots, N_{itr}$, where N_{itr} is the total number of iterations.

Now, the eqs. (13) translate into the following practical formulas for c :

$$\text{Fnd. max. of } f(x_i): c = |\min\{f(x_{l',i})\}|, f(x_{l',i}) < 0; \quad (14a)$$

$$\text{Fnd. min. of } f(x_i): c = |\max\{f(x_{l',i})\}|, f(x_{l',i}) > 0. \quad (14b)$$

After the above deliberation, a careful reader probably noted that the constant c could be applied even if for finding maxima (minima) there are no negative (positive) values of $f(x_i)$. In that case, c would be negative, to shift the fitness values closer to zero and thus expand the relative differences among the chromosomes. To achieve that, the absolute values around the minimum and maximum functions and the following range limits should be simply removed. With that, the formulas for $c \in \mathbb{R}(\mathbb{Z})$, now without restrictions, are:

$$\text{Fnd. max. of } f(x_i): c = \min\{f(x_{l',i})\}; \quad (15a)$$

$$\text{Fnd. min. of } f(x_i): c = \max\{f(x_{l',i})\}. \quad (15b)$$

Of course, if the achieved expanding of the fitness values is not desirable, one should stick to the formulas (12).

Finally, the extra control over the expansion (compression) of the fitness function can be achieved by introduction of the parameter $\gamma \in \mathbb{R}_0^+$, that would multiply the $f(x_i)$ and shrink it for $0 < \gamma < 1$ and expand it for $\gamma > 1$. With that factor, the formulas (11) become:

$$\text{Finding max. of } f(x_i): F(x_i) = \gamma f(x_i) + c. \quad (16a)$$

$$\text{Finding min. of } f(x_i): F(x_i) = -\gamma f(x_i) + c. \quad (16b)$$

4.3. Population, average and relative fitness values

In the l -th iteration of GA, we calculate the fitness values $F(x_{l',i})$ of the individuals from the $(l - 1) = l'$ -th population, $X_{l'}$, with generally $N_{l'}$ individuals.⁸ From these, the total fitness of the population l' is defined,

$$F(X_{l'}) = \sum_{i=1}^{N_{l'}} F(x_{l',i}), \quad (17)$$

as well as the average fitness of a chromosome within the population $X_{l'}$:

$$\overline{F(x_{l',i})} = \overline{F}_{l'} = \frac{F(X_{l'})}{N_{X_{l'}}}. \quad (18)$$

The ratio of the k -th chromosome fitness and the total population fitness gives the *relative fitness (goodness)* of the chromosome. This quantity will be chosen as the probability for the crossbreeding of that chromosome,

⁸ The numbers of chromosomes, $N_{l'}$, are kept population-dependent for the sake of generality (see also the discussion at the end of the subsection).

and denoted the same way:⁹

$$\Pr(x_{l,k}) = \frac{F(x_{l,k})}{F(X_l)} = \frac{1}{\sum_{i=1}^{N_l} F(x_{l,i})} F(x_{l,k}). \quad (19)$$

Having defined the probabilities of the chromosomes in the previous population, the set of N_l chromosomes for the next, $(l + 1) = l$ -th population is randomly selected as described in the step 3.1 of Algorithm 1. It should be noted that this could produce quite a different set of new individuals. Some of the previous chromosomes (presumably the very probably ones) can appear more than once, and some of them can disappear (presumably those with small probabilities).

We end this subsection with a comment why it could be useful to keep the number N_l of chromosomes general, despite it is standardly fixed to $N_l = N_0$ in all iterations l (as stated in §3.2). Namely, although it is known that the GA's efficiency and quality of results is not very dependent on the population cardinality, one might resort to changing it in some occasions. For instance, if the indirect termination indicators stall for several iterations, one may consider increasing N_l to (re)check the stability of obtained solutions. This idea could be implemented in some enhanced versions of GA.

4.4. The example and the implementation of the selection in MATLAB

We continue our example from §3.3, for finding the maximum of $f(x) = 36x - x^2$. The initial population (X_0) created there consists of $N_0 = 8$ chromosomes.

Now we proceed to the next (first) iteration of the GA. We calculate the fitness values of the previous population by applying the fitness function $F(x_{0,i}) = f(x_{0,i})$, because $f(x_{0,i}) \geq 0$ for each $x_{0,i}$, and also for all x_i . The results are shown in Table 1, with somewhat simplified notation: $x_{0,i} \mapsto x_i$, $F(x_{0,i}) = F(x_i)$. E.g., for $x_1 = 01000$, $F(x_1) = f[V(01000)] = f(8) = 224$.

The total fitness of the initial population is $F(X_0) = 1752$, so that the relative fitness, and in the same time the probability for selection of the chromosome x_1 , is

$$\Pr(x_1) = \frac{F(x_{0,k})}{F(X_0)} = \frac{F(x_{0,k})}{\sum_{i=1}^{N_0} F(x_{0,i})} = \frac{224}{1752} \cong 0.128.$$

On the basis of the chromosome probabilities $\Pr(x_i)$, $i = 1, 2, \dots, 8$, listed in Table 1, two new chromosomes will be selected to form a pair of parents (step 3.1.1 in Algorithm 1), and this will be—together with other actions—iterated four times (within the while-loop 3.1 in Algorithm 1).

The standard procedure for random choice is *roulette wheel parent selection*. It is illustrated in Figure 5 as a roulette on which each chromosome has its own sector, with the area percentage proportional to the chromosome's probability. For the right simulation of the chromosome sectors, the cumulative probabilities must be calculated from the chromosomes' probability distribution. In MATLAB, this is done by the `cumsum` function.

⁹ Of course, the relative fitness qualifies for a probability function because $0 \leq \Pr(x_{l,k}) \leq 1$ and $\sum_{i=1}^{N_l} \Pr(x_{l,i}) = 1$.

Table 1. Calculations prior the process of selection. For the chromosomes from the previous population, $x_{l-1,i} = x_{0,i} = x_i$, the table shows: $n_i(5)$ = 5-bit binary presentation, $V(n_i)$ = value, $F(x_i)$ = fitness value, $\Pr(x_i)$ = probability of selection in the next population, $\widehat{\Pr}(x_i)$ = cumulative probability.

x_i	$n_i(5)$	$V(n_i)$	$F(x_i)$	$\Pr(x_i)$	$\widehat{\Pr}(x_i)$
x_1	01000	8	224	0,128	12.8%
x_2	11110	30	180	0,103	23.1%
x_3	01010	10	260	0,148	37.9%
x_4	00001	1	35	0,020	39.9%
x_5	11010	26	260	0,148	54.7%
x_6	00101	5	155	0,088	63.5%
x_7	10001	17	323	0,185	82.0%
x_8	10101	21	315	0,180	100.0%
$\Sigma:$			1752	1.000	

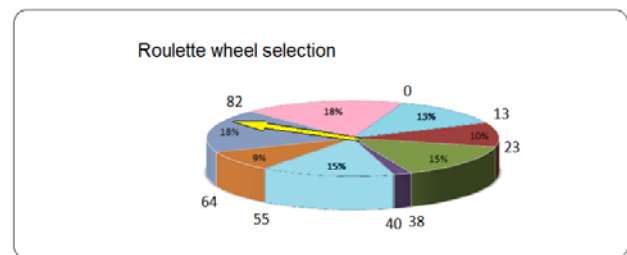


Figure 5. The roulette wheel parent selection for Example 1. To each of the 8 chromosomes of the initial population, a surface proportional to the chromosome probability is attributed.

In our example, the probability distribution \Pr is defined in Table 1,

$$\Pr = [0.128, 0.103, 0.148, 0.020, 0.148, 0.088, 0.185, 0.180] \quad (M3)$$

from which the cumulative probabilities are obtained by

$$\text{CumPr} = \text{cumsum}(\Pr) \quad (M4)$$

That gives the cumulative probability distribution:

$$\text{CumPr} = [0.128, 0.231, 0.379, 0.399, 0.547, 0.635, 0.820, 1.000] \quad (M5)$$

Now, a random number from the interval $[0,1]$ is generated; in MATLAB, by function `rand`. The value of the random number determines the position and the sector on the imaginary roulette, and thus also the belonging chromosome (the random number is compared with the intervals defined by the `CumPr`, and translated accordingly into the index of the corresponding chromosome).

The MATLAB function that does that (taken from [10]) is shown in Code Listing 3. Given the probability distribution $P (= \Pr)$, the function `RandChoseN(P, N)` returns the indices of N selected chromosomes. At the beginning of the function, the bin edges are defined from P by the `cumsum` function, and the vector `roulette` is zeroed. In the `for`-loop, the random number x is created. Then the histogram of its incidences (only one!) in the bins is made by function `histc` and stored in `Counts`. The index of `Counts` with the one (and only) hit is stored in `roulette`. The loop is repeated N times.

Code Listing 3. The MATLAB function for the roulette wheel parent selection. `RandChooseN(P,N)` gives the indices of N randomly selected chromosomes.

```
function roulette=RandChooseN(P,N)
BinEdges=[0, cumsum(P(:)')];
roulette=zeros(1,N);
for i=1:N
    x=rand;
    Counts=histc(x,BinEdges);
    roulette(i)=find(Counts==1);
end
```

4.5. A few comments on the selection process

The above depicted selection—implemented by the roulette method—is called *simple selection*. Another type of selection is *elimination selection*. While the simple selection deletes the old generation only after it is used for the selection process of all pairs of children for the new generation (before the step 3.3 in Algorithm 1), the elimination selection first detects *bad chromosomes* and deletes them prior the crossover and mutation operations. The shortage of chromosomes is then compensated by the additional offspring from the *good chromosomes*. To decrease or avoid the accumulation of duplicate chromosomes, some variants of this method check if the descendants are identical to their parents. If they are, the process of selection is repeated. This sort of selection is called the *elimination selection without duplicates*.

5. RECOMBINATION AND MUTATION

The recombination (crossover) and mutation in biological systems are complex processes of exchange of genetic material that are happening between the pairs of chromosomes (Figure 6). After the *interphase*, in which the chromosomes are duplicated, they align to each other, break in one or more places, and swap their fragments. This mixing results in the enhanced variability of the population.

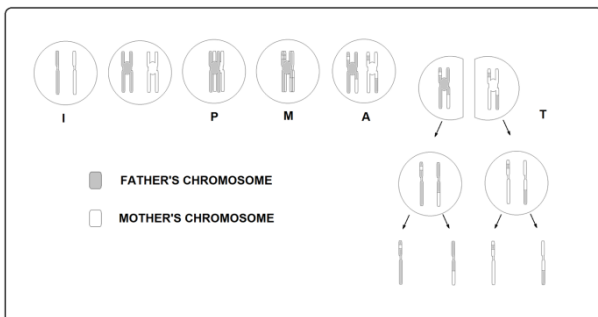


Figure 6. Meiosis, or reduction division. It starts from a somatic cell with a diploid number of chromosomes and ends with four sex cells that have the haploid number of chromosomes. The most important phase is *prophase* (P), in which the recombination and generation of gametes with completely different genetic material occurs.

5.1. Recombination in genetic algorithms

As it was already mentioned in §2.1, the process of recombination in evolutionary algorithms is mathematically abstracted to the action of the crossover operator. This *binary* operator—in the sense that it acts on two operands—exchanges the genes (bits) of two artificial chromosomes. As conceived by Holland in 1975, the crossbreeding performed by the crossover operator is a three-step process. [4] First, two individuals are taken from the parent (previous) population. Second, a point or several points of the chromosome splitting are chosen—the so-called *crossover points*. These points define the segments of genes (bits) between them. The contents of some of those segments are being exchanged, resulting in the generation of two new descendants with generally different chromosome structure (Figure 7).

The simplest way of choosing the crossover points is by random selection. Then some of the formed sections of bits are exchanged and some are not.¹⁰ This is the case of the ordinary crossbreeding, which is governed by the corresponding *ordinary crossover operator*.

In the simple example of Figure 7, the ordinary crossbreeding with single crossover point is applied. It defines the left and the right sections of the two chromosomes, of which the right sections are exchanged. Thus, the probability that the descendant has its corresponding (upper or lower) parent's genes in the left section is one, and in the right section is zero, meaning that the right section has the genes from the other, “crossed” parent.

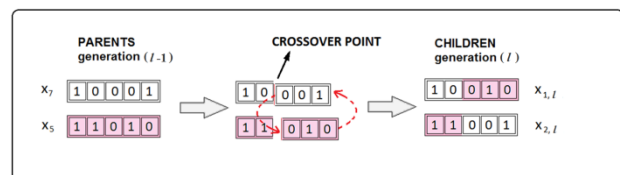


Figure 7. The recombination of chromosomes with one breaking point. From the previous generation ($l' = l - 1$), two parent chromosomes were selected. The crossover operator then splits them between the second and the third bit and exchanges their right parts. Thus, a pair of new chromosomes of the l -the generation is formed.

The above and all the other probability schemes can be generalized by the *crossover probability mask* \mathbf{m}_C ,

$$\mathbf{m}_C = (Pr(d_0), Pr(d_1), \dots, Pr(d_{b-1})). \quad (20a)$$

The mask consists of b -plets of probabilities $Pr(d_j)$, $j = 0, 1, \dots, b - 1$, each of which presents the probability that the descendant has the gene—here the binary digit d_j —inherited from its corresponding predecessor. If the mask for the first chromosome in a pair (the upper one in Figure 7) is \mathbf{m}_C , the mask applied to its conjugal partner (the lower one in Figure 7) must be $\overline{\mathbf{m}_C}$, with the complementary probabilities, $Pr(d_j) = 1 - Pr(d_j)$:

$$\overline{\mathbf{m}_C} = (Pr(d_0), Pr(d_1), \dots, Pr(d_{b-1})). \quad (20b)$$

With this notation, the probability masks for the example of ordinary crossover in Figure 7 are:

¹⁰ By exchanging all of them, the net result would be the two starting chromosomes with swapped indices.

$$\mathbf{m}_{Cord} = (1, 1, 0, 0, 0), \overline{\mathbf{m}_{Cord}} = (0, 0, 1, 1, 1).$$

As we have already pointed out, there can be more than one breaking point. For b bits there are maximally $b - 1$ breaking points. The introduced notation enables the specification of such and other cases, by forming the adequate recombination probability masks.

The *uniform crossover* operator allows equal-chance swapping of all bits, meaning that all the probabilities in the mask are equal, $Pr(d_j) = Pr(\overline{d_j}) = 1/2$, leading to

$$\mathbf{m}_{CUnif} = (0.5, 0.5, \dots, 0.5). \quad (21)$$

In other words, this mask states that all genes from the first parent have the opportunity of $1/2$ to end up in the corresponding (first) descendant chromosome, and that the same is valid for the genes of the second parent and the corresponding (second) descendant chromosome.

Finally, the fully general form of the mask in eq. (20a) allows the fully variant recombination (sometimes misleadingly called the *p-uniform crossover*). We shall call it the *variant crossover* and denote it by *CVar* index. To affirm the meaning of their masks, we give the following example:

$$\mathbf{m}_{CVar} = (0.2, 0.3, 1.0, 1.0, 0.0).$$

Here, the first child will inherit the first gene from her/his first parent with probability 0.2, and the second gene with probability 0.3 (meaning that the probabilities that these genes will be inherited from the second parent are 0.8, and 0.7, respectively). The third and fourth genes will be surely inherited from the parent one (i.e. they stay as they were in the first parent), and the last gene will be surely inherited from the second parent (i.e. it is surely exchanged from what it was in the first parent).

The recombination does not have to be done on all individuals within a population. The relative portion of the chromosomes that participate in the recombination—which can be also formulated as the rate of the activation of the crossover operator—is called the *crossover rate* or *crossover probability*. We shall denote it as γ_C , $\gamma_C \in [0, 1]$. If in population (iteration) l the N_l chromosomes were selected, only $N_{l,C}$ of them will be selected for crossbreeding,

$$N_{l,C} = \gamma_C \times N_l n. \quad (22)$$

The values of γ_C that are reported to give the best behavior of GA are between 0.5 and 1.0. [5]

5.2. Implementation of recombination in MATLAB

A simple implementation of recombination in MATLAB is shown in Code Listing 4. It selects one breaking point by using the function `randi(nbits-1)`, which randomly picks an integer between 1 and $b - 1$. Then the part of the chromosome to the right of the breaking point is exchanged. The exchange of these chromosome parts is performed with the last two statements of the code.

5.3. Mutation in biology

As a motivation for the implementation of mutation in GA, here we give a short reminder of the influence of mutation on living organisms. Unlike the recombination, the mutation in biology is a random change of genetic material in a somatic or a sex cell. That change can be

Code Listing 4. Implementation of the recombination with one randomly chosen crossover point in MATLAB. Prior to this code, the vectors of indices for dad and mom are to be defined. They denote the rows of the population matrix that present the corresponding parents.

```
%Calculate the probability of selection:
probs=fitness/sum(fitness);
%Selection of parents:
M=popsize/2;
dad=RandChooseN(probs,M);
mom=RandChooseN(probs,M);
%%CROSSOVER
%Choose the crossover point:
xp=randi(nbits-1)
%Take every 2nd dad's chromosomes
%and exchange genes with mom
popul(1:2:popsize,:)=...
[popul(dad,1:xp) popul(mom,xp+1:nbits)];
popul(2:2:popsize,:)=...
[popul(mom,1:xp) popul(dad,xp+1:nbits)];
```

influenced or stimulated by outer factors, like radiation, and sudden environmental changes. In natural conditions, it is very rare. If it happens to a somatic cell, it can cause its damage or death. It can occasionally trigger uncontrolled division and malign diseases. However, the consequences of such mutations are not inherited by the future generations. So, from the evolutionary point of view, much more significant are mutations that happen in the sex cells, because they are transferred to the next generations. They are manifested in the changes of the organisms' phenotypes, i.e. as new inherent characteristics of the descendants. This makes the mutation the second important cause of the variability of biological populations.

5.4. Mutation in genetic algorithms

In a genetic algorithm, the mutation will be performed by a *mutation operator*. It acts on a single chromosome and is therefore a unary operator. It changes one or more randomly chosen genes (bits) of the artificial chromosome. For instance, the mutation operator can change a chromosome $x_i = 11111$ to its mutant $x'_i = 11101$.

We formalize the action of the mutation operator in a way similar to the one used for the crossover operator. First, we introduce the mutation rate $\gamma_M \in [0, 1]$, which decides what percentage of the whole *gene pool* will be influenced by mutation. That is, with N_l chromosomes in a population, of which each has n genes, the gene pool contains a total of $N \cdot n$ genes. Then the number of mutations performed in each iteration of the GA is

$$N_{l,M} = \gamma_M \times N_l n. \quad (23)$$

Following the example of the natural mutation, γ_M in GA is normally made quite small, typically between 0.001 and 0.01. E.g., with $\gamma_M = 0.01$ and a gene pool with 20 5-bit chromosomes, only one gene (bit) and one chromosome are expected to undergo the mutation.

To further generalize the action of the mutation operator, one can introduce the *mutation probability mask*, \mathbf{m}_M , which is fully analogous to the crossover probability mask, defined by eq. (20a).

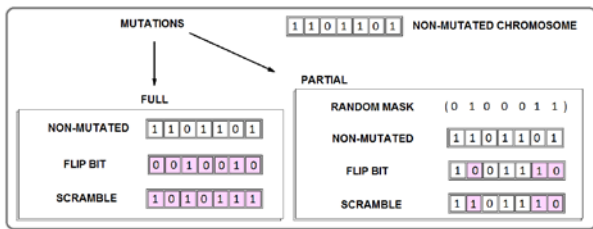


Figure 8. The action of inverting and mixing mutations illustrated on the chromosome 1101101. The inverting (flip) mutation inverts the zeros into ones and vice-versa. The mixing mutation permutes (scrambles) the bits while conserving their parity (the numbers of both zeros and ones stay the same). The partial versions of the mutations operate only on the selected fields of bits (shaded).

In a *simple mutation*, $N_{p,M}$ randomly chosen genes are mutated, meaning that its mask is the same as the uniform crossover mask in eq. (21). Besides that, the *mixing* and *inverting mutations* are used. The mixing mutation permutes the genes within the $N_{p,M}$ randomly chosen chromosomes or within their parts specified by a

mutation mask. The parameters of the mutation mask can also be generated randomly. In the *inverting mutation*, the bits specified by the mutation mask are inverted. [6] Both mutations are sketched in Figure 8.

6. EXAMPLES IN MATLAB

Two complete MATLAB programs for finding extrema of the polynomial functions are given in Appendix A. Relying on the provided comments, the readers acquainted with MATLAB basics should follow their code easily.

The Appendix A.1 contains the code for our simple Example 1, introduced in §3.3. The performance of GA for this case is shown by two diagrams of Figure 9. The upper diagram shows that the average fitness value rises to its upper plateau in only about 20 iterations, but keeps oscillating. In fact, it looks like the GA is quite struggling to get to the maximum of this simple 2nd order function. A few iterations prior 30 and 40, it finds that

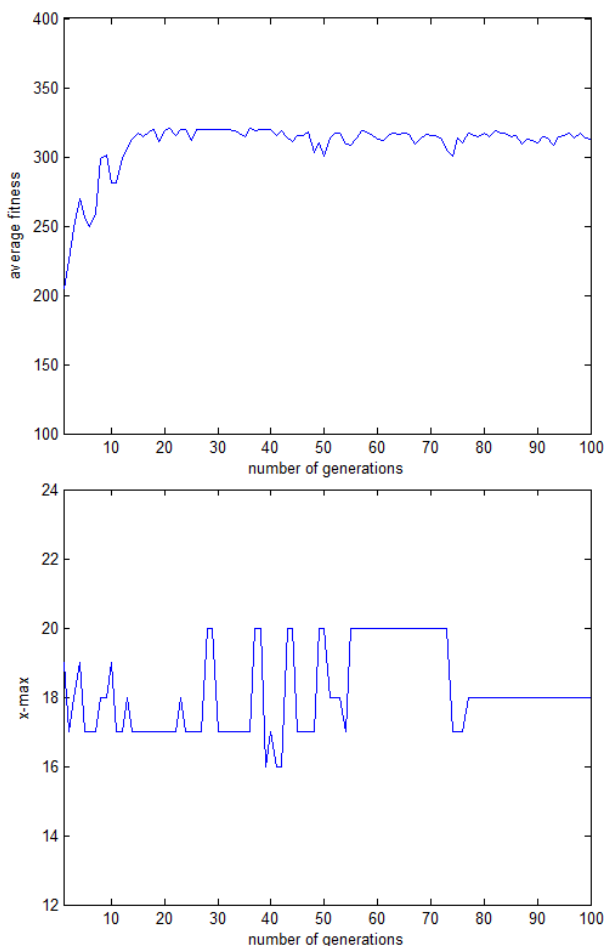


Figure 9. Diagrams of the average fitness (up) and the fittest GA solution (down), for square function of Exmpl. 1. The population average fitness increases quickly, but there is no sure indicator of the optimal solution. During the generations 55-75, the fittest chromosome is $x_{i,max} = 20$. After 75 generations, GA finally finds the exact solution, $x_{i,max} = 18$.

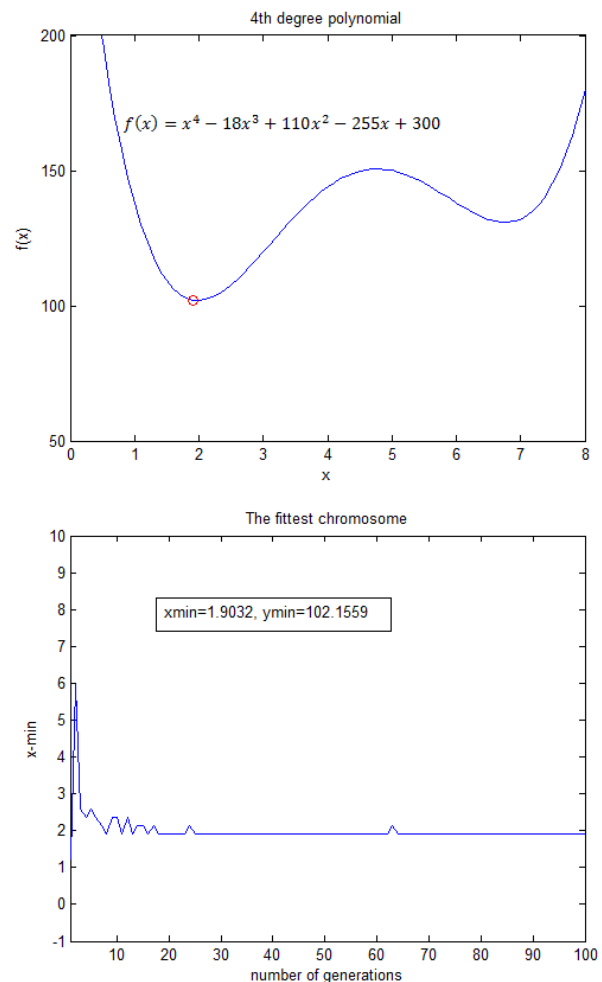


Figure 10. Diagrams of the 4th-degree polynomial (up) and the fittest GA solution. As can be seen by inspecting both diagrams, the algorithm successfully finds the global minimum and gives its accurate coordinates without being trapped in the local minimum (around $x = 6.75$).

the maximum is at $x = 20$, but does not converge immediately to it. Then, from 55th to 75th iteration it stabilizes at that value. However, the average fitness value keeps on oscillating and shows a few dips. The right answer, $x = 18$, is finally found after 75 iterations.

The Appendix A.2 gives the code for GA that finds the global minimum of the 4th-degree polynomial. The 5-bit chromosome representation is adjusted to the interval [1, 8] by formula (3b). As can be seen in the upper diagram of Figure 10, the polynomial has two minima (of course, with a local maximum between them). The right minimum is only local. On the lower diagram, one can see how the GA hits the global minimum in less than 30 iterations. It is found for the chromosome $n\langle 5 \rangle = 00100$, with the value $V(n\langle 5 \rangle) = n = 4$, for which eq. (3c) gives $x = x_{\min} = 1.9032$. This abscise value is marked on the polynomial curve as a small circle. It can be seen that the result is very accurate.¹¹ All in all, it looks like the previous simple function wasn't enough of a challenge for this mighty algorithm!

However, a careful reader will notice that not everything is in a steady state. Slightly below 65 iterations there is an instability, showing slightly higher value for the x_{\min} . Such behavior is quite common for genetic algorithms, due to the action of the variation operators.

7. USE OF THE GENETIC ALGORITHM IN THE STOCHASTIC ITERATED PRISONER DILEMMA

After showing the efficiency of the genetic algorithm for finding global extrema of the single-variable functions, here we elaborate on how it was used for a function that depicts cooperation in the heterogeneous population of selfish individuals in the problem known as *Stochastic Iterated Prisoner's Dilemma* (SIPD), which is a version of the *Iterated Prisoner's Dilemma* (IPD).¹²

¹¹ The accuracy would be significantly diminished if the interval [0, 8] was chosen. For it, $\Delta x = 0.25806$, and the individual closest to the minimum is 00111, with value 7, giving $x = 1.8065$ (0.0967 lower than x_{\min}). The second best is 01000, with value 8, giving $x = 2.0645$ (0.1613 greater than x_{\min}). The high dependence of the result on the choice of interval is an obvious consequence of the low resolution of the search space, i.e. of the low number of the chromosome bits.

¹² The Prisoner's Dilemma is a well-known game in which two players can cooperate with or betray each other. The outcome for each player varies according to the combined outcome for them both. It is rational that each player defect (D), even though they would both gain more if they cooperated (C). If there is another encounter of the players, in another round of the game, the cooperation may be really profitable. This kind of game is called *Iterated Prisoner's Dilemma* (IPD). It is considered as the paradigm for the evolution of cooperation among selfish individuals. [7] In the context of biology, the game payoff (food, water, etc.) may be considered as fitness. To find out which IPD strategy is the most effective, the mathematician, political scientist and game theorist Robert Axelrod organized a tournament in 1979, and invited the scientists to submit their solutions. The simplest strategy, known as *Tit for Tat* (TFT), won the tournament. This was a big surprise because it was well known by then that the strategy of defecting on every

We shall expose the problem briefly at the expense of accuracy (and hopefully not of the clarity). In the classic form of the IPD, the population usually consists of players represented by deterministic strategies that always follow their algorithms. For example, the ALLC strategy plays cooperatively always, and the strategy ALT plays cooperatively in every 2nd round. The TFT strategy¹¹ simply copies the moves of the opponent player from the previous round. However, in the real-life situations, both animals and humans make mistakes. This invites for the implementation of the uncertainty into the players' moves. The IPD that includes that is the above mentioned Stochastic IPD. In SIPD, each player is represented by a pair of probability values (p, q) , whereby p stands for the probability of cooperation after the opponent's cooperation, and q stands for the probability of cooperation after the opponent's defection.¹³ Now suppose that we want to find the best strategy of the SIPD in which the total payoff for a particular player equals to the sum of payoffs gained in the duels with all other players. The payoff as a function of (p, q) depends on various parameters, such as the total number of players, the strategies of the players and the number of the game rounds. Interpreted in another way, the payoff is a multivariable function, whose maximum cannot be found by the classical optimization algorithms.

One possibility to find the extrema of such payoff function is to simulate the natural selection. One can generate a set of strategies and then "leave it to the natural selection." The best strategy will be the one that becomes dominant in a population.

Most of the studies in this field have been done under the assumption that the individuals reproduce asexually; the strategies fight among each other, the generation after generation, with relative frequencies proportional to their payoff in the previous generation. It means that particular strategy could be, and usually is used by more than just one player. The players with copied strategies might be considered as the *clones* of the corresponding original strategies. It should be stressed that in this approach there is no crossbreeding between different strategies.

On the other hand, the GA could be applied to the SIPD if the strategies are suitably encoded in the form of artificial chromosomes. An example of such approach is our model, in which each reactive strategy (p, q) is represented by a 10-bit chromosome. [8] The first five bits in the chromosome encode the probability p , and the remaining five bits encode the probability q (Figure 11).

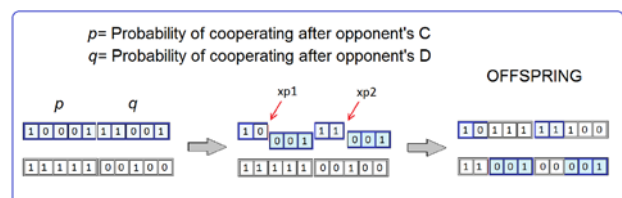


Figure 11. Double-point crossover operator applied to the parent chromosomes which represent a (p, q) SIPD strategy.

round (ALLD) is the only strategy that is generally evolutionarily stable (in more details commented in [8]).

¹³ This kind of strategy is known as *reactive strategy*.

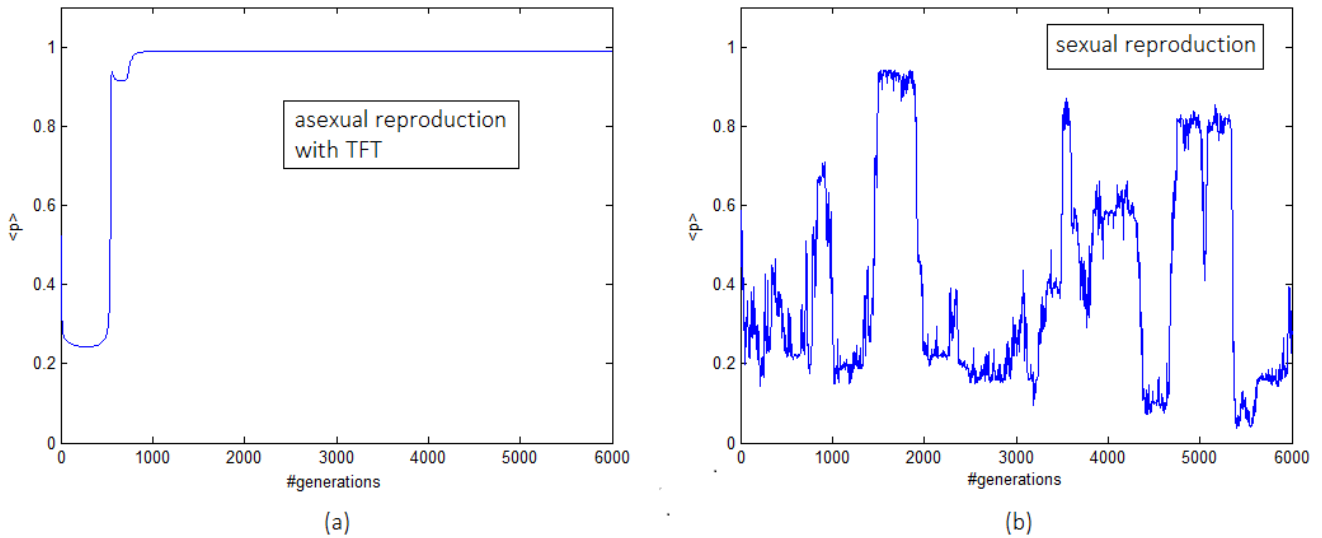


Figure 12. The cooperation coefficients over time in (a) populations that reproduce asexually, (b) populations with sexual reproduction. For the asexual reproduction, the cooperative strategies win after around 1000 generations. The sexual reproduction does not allow the extinction of different strategies and results in their erratic and cyclic exchanges.

The payoff gained in one round serves as a fitness function for the evaluation of strategies — the most successful strategies will have the highest chances for mating. After being selected, every chromosome is subjected to double point crossover operator. One crossover point is randomly selected on the p and another on the q chromosome segment (confer Figure 11).

At the beginning of each iteration (each round of the game), the *cooperation coefficients* are calculated as the averages of the strategy p -probabilities,

$$\bar{p} = \sum_{i=1}^{N_{str}} \omega_i p_i. \tag{24}$$

Here ω_i stands for the relative frequency of the i -th strategy with the cooperation probability p_i , and the summation is over all N_{str} strategies.

This, sexually reproduced SIPD model have shown that the subsequent populations are going through the erratic and cyclic exchanges of cooperation and exploitation. Such result is just the opposite from what the previous models—with asexual reproduction of individuals—are giving. In them, once some strategy is extinct, its restoration is impossible. Figure 12 shows the cooperation coefficients for both of these cases.

The instabilities in our model are the consequence of the GA variation operators. They preserve the genetic variability and diversity of the dominant strategies. In this case, the genetic algorithm does not deliver an optimal solution (the best strategy). On the contrary, it restores the defective strategies and leads to the instability and divergence. There is no dominant strategy that would eliminate the opponent players for good. Both, the co-

operators and the exploiters can rule the world by themselves just temporarily.

8. CONCLUSION

When some optimization problem is being solved using a genetic algorithm (GA), it is not guaranteed that it will give a perfect or even a very good solution. But quite often it will deliver a “good enough solution”, and almost always it will provide some kind of useful information about the problem.

The examples presented in this paper have shown that the global extremum of the single-variable functions was found very effectively, especially in the case of the 4th-degree polynomial. Its derivative gives a third order equation that cannot be solved easily. Obviously, the strength and the justification for the use of GA increase with the number of function’s local extrema and generally with the degree of the function complexity.

On the other hand, in the case of the Stochastic Iterated Prisoner’s Dilemma, the GA did not perform that efficiently. The populations of strategies do not evolve toward any dominant type of strategy. Instead, they diverge and jump from one near-optimal solution to another, showing that there is no clear winning strategy. However, although “the best” strategy wasn’t found, the GA revealed erratic and circular patterns in the level of cooperation over time.

Henceforth, we conclude that—besides the determination of the function extrema—the genetic algorithm can occasionally give us something quite different — a new insight into the subject of study.

9. REFERENCES

- [1] Mitchell, M.: An Introduction to Genetic Algorithms. Bradford Book MIT Press, Cambridge, Massachusetts, 1996.
- [2] Gondra, I.: Parallelizing Genetic Algorithms, in Artificial Intelligence for Advanced Problem Solving Techniques, Vrakas, D. & Vlahavas, I. eds., Hershey, Information Science Reference, 2008.
- [3] Negnevitsky, M.: Artificial Intelligence – A Guide to Intelligent Systems, Addison-Wesley, Harlow, 2005.
- [4] Booker, L. B.: Recombination, in Handbook of Evolutionary Computation, Kenneth de Jong ed., Oxford University Press, 1997.
- [5] Lin, W. Y.; Lee W. Y., Hong, T. P.: Adapting Crossover and Mutation Rates, Journal of Information Science and Engineering, No. 19, 2003, pp. 889-903.
- [6] Soni, N.; Kumar, T.: Study of Various Mutation Operators in Genetic Algorithms, International Journal of Computer Science and Information Technologies, Vol. 5, No 3, 2014, pp. 4519-4521.
- [7] Nowak, S.: Tit for tat in heterogeneous populations, Nature, Vol 355, 1992, pp. 250-253.
- [8] Hižak, J.: Genetic Algorithm Applied to the Stochastic Iterated Prisoner's Dilemma, conference paper, Basoti 2016, Tallinn, Estonia (to be published) https://www.researchgate.net/publication/305768564_Genetic_Algorithm_Applied_to_the_Stochastic_Iterated_Prisoner_Dilemma.
- [9] Obitko, M.: Introduction to Genetic Algorithms, Web tutorial, <http://www.obitko.com/tutorials/genetic-algorithms/index.php>.
- [10] Hundley, D. R.: Lectures on Math Modeling, Ch. 4 Genetic Algorithm, Walla Walla: Whitman College, <http://people.whitman.edu/~hundledr/courses/M350/Note02.pdf>.
- [11] Wkp2: Wikipedia articles: Genetic Code, Codons, <https://en.wikipedia.org>.
- [12] Wkp1: Wikipedia article: Space Technology, https://en.wikipedia.org/wiki/Space_Technology_5.

* All cited Web sites and Web pages were accessible and their URLs were correct in December 2016.

Authors' contacts:

Jurica Hižak, M.Sc.

University North, Dpt. of Electrical Engineering
104. brigade 3, HR-42000 Varaždin
jurica.hizak@unin.hr

Robert Logožar, Ph.D.

University North, Dpt. of Multimedia.
104. brigade 3, HR-42000 Varaždin
robert.logozar@unin.hr

APPENDIX A. FINDING EXTREMA OF TWO POLYNOMIAL FUNCTIONS BY THE GENETIC ALGORITHM — MATLAB CODE

A.1. Genetic algorithm for finding the maximum of a square function

```
%%MAXIMUM
%This program finds the x-value for which
%the function f(x)=36x-x^2 reaches the
%maximum value.
%Program written by Jurica Hižak
%University North, Varaždin, 2016

%FITNESS FUNCTION:
ff=inline('36.*x-x.^2')
%Parameters:
n=100           %number of generations
popsize=40     %population size
mutrate=0.001 %mutation rate
nbits=5        %number of bits in a
               %chromosome

%CREATE an initial population:
popul=round(rand(popsize,nbits))
%Create a vector that will record near-
%optimal solutions across the generations:
best=zeros(1,n)
%Create a vector that will track the
%average the fitness of the population:
avg_fitness=zeros(1,n)

%EVOLUTION
iter=0
while iter<n
    iter=iter+1
    %Calculate the value of each chromosome:
    pop_dec= bi2de(popul)
    %Calculate the fitness:
    f=feval(ff,pop_dec')
    %Average fitness of the population:
    avg_fitness(iter)=sum(f)/popsize
    %Sort fitness vector and find the indices:
    [f,ind]=sort(f, 'descend')
    %Sort chromosomes according to their
    %fitness:
    popul=popul(ind,:)
    %The x-values:
    pop_dec=bi2de(popul)
    %The x-value of the chromosome with the
    %highest fitness:
    best(iter)=pop_dec(1)
    %Calculate the probability of selection:
    probs=f/sum(f)
    %Selection of parents:
    M=popsize/2
    dad=RandChooseN(probs,M)
    mom=RandChooseN(probs,M)

    %CROSSOVER
    %Choose the crossover point:
    xp=randi(nbits-1)
    %Take every 2nd dad's chromosomes
    %and exchange the genes with mom's:
    popul(1:2:popsize,:)= [popul(dad,1:xp)...
    popul(mom,xp+1:nbits)]
    popul(2:2:popsize,:)= [popul(mom,1:xp)...
    popul(dad,xp+1:nbits)]
```

```

%MUTATION
%Number of mutations in the population:
nmut=ceil(popsize*nbits*mutrate)
for i=1:nmut
    col=randi(nbits)
    row=randi(popsize)
    if popul(row,col)==1
        popul(row,col)=0
    else
        popul(row,col)=1
    end
end
end

%PLOT the x-value of the best chromosome
%over time:
figure
%Generate an array of integers from first
%to the last generation:
t=1:n
plot(t,best)
axis([1 n 12 24 ])
xlabel('number of generations')
ylabel('x-max')
%Plot the average fitness value of the
%population over time and label the axes:
figure
plot(t,avg_fitness)
axis([1 n 100 400])
xlabel('number of generations')
ylabel('average fitness')

```

A.2. Genetic algorithm for finding the global minimum of the 4-th degree polynomial

```

%%MINIMUM OF THE 4th DEGREE POLYNOMIAL
%The program finds the x-value for which
%the function
%f(x)=x^4-18x^3+110x^2-255x+300
%reaches the minimum.
%Program written by Jurica Hižak
%University North, Varaždin, 2016.

%FITNESS FUNCTION:
clear all
f=inline('x.^4-18*x.^3+110*x.^2-...
255*x+300')
%Plot the function and hold the figure:
x=0:0.1:8;
figure
ymin=fval(f,x);
plot(x,ymin)
axis([0 8 50 200 ])
xlabel('x')
ylabel('f(x)')
hold on
n=100           %number of generations
popsize=40     %population size
mutrate=0.001 %mutation rate
nbits=5        %number of bits in a
               %chromosome

%CREATE an initial population:
popul=round(rand(popsize,nbits))
%Create a vector that will record
%near-optimal solutions across
%the generations:
best=zeros(1,n);

```

```

%Create a vector that will track
%the average fitness of the population:
avg_fitness=zeros(1,n);

%EVOLUTION
iter=0
while iter<n
    iter=iter+1
    %Having assumed that the solution takes
    %place somewhere inside the interval(1,8),
    %insert as many real values as possible
    %considering the number of bits nbits
    %(e.g. 5-bits string allows 32 values).
    %Therefore, the decoded value of each
    %chromosome is:
    pop_dec= 1+bi2de(popul).*(8-1)/(2^nbits-1)

    %FITNESS
    %First, find the function value fv
    %of each chromosome:
    fv=fval(f,pop_dec');
    %Since we are looking for the MINIMUM,
    %the fitness function will be defined in
    %respect to "the worst chromosome" whose
    %fv-value is actually the highest:
    fit=max(fv)-fv;
    %Average fitness:
    avg_fitness(iter)=sum(fit)/popsize;
    %Sort fitness vector and find the indices:
    [fit,ind]=sort(fit, 'descend');
    %Sort chromosomes according to their
    %fitness:
    popul=popul(ind,:);
    %The x-value of the chromosome with
    %the highest fitness:
    best(iter)=pop_dec(1);
    %Calculate the probability of selection:
    probs=fit/sum(fit);
    %Selection of parents:
    M=popsize/2;
    dad=RandChooseN(probs,M);
    mom=RandChooseN(probs,M);

    %CROSSOVER
    %Choose the crossover point:
    xp=randi(nbits-1)
    %Take every 2nd dad's chromosomes
    %and exchange the genes with mom's:
    popul(1:2:popsize,:)= [popul(dad,1:xp)...
    popul(mom,xp+1:nbits)];
    popul(2:2:popsize,:)= [popul(mom,1:xp)...
    popul(dad,xp+1:nbits)];

    %MUTATION
    %Number of mutations in the population:
    nmut=ceil(popsize*nbits*mutrate);

    for i=1:nmut;
        col=randi(nbits);
        row=randi(popsize);
        if popul(row,col)==1;
            popul(row,col)=0;
        else
            popul(row,col)=1;
        end
    end
end

```

```
%MINIMUM:
xmin=best(n)
ymin=feval(f,xmin)
%Plot (xmin,ymin) as a red ring on the
%current figure:
plot(xmin,ymin, 'ro')

%PLOT the x-value of the best chromosome
%over time:
figure
%Generate an array of integers from the
%first to the last generation:
t=1:n
plot(t,best)
axis([1 n -1 10 ])
xlabel('number of generations')
ylabel('x-min')
%Show textbox with the output value
%(xmin,ymin)
dim = [.26, .2, .2, .6];
str = ['xmin=',num2str(xmin),...
      'ymin=',num2str(ymin)];
annotation('textbox',dim,'String',...
          str,'FitBoxToText','on')
```

BARRIERS TO THE IMPLEMENTATION OF KEY ENABLING TECHNOLOGIES

IZAZOVI IMPLEMENTACIJE KLJUČNIH RAZVOJNIH TEHNOLOGIJA

Jasna Prester, Petra Jung Erceg, Ivan Kumić

Original scientific paper

Abstract: Key enabling technologies (KET) are often crucial technological prerequisites for the advances in the production processes and product quality. They are expected to impact the existing technologies by expanding their usefulness, to enable new technological approaches and to trigger wider applications in a number of industries. Enabling technologies often have no direct easily recognizable connection with the applications, which makes it difficult to even determine the relevant impact categories. In order to stay competitive, Europe has built a fund for enhancing the usage and production of KET [1]. Since these technologies are new and their impact on the industry is still not easily identified, more research is needed. A literature review revealed many obstacles in the KET-related manufacturing, which is why in depth interviews with companies are needed. A survey research was conducted in Croatia on the level of the adoption of KET, followed by a workshop with companies that use KET in order to identify the problems they came across during the implementation.

Keywords: key enabling technologies, KET, transfer of technologies, European manufacturing, survey, implementation problems

Izvorni znanstveni rad

Sažetak: Ključne razvojne tehnologije obično su tehnologije koje su nužne za rad drugih tehnologija, proizvoda i procesa. One utječu na postojeće tehnologije povećavajući mogućnosti proizvodnih procesa i poboljšanje kvalitete. Omogućavaju nove primjene postojećih tehnologija i primjene u brojnim drugim industrijama. Takve razvojne tehnologije obično nemaju vidljiv direktan utjecaj na primjenu pa ih je teško kategorizirati i pratiti. Da bi ostala konkurentna Europa je pokrenula fond čija je jedina uloga poticanje na snažniju primjenu spomenutih tehnologija [1]. Budući da su ove tehnologije nove, nema puno istraživanja na tu temu. Istraživanje literature pokazalo je brojne prepreke u prihvaćanju naprednih razvojnih tehnologija, pa se vidi potreba za dubinskim intervjuima i pokušaju kvalifikacija tih tehnologija. U Hrvatskoj je proveden upitnik o korištenju tih razvojnih tehnologija, a zatim je uslijedila radionica s poduzećima koja koriste razvojne tehnologije da se vidi s kojim izazovima su se susretali prilikom implementacije.

Ključne riječi: ključne razvojne tehnologije, KET, transfer tehnologije, europska proizvodnja, implementacijski problemi

1. INTRODUCTION

Key enabling technologies (KET) are often crucial technological prerequisites for other technologies, products and processes which are expected to impact the existing technologies by expanding their usefulness, to enable new technological approaches and to trigger wider applications in a number of industries. They often have no direct easily recognizable connection with the applications, which makes it difficult to even determine the relevant impact categories [2]. Those technologies are in the nascent stage and there are many production challenges, dominantly the high production costs and the public's general reluctance to embrace an innovative technology without the real safety data [3]. Some speak of KETs as a new industrial revolution, because different laws of physics come into play. Traditional materials

such as metals and ceramics show radically enhanced properties and new functionalities, and the behavior of surfaces starts to dominate the behavior of bulk materials, and whole new realms opens up. Contrary to the popular belief, in the field of only nanotechnology, many industries already produce or employ products which are either nano-sized or exploit the nano effects, and are generating substantial revenues [4].

Key Enabling Technologies (KETs) are nanotechnology, micro- and nanoelectronics, including semiconductors, advanced materials, biotechnology and photonics, and advanced manufacturing systems. Mastering these technologies might mean a shift to a low carbon, knowledge-based economy. KETs play an important role in the R&D, innovation and cluster strategies of many industries, and are regarded as crucial for ensuring the competitiveness of European industries

in the knowledge economy [5]. KETs have recently become one of the “hottest” areas in research and development worldwide in terms of issued patents, and have also attracted considerable attention in the media and investment community [6]. To stay competitive, Europe has built a fund for enhancing the usage and production of KET [1].

KET is multidisciplinary and in order to apply it, knowledge from physics, chemistry, biology and other areas are needed. A second problem is that companies stick to their core activities and are reluctant to introduce new risky technologies. Such a mental picture coupled with a limited understanding of KET and how an enterprise could exploit KET explains the absence of the concepts. The situation is particularly difficult in small or less developed economies [7]. No single professional has all the necessary skills to bring a KET product to the market on his/her own. Furthermore, those in the scientific field generally lack the understanding or the business acumen required to convert technology into a commercialized product. On the other hand, investors want to get involved with the next big thing but generally lack the patience and technical expertise required in the development and evaluation of these KET-based products [6].

Although it is widely agreed that the emerging technologies such as nanotechnology, biotechnology, etc. will have increasing socio-economic impacts, there are significant boundaries in terms of available economic resources and social and political accountability (“value for money”). This has led to the necessity of setting research priorities not only at the macro-level (e.g. choosing between the broad fields such as biotechnology, nanotechnology, ICT, etc.) but also at the country (macro) level [8]. Countries and regions invest heavily in the selected KETs in order to become a global player in the field. Reports on abundant government funding in various regions are heavily cited. However, competing with the best in the globalizing world is a tough challenge even for large emerging countries. Small countries face even more challenges. Since it is extremely difficult for a country to achieve competitiveness in many industries, [9] it is proposed that a country makes a choice of industries with high impact.

KETs are potential economic engines that have the capability to become the basis for a regional and national job and wealth creation [10]. [10] researched only the nanocenters, which by their survey are growing, but those centers are dominantly scientific research centers. Only 3% of their responders labeled themselves as industrial centers. As far as the funding goes, those nanocenters were dominantly financed by national governments or in the EU by the FP7 or Horizon 2020 funding scheme [11].

However, the key point is getting revenues and competitiveness by using those KET technologies. In their technology strategies, governments so far point to a specific technology or technologies that they find to be the most relevant for their settings, and they write strategies and devise policies and based on them fund the research on selected technologies. Albeit, the dominant effects of such government schemes are the increased

scientific publications by research centers (not companies), which is not that relevant to the industry. According to the research done by [12], companies are more interested in patents and conference participation. If positive effects are to be achieved, then the commercialization of KETs is important. Commercialization is the process of turning new technologies into successful commercial ventures, which may involve an array of professionals from technical, commercial, and economic background to successfully transform a new technology into useful products or services. So far commercial applications are in industries that usually generate high revenues, e.g. cosmetics, medicine, various coatings and powder used in textile or building. The majority of companies name the lack of funding as the main barrier to the application and commercialization of novel products. Moreover, for quality control, more sophisticated equipment is needed, e.g. microscopy (atomic force microscopy, transmission electron microscopy (TEM), and scanning electron microscopy; measurement of particle size and size distribution with light scattering (static and dynamic); analytical ultracentrifugation, capillary electrophoresis; analysis of surface charge or zeta potential; examination of surface chemistry by X-ray photoelectron spectroscopy or Fourier transform infrared spectroscopy; differential scanning calorimetry and X-ray diffraction, among others. Such analytical equipment and the performance of these checks are not just expensive, but also require trained personnel to carry out the analysis and interpret the results. This would substantially add to the cost of manufacture and would definitely deter a company from investing in the development of such a product. Even if the industry plans to outsource these analyses to other firms, it would still be expensive as each and every batch would have to be run through several tests and transported to the premises of the controlling institute/company [6].

The main objective of this work is to find out what the level of the adoption of KETs in the least advanced member of EU – Croatia – is. However, since Croatian manufacturing largely exports its products, it is hypothesized that there some level of adoption of these technologies will be found. After a survey that revealed that 28% of surveyed companies do in fact use some of KET technologies, a workshop was conducted in order to find out what their experiences, issues and problems regarding the implementation of KETs were. Moreover, during the workshop, some possible further actions in order to facilitate the transfer of KET technologies were revealed. However, in order to talk about KETs, it is first necessary to define them.

2. OVERVIEW OF THE KEY ENABLING TECHNOLOGIES

KETs are knowledge intensive and are associated with high R&D intensity, rapid innovation cycles, high capital expenditure and highly-skilled employment. They enable the production of new products and therefore augment the competitiveness of a company and then of

the region. They are multidisciplinary, cutting across many technology areas with a trend towards convergence and integration. KETs necessitate large investments, but those investments could bring positive effects in the long run [13].

The following section provides a brief description of the multidisciplinary characteristics of some KETs in the EU and explains why advanced materials, nanotechnology, micro- and nano-electronics, industrial biotech and photonics and advanced manufacturing systems have been identified as a priority to improve the European industrial competitiveness.

2.1. Advanced materials

Advanced materials technologies lead both to new reduced cost substitutes to the existing materials and to new higher added-value products and services. This will reduce resource dependency and environmental waste and hazards at the same time. Besides the costs of capital, expenditure on materials is the most important cost factor in high-technology related industries. They are of key importance for the competitiveness of the EU industry, especially since Europe is not well endowed with natural resources [13].

2.2. Nanotechnology

Nanotechnology is an umbrella term that covers the design, characterization, production and application of structures, devices and systems by controlling the shape and size at the nanometer scale. European SMEs using nanomaterials are mostly present in the automotive and medical and healthcare sectors, followed by energy. Within the medical system and healthcare, implants (44%), molecular diagnostics (28%) and drug delivery (27%) are the most important fields of application. Applications in the energy field are mostly related to energy conversion or production (66%), followed by energy saving (38%) and energy storage (28%) [13].

2.3. Micro- and nanoelectronics

Micro- and nanoelectronics deal with semiconductor components and highly miniaturized electronic subsystems and their integration in larger products and systems. Europe has a declining share of worldwide investment in microelectronics. From a total investment of €28bn in microelectronics in 2007, only 10% was made in the EU compared to 48% in Asia. Europe's semiconductor market share has declined from 21% to 16% since 2000. However, total direct employment in microelectronics in Europe is over 110 000 plus 105 000 in equipment manufacturers. Europe has a number of dedicated regions with a critical mass and particular semiconductor competencies which are recognized world-wide. These clusters have access to the most advanced technologies and are the key assets for the European industrial competitiveness [13].

2.4. Industrial biotechnology

Industrial biotech is the application of biotechnology for the industrial processing and production of chemicals, materials and fuels. It includes the practice of using microorganisms or components of micro-organisms such as enzymes to generate industrially useful products, substances and chemical building blocks with specific capabilities that conventional petrochemical processes cannot provide. There are many examples of such bio-based products already on the market. The most mature applications are related to the enzymes used in the food, feed and detergents sectors. More recent applications include the production of biochemical, biopolymers and biofuels from agricultural or forest wastes [13].

2.5. Photonics

Photonics is a multidisciplinary domain dealing with the science and technology of light, encompassing its generation, detection and management. The EU has strong positions in many photonics applications such as solid state lighting (including LEDs), solar cells, and laser assisted manufacturing. Photonics is a good example of an enabling technology, as there are around 5000 photonics manufacturers in Europe employing around 246 000 persons (excluding subcontractors) directly. In addition to that, the jobs of over 2 million more employees in the EU's manufacturing sector depend directly on photonic products. Germany accounts for 39% of European production volume, followed by France and the UK (12% each), the Netherlands (10%) and Italy (8%) [13].

2.6. Advanced manufacturing systems

Advanced manufacturing systems denote the range of high technologies involved in manufacturing, leading to improvements in terms of new product properties, production speed, cost, energy and materials consumption, operating precision, waste and pollution management. This is especially relevant in capital intensive industries with complex assembly methods. They are needed to help create marketable knowledge-based goods and the related services (e.g. modern robotics). For example, the production and assembly of modern aircraft involves the whole spectrum of manufacturing technologies from the simulation and programming of robotic assembly lines to reducing energy and materials consumption. Other examples include intelligent control systems, automation for modelling and production. They can be applied in all manufacturing industries and form an important element in the supply chain of many high value manufacturing businesses [13].

These are only general descriptions of technologies, but in order to conduct a survey, a more detailed description of the technologies was necessary.

3. METHODOLOGY

The questionnaire was developed through a massive literature research dominantly on Status Implementation reports from the European Commission, on each KET field. Even though the complexity of each technology is described in the previous section, for the survey process it was crucial to extract the enabling technologies that might be used by manufacturing companies. The sampling procedure was facilitated by obtaining e-mail addresses from the Croatian Chamber of Commerce, and it covered the whole manufacturing sector with over 10 employees. 2037 addresses of manufacturing companies in Croatia with over 10 employees were obtained. It was believed that micro companies with less than 10 employees hardly use such sophisticated technologies. The survey was launched twice, once at the beginning of September 2014, followed by the next round in October 2014. Responders usually answered a couple of days after the launch of the survey. That enabled the checking of non-response biases, which is highly necessary in this study since the return rate was only 2%. The rate is truly small but as [14] shows, the response rates are almost linearly declining and therefore scientists more often than not engage in case study research. Moreover, such a small sample is due to the fact that KETs are still not in wide usage even in the advanced economies.

Richards et al. [15] have identified that there are both psychological and mechanical reasons for low response rates with web-based surveys. Psychological reasons include: people may have forgotten about it; they may be so busy that they do not want to take the time to fill the survey out; some people find surveys a disruption to their personal lives; or the survey is too long. Mechanical reasons may include a lack of Internet access, concerns with the security and data integrity, and technical problems and other reasons of unwillingness or inability to participate in the survey. Given these issues and generally low response rates with self-administered surveys, non-response bias is a significant concern and particularly salient for web-based research [16], [17]. Among various methods of checking for non-response biases described by [18], Wave Analysis was used, which consists of comparing late respondents to early respondents. Wagner and [19] cite [20] the rule of thumb as a minimal response rate of $n=30$. Our sample fulfils this minimal criterion, as 37 companies returned filled in questionnaires.

Since this is an extremely low response rate, it was necessary to check the representativeness of the sample according to the industry and size of companies. The calculation of representativeness by NACE codes is given in Table 1. The methodology used can be found in [21]. A group is considered representative if its Z value does not surpass 1.96 which is the critical value at 5% significance level, meaning that the null hypothesis that the sample represents the parent population can be accepted.

Table 1. Representativeness by industry

NACE code	Population	Sample	Z	Representative
10 Manufacture of food products	311	3	-1.44	Rep
11 Manufacture of beverages	50	0	0	
12 Manufacture of tobacco products	2	0	0	
13 Manufacture of textiles	55	0	0	
14 Manufacture of wearing apparel	139	2	-0.41	Rep
15 Manufacture of leather and related products	47	2	0.60	Rep
16 Manufacture of wood and products of wood and cork; except furniture; manufacture of articles of straw and plaiting materials	190	3	-0.34	Rep
17 Manufacture of paper and paper products	47	2	0.60	Rep
18 Printing of the reproduction of recorded media	95	1	-0.68	Rep
19 Manufacture of coke and refined petroleum products	2	0	0	
20 Manufacture of chemicals and chemical products	61	3	0.83	Rep
21 Manufacture of basic pharmaceutical products and pharmaceutical preparations	15	0	0	
22 Manufacture of rubber and plastic products	144	3	0.08	Rep
23 Manufacture of other non-metallic mineral products	139	5	0.83	Rep
24 Manufacture of basic metals	36	0	0	
25 Manufacture of fabricated metal products, except machinery and equipment	364	2	-2.88	
26 Manufacture of computer, electronic and optical products	66	1	-0.23	Rep
27 Manufacture of electrical equipment	90	3	0.57	Rep
28 Manufacture of machinery and equipment n.e.c.	133	3	0.18	Rep
29 Manufacture of motor vehicles, trailers and semi-trailers	24	2	0.85	Rep
30 Manufacture of other transport equipment	52	0		
31 Manufacture of furniture	102	3	0.46	Rep
32 Other manufacturing	46	1	0.07	Rep

As it can be seen from Table 1, there are several industries that are not represented. However, those industries are the least mentioned as the ones applying the KET technologies, so the rest of the sample is representative for the analysis. Representativeness according to size is given in Table 2, and the sample is representative.

Table 2: Representativeness according to size in terms of the number of employees

	Population	Sample	Z	Representative
> 10 and < 50	1606	19	-1.12	Rep
51 to 250	567	3	-1.36	Rep
> 250 employees	139	13	0.97	Rep

4. RESULTS

In the whole sample, 28% of companies use some key enabling technology, 72% do not use the technology, but out of those who do not use KETs, 24% think or plan to use them. Table 3 presents the used technologies.

Table 3: Used technologies

Technology	Number of companies using
Advanced materials	
Advanced steel (iron) alloy	5
Advanced non-ferrous alloys	5
Super alloys	1
Polymeric composites (polymer-matrix composites)	8
Polymeric composites (metal-matrix composites)	3
Ceramic composites (composites with ceramic matrix)	2
Synthetic non-conductive polymeric materials	4
Conductive polymers	2
Nanofibers (nanotubes, fullerenes)	0
Nanocomposites	1
Nanoceramic	0
Nanopowders	0
Nanocrystals	0
Piezoelectric ceramics	1
Advanced coatings (multifunction, nanostructured, gradient ...)	1
Biomaterials	2
Micro- and nanoelectronics	
Semiconductors in the information and communication technology	5
Semiconductors for the medical industry	0
Nano materials	
Usage in construction (antibacterial coatings, coating against fire, ...)	1
Environment/energy (storage batteries, catalysts, heat exchangers, filters, solar cells, ...)	2
Textiles (fabrics resistant to heat, antibacterial textiles, ...)	3
Chemistry (nanosilica, polymers, ferrofluids, carbon nano tubes, artificial silk, nanopigments ...)	1
Automotive industry (fasteners rubber, anti-fogging coatings, anti-reflective displays, ...)	0
Electronics (hard drives with GMR heads, silicone and polymer electronics, phase shifting, ferroelectric and magnetic memory, ...)	2
Optics (ultra precision optics, optical microprocessors, EUV optical lithography, ...)	2
Medicine (marker substances, contrast agents, biocompatible implants, ...)	0
Industrial Biotechnology	
Biopolymers fibers	1
Biodegradable plastics	1
Biofuel	3
Industrial enzymes	2
Antibiotics and vitamins	2
Chemicals (amino acids, organic acids, detergents, cosmetics ...)	2
Photonics	
Consumer electronics (lighting, displays, CD / DVD ...)	8
Conversion of solar energy	0
Optical fiber cables (telecommunications)	7

Optical systems (various scanners, sensors, lasers, ...)	7
Medical diagnosis, contact lenses, microscopes, medical lasers, ...	0
Advanced manufacturing systems	
Production system that produces at a higher speed compared to conventional production	8
Production system that reduces material consumption	8
Production system which increases accuracy	9
Production system that reduces environmental impact	8
Production system that is smaller in size	3

Figures 1 and 2 display the usage of KET technologies by industry and by size.

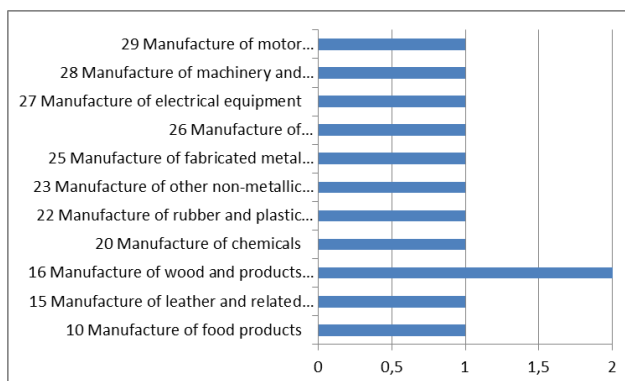


Figure 1. Usage of KET-related technologies by industries

Looking into the industries, it can be seen that in almost all industries that were representative for the sample there is at least one company using KET-related technologies. This proves the general applicability of KET technologies.

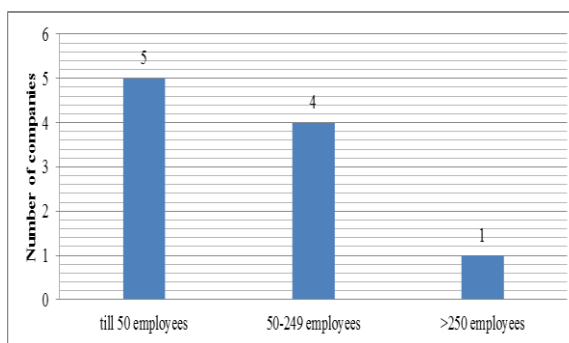


Figure 2. Usage of KET-related technologies by the size of the company

The hypothesis that small companies do not use KET-related technologies seems to be wrong as the majority of KET users fall into small companies. This was further investigated during the workshop and indeed it is usually easier for a small company to acquire the latest technology, which then does not necessitates much labor work, and therefore the result is that more micro companies use these latest technologies.

Further in the questionnaire were the questions addressing the barriers of the implementation of KET-related technologies. Table 4 presents the main barriers.

Table 4. Main obstacles in applying KETs

Reasons for not using KET technologies	Number of companies
Lack of financial resources	13
Unknown application potentials	11
Uninformed	11
Lack of knowledge	9
Not applicable for our production	6

The reasons from Table 4 fall into three categories: lack of financial resources, lack of knowledge and not applicable. The workshop had to reveal the problems associated with the two dominant problems, that is, the lack of financial resources and lack of knowledge.

One way to enhance the transfer of technology from research institutions to companies is their cooperation. In the questionnaire there was an open question regarding why companies and research institutions do not cooperate more. The answers fall into these five categories:

- communication problems
- it is unknown to the industry what research institutions explore and vice versa, the research institutions are not aware of the practical problems in the industry
- a lack of workshops between the research and industry in a simple understandable language
- high cost of Croatian research institution's fees
- corruption in Croatia

Apart from corruption in Croatia, the problems of cooperation are universally the same as in the rest of the world [22], [23].

5. WORKSHOP RESULTS

At the beginning of the survey process all companies (2037) were invited to a free workshop on KETs. The workshop was marketed several times during the conduction and the end of the survey. The workshop consisted of an introductory overview on why KETs are important for Europe and some practical applications of KETs in everyday products. That was followed by the results of a similar survey in Slovenia, and a presentation on how German institutes cooperate with companies on technologies that Germany adopted as strategically important. Finally, the obstacles were addressed.

5.1. Lack of financial resources

A small presentation was done on the subject by giving the examples on how companies from Poland, Slovenia and China surmounted this problem. The point was that companies, in cooperation with research institutions, should apply for EU or government funds. Two problems regarding this came up in the workshop. First, companies already applied in such a way for the funding, but did not obtain it. A careful talk about this proposal revealed that what was too high was a consortium of manufacturing companies and the level of detail about the company that had to be disclosed. It was

then suggested that in order to increase the chances of getting funds, companies should cooperate with research institutions or education institutions, and the second point was that the choice of the leading partner that has the know-how of writing a research proposal is extremely important. Another problem that the participants mentioned was that even when it is directed by the CEO to apply for funding, the employees do not get extra time for writing proposals, rather it becomes an after work duty which is certainly not convenient and leads to many errors.

5.2. Lack of knowledge

Companies using KETs or planning to use KETs obtained the knowledge from companies that provide KET technologies. Companies did not do research about the technologies themselves. In fact, the information about KET technologies in Croatia are extremely scarce, unlike in Germany where national chambers and ministries send brochures educating the companies of the potential positive use of technologies. All participating companies revealed an interest in quarterly workshops on a certain technology where they would get the knowledge of potential applications, but where they would also meet each other and discuss how to implement a certain technology and how they solved the obstacles.

5.3. Collaboration with research institutions

There is a substantial problem in cooperation between the companies and research or education institutions. Participants of the workshop indeed said that this was the first workshop in an easily understandable language about advanced technologies. Additionally, it was free. Participants from the Faculty of Mechanical Engineering did in fact confess that they only do commercial cooperation with companies mostly by lending the newest equipment, which they in fact obtained by applying for the national or EU research grants. It seems that the problems with cooperation are truly serious and cannot be easily remediated. Rather, it is necessary to start building trust between the research institutions and companies, in a way that research institutions and education institutions devote some of their time to giving free workshops to the industry in order to build this trust. The leading countries in technology and competitiveness (USA, Japan, China) do in fact conduct more applicative rather than basic research, unlike Europe, where fundamental research is more dominant [1]. It means that the research and higher education institutions in Croatia should start building this relationship for a mutual benefit.

6. CONCLUSION

Even in a small country such as Croatia, research showed that 28% of surveyed companies do use some of the key enabling technologies. Among the dominant reasons for not using the technologies are a lack of financial resources, unknown application potentials and a

general lack of knowledge on key enabling technologies. It is advised to companies to use the European structures funds or national funds [24]. However, the communication problems are serious and may be even more serious than in the developed and developing countries. The workshop revealed that companies would in fact truly appreciate quarterly workshops on a certain technology to start building the trust in research and higher education institutions. In this way, the applicative problems would also be discussed, which could enhance the number of applicative research instead of fundamental research. This would enhance the technology transfer and it would help companies to gain more knowledge about the technologies and in that way be better in communicating with the KET providers that approach them.

7. REFERENCES

- [1] EC (European Commission), Key enabling technologies – Status Implementation Report, (2013) http://ec.europa.eu/enterprise/sectors/ict/files/kets/hlg_ket_status_implementation_report_final_en.pdf, (Accessed 02.10.2014).
- [2] Fleischer, T.; Decker, M.; Fiedeler, U. Assessing emerging technologies—Methodological challenges and the case of nanotechnologies, *Technological Forecasting and Social Change*, Vol. 72, No. 9 (2005) 1112-1121.
- [3] Hunt, W. H. Jr., Nanomaterials: Nomenclature, novelty, and necessity, *Journal of Operations Management*, Vol. 56, No. 10 (2004) 13-18.
- [4] Fleischer, T.; Grunwald, A. Making nanotechnology developments sustainable. A role for technology assessment?, *Journal of Cleaner Production*, Vol. 16, No. 8–9 (2008) 889-898.
- [5] EC (European Commission), Key enabling technologies, (2014), available at: http://ec.europa.eu/enterprise/sectors/ict/key_technologies/index_en.htm (Accessed 01.10.2014).
- [6] Kaur, I. P.; Kakkar, V.; Deol, P. K.; Yadav, M.; Singh, M.; Sharma, I. Issues and concerns in nanotech product development and its commercialization, *Journal of Controlled Release*, Vol. 193 (2014) 51–62.
- [7] Tegart, G. Nanotechnology: the technology for the twenty first century, *Foresight*, Vol. 6, No. 6 (2004) 364 – 370.
- [8] Salerno, M.; Landoni, P.; Verganti, R. Designing foresight studies for Nanoscience and Nanotechnology (NST) future developments, *Technological Forecasting and Social Change*, Vol. 75, No. 8 (2008) 1202-1223.
- [9] Momaya, K. Cooperation for competitiveness of emerging countries: learning from a case of nanotechnology, *Competitiveness Review: An International Business Journal*, Vol. 21, No. 2 (2011) 152 – 170.
- [10] Kautt, M.; Walsh, S. T.; Bittner, K. Global distribution of micro–nano technology and fabrication centers: A portfolio analysis approach, *Technological Forecasting and Social Change*, Vol. 74, No. 9 (2007) 1697-1717.
- [11] Brousseau, N. I. E. Implementing a multi-staged methodology to micro and nanotechnology, *International Journal of Productivity and Performance Management*, Vol. 63, No. 2 (2014) 170-193.
- [12] Blind, K.; Gauch, S. Research and standardization in nanotechnology: Evidence from Germany, *The journal of technology transfer*, Vol. 34, No. 3, (2009) 320-342.
- [13] EU (European Union), Preparing for our future: Developing a common strategy for key enabling technologies in the EU, Current situation of key enabling technologies in Europe (2009), <http://eur-lex.europa.eu/legal-content/EN/TXT/PDF/?uri=CELEX:52009SC1257&from=EN> (Accessed 02.10.2014).
- [14] Larson, P. D. A Note On Mail Surveys And Response Rates In Logistics Research, *Journal of Business Logistics*, Vol. 26, No. 2 (2005) 211-222.
- [15] Atif, A.; Richards, D.; Bilgin, A. Estimating Non-Response Bias in a Web-based Survey of Technology Acceptance: A Case Study of Unit Guide Information Systems, 23rd Australasian Conference on Information Systems (2012) <http://dro.deakin.edu.au/eserv/DU:30049121/atif-estimatingnon-2012.pdf> (Accessed 01.10.2014).
- [16] Dillman, D. A. Mail and Internet Surveys: The Tailored Design Method. New York: John Wiley & Sons (2000).
- [17] Hansen, R. A.; Henley, A. C.; Brouwer, E. S.; Oraefo, A. N.; Roth, M. T. Geographic Information System Mapping as a Tool to Assess Nonresponse Bias in Survey Research, *Research in Social and Administrative Pharmacy*, Vol. 3, No. 3 (2007) 49-64.
- [18] Rogelberg, S. G.; Stanton, J. M. Understanding and Dealing with Organizational Survey Nonresponse, *Organizational Research Methods*, Vo. 10, No. 2 (2007) 195-209.
- [19] Wagner, S. M.; Kemmerling, R. Handling Nonresponse in Logistics Research, *Journal of Business Logistics*, Vol. 31, No. 2 (2010) 357-381.
- [20] Mentzer, J. T.; Flint, D. J. Validity in Logistics Research, *Journal of Business Logistics*, Vol. 18, No. 1 (1997) 199-216.
- [21] Telhaj, S.; Hutton, D.; Davies, P.; Adnett, N.; Coe R. Competition within Schools: Representativeness of Yellis Sample Schools in a Study of Subject Enrollment of 14-16 Year Olds, (2004), <http://www.staffs.ac.uk/schools/business/iepr/docs/Working-paper11.doc>, (Accessed 18.07. 2004).
- [22] Allarakhia, M.; Walsh, S. Analyzing and organizing nanotechnology development: Application of the institutional analysis development framework to nanotechnology consortia, *Technovation*, Vol. 32, No. 3-4 (2012) 216–226.
- [23] Nikulainen, T.; Palmberg, C. Transferring science-based technologies to industry—Does nanotechnology make a difference?, *Technovation*, Vol. 30, No. 1 (2010) 3-11.

- [24] Shapira, L. T. P.; Meng, Y. Developing an innovative materials enterprise in China: a nanotechnology small business case study, Chinese Management Studies, Vol. 8, No. 2 (2014) 201-217.

Acknowledgements: This work is conducted and financed thanks to the Croatian National Foundation, Grant No. O-1861-2014-3535 Building Competitiveness of Croatian Manufacturing.

Authors would also like to thank the anonymous reviewers for their useful comments for making this paper better.

Contact addresses

Jasna Prester, Ph.D, Associate Professor

University of Zagreb,
Faculty of Business and Economics
Kennedyev trg 6, Zagreb, Croatia
Tel: 00385 1 238 32 61,
Fax: 00385 1 233 56 33Tel.
e-mail: jprester@efzg.hr

Dr. Petra Jung Erceg

Fraunhofer-Institut für System- und
Innovationsforschung
Breslauer Straße 48 | 76139 Karlsruhe
Telefon +49 721 6809-306
e-mail: petra.jung-erceg@isi.fraunhofer.de

Ivan Kumić, PhD, Postdoctoral Researcher

University of Zagreb, Faculty of Mechanical
Engineering and Naval Architecture, Department of
Materials
I. Lučića 5, HR-10000 Zagreb, Croatia
Tel. +38516168304
e-mail: ivan.kumic@fsb.hr

AN APPROXIMATE SOLUTION FOR THE PLANE WAVE DIFFRACTION BY AN IMPEDANCE STRIP: H-POLARIZATION CASE

OKVIRNO RJEŠENJE ZA DIFRAKCIJU RAVNOG VALA IMPEDACIJSKOM TRAKOM: SLUČAJ H-POLARIZACIJE

Emine Avşar Aydın, Turgut İköz

Original scientific paper

Abstract: In this study, the diffraction of H-polarized plane wave by an infinitely long strip which has the same impedance on both faces with a width of $2a$ is investigated by using an analytical-numerical method. The diffracted field is obtained by an integral equation in terms of the electric and magnetic currents induced by the incident field. This integral equation is reduced to two uncoupled integral equations that include only induced electric and magnetic currents separately. Both of the currents are defined as a sum of infinite series of Gegenbauer polynomials with unknown coefficients satisfying the edge conditions. The integral equations are transformed to linear algebraic equations by using analytical methods and the unknown coefficients are determined by solving numerically obtained matrix equations. Numerical examples on the RCS (radar cross section) are presented, and the far field scattering characteristics of the strip are discussed in detail. Some of the obtained results are compared with the other existing method.

Keywords: impedance, strip, analytic, numeric, diffraction

Izvorni znanstveni članak

Sažetak: U ovom radu istražuje se difrakcija H-polariziranog ravnog vala od beskonačno duge trake koja ima jednak otpor na obje strane i širinu $2a$ korištenjem analitičkog-numeričke metode. Difraktirano polje dobiveno je putem integralne jednadžbe u smislu električnih i magnetskih struja induciranih upadnim poljem. Ova integralna jednadžba svedena je na dvije odvojene integralne jednadžbe koje zasebno uključuju samo inducirane električne i magnetske struje. Objke struje definirane su kao zbroj beskonačnog niza Gegenbauerovih polinoma s nepoznatim koeficijentima koji zadovoljavaju rubne uvjete. Integralne jednadžbe pretvorene su u linearne algebarske jednadžbe pomoću analitičkih metoda i nepoznati su koeficijenti utvrđeni rješavanjem numerički dobivenih matricnih jednadžbi. Predstavljani su numerički primjeri na PRP-u (površina radarskog presjeka), a karakteristike rasipanja na dalekom polju kod traka detaljno su raspravljani. Neki od dobivenih rezultata uspoređeni su s drugom postojećom metodom.

Ključne riječi: impedacija, traka, analitički, numerički, difrakcija

1. INTRODUCTION

The scattering of electromagnetic waves from geometrical and physical discontinuities is one of the most essential fields in the electromagnetic wave theory. However, the first considerable steps in this area of research are due to Lord Rayleigh and A.Sommerfeld. Almost a century ago, Rayleigh [39] (from Born M. [5]) investigated the problem of scattering by a perfectly conducting sphere; and Sommerfeld [45] overcame the problem of diffraction of plane electromagnetic waves by an absolutely conducting semi-infinite plane. Over the last few decades, the researches in the scattering of electromagnetic waves by several objects have been developed as a result of its direct applicability to civilian applications, including military ones, such as remote sensing, non-invasive diagnostics in medicine and non-destructive testing.

The received signal, which is spread by an object, can be used to resolve some of the geometrical and physical properties of the scatterer. Since the received scattered signal power is directly corresponds to the scattered field or radar cross section (RCS) of the object. Therefore, in military applications, in order to avoid the echo signal, the RCS of targets like air crafts must be cut down to a minimum level. Additionally, in order to decrease the inference caused by obstacle as buildings for instance, the RCS of such obstacles that are close to radars should also be reduced. Correspondingly, groups of engineers and scientists are also researching to extract as sufficient information as possible from low RCS values for both military and civilian applications.

Several methods exist, which are applicable to reduce the RCS of some obstacles. For instance, if the shape of the target is to be modified, scattered energy somehow may be directed toward some desired regions. But some other situations exist where shape modification is

confined by the aerodynamic structure of that target, and another technique such as absorbing layer is applied for the same purpose. The absorber may consist of dielectric or magnetic materials, partially dielectric and/or magnetic materials or a number of layers of such materials. Even though such mixtures of shapes and materials propose more degrees of freedom in terms of design within controlling the RCS of the target, similarly, the complexity of the solution procedure is also increased.

Solutions for recognized problems including half-plane, cylinder or sphere are apparently essential regarding the diffraction theory, and strip is considered to be one of the most important familiar structures due to its geometry, strips are usually accustomed to investigate the multiple diffraction phenomenon. Furthermore, a large amount of applicable issues, especially in remote sensing, modeling by conducting, impedance or resistive strips is possible. Additionally, by using the duality principle diffracting a slit in an absolute conducting plane can be reduced to a perfectly conducting strip problem.

Scattering of cracks or gaps that may occur on the obstacle's surface, which is completely or partially filled with some material, may provide a significant contribution to the overall scattering pattern. In such issues the gaps or cracks may be modeled by strips and/or slits. Accordingly, due to its adjustment to many practical problems, strips have been broadly researched by many authors by using distinctive analytical and numerical strategies.

1.1. Literature Review

A large number of analytical techniques have been developed considering diffraction by scatterers with several shapes, sizes and constituent materials. These methods can be categorized in two groups, namely, exact and approximate methods. Using an exact method is possible, when the obstacle's geometry corresponds to a coordinate system having the wave equation separable.

Furthermore, exact solutions usually include sophisticated integral expressions, which are required to apply near-field, far-field or high-frequency asymptotic for engineering purposes. Due to these constraints not many practical problems have exact solutions, and mostly severe asymptotic expressions are acquired. Approximate analytical techniques were obtained from the extension of classical optics by geometrical Theory of Diffraction (GTD) introduced by Keller [23] and Physical Theory of Diffraction (PTD) introduced by Ufimtsev (from Bhattacharyya, A.K. [4]).

In geometrical optics zero wavelength approximation is implemented and space is divided into distinct illuminated and shadow regions. It is considered that energy spreads in tube of rays, obviously the diffraction impacts are discarded in previous estimates; where these effects were first studied by GTD. At both incidence and reflection boundaries, the diffracted field becomes infinite and also at the edge which is caustic for the diffracted field. The term of a diffraction coefficient can be acquired simply by expressing the identical solution of a recognized problem in GTD form. In order to

enhance GTD and overcome some of the methods' drawbacks two fundamental techniques have been developed namely, Uniform Asymptotic Theory of Diffraction (UAT) and Uniform Theory of Diffraction (UTD) introduced by Ahluwalia et.al [2] and Kouyoumjian and Pathak [24] respectively. In UAT it is considered that the field solution that occurs in an edge diffraction problem can be extended in a specific asymptotic series including a Fresnel integral, whereas in UTD Keller's diffraction, the coefficient is multiplied by a factor involving a Fresnel integral. The multiplication factor has a feature such that the field point approaches the shadow boundary and a finite field is obtained at the shadow boundaries while approaching zero.

In physical optics, surface currents are assumed to induce only at the illuminated part of the scatterer that functions as the supply of the scattered field. The accuracy of the technique can be raised by enhancing the assumed current distributions, however, it may not be able to account utterly for the presence of discontinuities on the obstacle. By PTD, Ufimtsev introduced the fringe current concept as a result of the physical or geometrical discontinuities. It was assumed that the entire current on a conducting surface includes a fringe current (nonuniform part) along with physical optics current. In distinction to GTD, PTD yields the finite fields everywhere including the shadow boundaries at the caustics.

Since its geometry is simple, the strip issue was researched by many scientists. Many techniques were proposed, but none yielded an efficient solution. So far, a severe solution for the problem of diffraction by a strip doesn't exist. However explaining the attempts to solve this problem which had yielded significant solutions, is worth it. Some of the considerations made will be given in a sequential order as follows.

Morse and Rubenstein [33] used a Mathieu function expansion for electromagnetic fields to obtain the exact series representation for the solution of the diffraction by strips. According to the rapid convergence of the Mathieu series, their solution yields improvement for low frequencies. However, when it comes to high frequency range their proposed method is not accurate since there is a necessity to include large number of terms while computing the infinite series.

Grinberg [16] proposed shadow current concept for diffraction issues regarding electromagnetic waves by a conducting slit by implementing the integral equation method. However, the same method could be applied to solve the problem of diffraction by a conducting strip, which is achieved by using the duality principle. The problem with this method is reduced to the solution of a second kind Fredholm equation. According to this formulation, the asymptotic form of the solution for the high frequency case can be obtained easily. It should be taken into account that the application of integral equation method have been used by other researches before Grinberg, in previous studies, e.g. Copson [12], Levine and Schwinger [27] and Miles [32]. Integral equation based formulation was firstly implemented by Copson [12] (from Senior, T.B.A. [42]) for a specific case of the Sommerfield half-plane which was an equation of the Wiener-Hopf type.

Up to 1950s, approximately all researches were focused on the diffraction by perfectly conducting structures. Senior [42] proposed the first study for the issue of finite conductivity, by using a semi-infinite metallic sheet as the diffracting structure. The stipulation used in this study was the standard impedance condition. For E-polarization, Senior defined two induced currents namely electric and magnetic, and by using Green's theory Senior had acquired the total field at any point off the plate in terms of these induced currents and incident field. The edge conditions for current components were being given as $O(x^{-1/2})$ and $O(x^{1/2})$ for $x \rightarrow 0$, for the tangential and normal components, respectively, of the electric and magnetic currents. The asymptotic behavior introduced by Senior [42] for the currents correspond to asymptotic behavior of the field components proposed by Meixner [31]. This is considered as one of the most essential information for our method. Accordingly, the information behind this behavior of currents at the edges give us the possibility to explain the currents in a series of some special functions with some unknowns.

It may be noted that the strip is used as a basic element in the formation of gratings. Diffraction by an impedance strip was researched by Faulkner [14] (from Bowman, J. J. [6]) via a Wiener-Hopf primarily based method, where the width of the strip was considered large compared to both the wavelength and the magnitude of the surface impedance such that it was being restricted to limited values. Maliuzhinets [28] (from Bowman, J. J. [6]) thought-out the wide strip drawback, furthermore, where the mutual interaction between the edges was neglected: then, the two edges were assumed as independent semi-infinite half planes, within the absence of the other being excited by an equivalent field alone.

Bowman [6] has also researched the high frequency back-scattering from an absorbing wide strip with random face impedances by using an approximation based on the known half plane solutions obtained by Maliuzhinets [28].

Multiple diffraction or the interaction among the diffracting edges of a strip is of great applicable importance additionally, diffraction problems which involve both slit and or strip geometry represent a three-part mixed boundary-value issue which strictly may be represented via triple integral equation approach that generally yields correspondingly to a modified Wiener-Hopf equation. Possibly, the solution for multiple diffractions are obtained by a repetitive procedure presented by Jones [22] (from Serbest A.H. and Büyükaksoy A. [44]). Kobayashi [25] had researched numerous types of modified Wiener-Hopf geometries and conjointly conferred the solution for H and E polarization cases. Another approximate method is presented by

Tiberio and Kouyoumjian [47] and is called extended spectral ray method which includes interpreting the incident field to the second edge as a sum of inhomogeneous plane waves that can be treated separately. By using this method, Herman and Volakis [18] had researched several diffraction by a conductive, resistive and impedance strips where the asymptotic solutions presented for these cases also involved the

impacts of surface waves. The spectral iteration technique introduced by Büyükaksoy et al. [9] is considered an alternative spectral domain method furthermore, assuming that the edge is illuminated by the field diffracted from the other edge, it is possible to obtain the doubly diffracted field additionally, constructing another Wiener-Hopf problem for this configuration. A detailed discussion of the mentioned methods are given by Serbest and Büyükaksoy [44].

The development in numerical techniques for the solution of the scattering problems has always been parallel to the evolution in computer technology. Although numerical methods may be considered as more obvious compared to analytical methods, since the matrix inversion procedure for the analysis, computer capacity limits the size of the issue that can be dealt with. Generally, for the barriers having a maximum dimension of a few wavelengths, numerical methods are able to maintain precise solutions. The Method of Moments (MOM) and Galerkin's Method [17] are the popularly used numerical techniques. In MOM both the basic functions and the weighting functions are distinct however, they are considered similar functions in Galerkin's Method.

In numerical methods, the scattering drawbacks are presented as integral equations of both unknown field quantity and unknown induced surface current density by applying Green's theorem:

$$\vec{E}(\mathbf{r}) = -\frac{1}{4\pi} \int_s \left\{ \begin{aligned} & i\omega\mu [\vec{n} \times \vec{H}] G(\mathbf{r}, \mathbf{r}') \\ & + [\vec{n} \times \vec{E}] \times \nabla G(\mathbf{r}, \mathbf{r}') \\ & + (\vec{n} \cdot \vec{E}) \nabla G(\mathbf{r}, \mathbf{r}') \end{aligned} \right\} ds \quad (1.1)$$

or in terms of surface current densities.

$$E(\mathbf{r}) = E^i - \frac{i}{4} \int_s \left\{ -iJ(\mathbf{r}') + M(\mathbf{r}') \frac{\partial}{\partial n} \right\} G(\mathbf{r}, \mathbf{r}') ds \quad (1.2)$$

The fundamental functions are broadly used for representing the currents on a given surface. However, in most studies the integral equation is achieved directly by applying the well-known methods such as Moment Method, Galerkin's Method or Finite Element Method.

Wandzura [53] investigated the current fundamental functions for curved surfaces in general. Volakis [52] researched the scattering by a narrow groove in an impedance plane, and solved the integral equations by presenting a single-basis study of the equivalent current on the narrow impedance insert. Based on these studies, the obtained integral equations are solved directly by applying either one of the above-mentioned numerical methods.

The GTD was used by Senior [43] to obtain the expression of the scattered field by a resistive strip where the results meet the ones obtained by the numerical solution of the integral equation including strips a narrow as a sixth of a wavelength. Senior also applied MOM to inspect the contribution of front and rear-edges to the far fields. It has been represented that, for strips with a width greater than about a half wavelength, the contribution regarding the front edge is similar to a half plane one, having similar resistance and the contribution of the rear edge is proportional to the square of the current at that

point on the half plane corresponding to the rear edge of the strip.

Generally, the integral equations in Eq. (1.1) and Eq. (1.2) are usually solved by numerical methods. However, they can also be reformed to a set of algebraic equations by applying some analytical techniques. Additionally, it is possible to solve the matrix equation obtained, by using standard matrix inversion algorithms. The time needed for the solution of this matrix equation is proportional to the size of the developed matrix. In the case of large bodies, the time required can be enormously large particularly for RCS estimation: Accordingly, the size of the matrix must be maintained as small as possible.

Emets and Rogowski [13] solved a two-dimensional problem of electromagnetic wave diffraction by a plane strip with different boundary conditions on its surfaces. The diffracted field was expressed by an integral in terms of the induced electric and magnetic current densities. The related boundary-value problem in the domain of the short-wavelength was occurred as a matrix Wiener-Hopf equation which was solved through the Khrapkov method. This analytical solution is a powerful tool to study the effects of a single strip under the incidence of plane waves. It can be used to validate the numerical methods.

Apaydin and Sevgi [3] studied on methods of moments (MoM) for modeling and simulation of scattered fields around infinite strip with one face soft and the other hard boundary conditions. Scattering cross-section was calculated numerically and compared with high-frequency asymptotics (HFA) models such as physical theory of diffraction (PTD) and theory of edge diffraction (TED). According to authors' knowledge, this method is the first application of MoM on the strip with one face soft and the other hard.

The H-polarized plane wave diffraction by a thin material strip has been solved using the Wiener-Hopf technique and approximate boundary conditions by Nagasaka and Kobayashi [34]. Employing a rigorous asymptotics, a high frequency solution for large strip width has been obtained. The numerical examples have been done on both the radar cross-section (RCS) and the far field scattering characteristics of the strip. Some of these examples have been compared with existing method and results agree reasonably well with existing method.

1.2. Comparison of Numerical-Analytical Methods

Commonly, the electrical size of the body restricts the tractability of numerical techniques, however, the geometrical complexity of the object restricts the applicability of the analytical methods. Furthermore, hybrid methods are used along with techniques based upon the extension of classical optics in order to obtain an asymptotic solution for problems regarding high region frequencies. Hybrid methods including both numerical and high frequency asymptotic techniques may have the ability to extend the class of electromagnetic scattering problems that can be handled.

The hybrid approach can be reformed as a field-based analysis where the GTD solution for the field associated with edge or surface diffraction are used as the initial point. These solutions function as the ansatz to the MoM formulation and represent the elements of a scatterer not meeting the requirements of a recognized geometry which is not cooperative with a GTD solution itself. (Burnside et.al. [7] and Sahalov and Thiele [41]). Alternatively, current-based formulation is possible in a situation such that the analysis proceeds from ansatz solutions for the currents obtained from physical optics and PTD (Thiele and Newhouse (1975), Ekelman and Thiele (1980) (from Medgyesi-Mitschang, L. N., 1989)) and Medgyesi-Mitschang and Wang (1983) (from Medgyesi-Mitschang, L. N., [29-30])). The option of a mixed field-current based approach also exists.

Generally, rigorous scattering theory, relies on the theory of boundary-value problems in which the progress is closely dependent, to mathematical branches. The main approach for the solution behind wave scattering is to reform the problem in terms of the integral equations satisfied by the unknown functions along with the current induced on the scatterer surface. Numerical techniques are utilized to shrink these integral equations to a system of linear algebraic equations. The presence of edges on the integration contour produce errors in current density calculations. In order to enhance the accuracy of the solution, some approaches accounting for the Meixner's edge condition in explicit form have been suggested by Shafai (1973) (from Veliev, I. E. [50]).

A similar technique was used by Butler [8] in which the analytical solution of the integral equation was obtained for the current induced on a confined conducting strip. In this solution the current mass was expressed as a product of a Chebyshev polynomial and a weighting operator which fulfill the edge condition and after specifying the Fourier type coefficients, the expression of far fields were obtained. So an integral equation which contains the current density and excitation was obtained as follows,

$$E_z^i(x) = -j \frac{k\eta}{2\pi} \left\{ \int_{-\infty}^{\infty} J_z(x') \ln|x-x'| dx' + (c + \ln \frac{k}{2}) \int_{-\infty}^{\infty} J_z(x') dx' \right\} \quad |x| \leq \omega \tag{1.3}$$

Where J_z is the unknown current density. $\eta = \sqrt{\mu/\epsilon}$ and $c = \gamma + j(\pi/2)$, ($c = 0.5772\dots$ is the Euler's constant). The solution for the current density was expressed as,

$$J_z(x) = [1 - (\frac{x}{\omega})^2]^{-1/2} \frac{f_0}{2} + \sum_{n=1}^{\infty} f_n T_n(\frac{x}{\omega}) \tag{1.4}$$

where $T_n(\cdot)$ denotes the Chebyshev polynomials of the first kind and f_n 's are the unknown coefficients. By using the orthogonality properties of the polynomials, the unknown coefficients and so the expression of the current density were obtained for both E and H-polarization cases.

A substitute technique was proposed by Veliev et al. [49-50] where the solution encompasses any preassigned accuracy. The distributed field was represented using the Fourier transform of the corresponding surface current density which offers a number of enhancements to overcome the problem. A hybrid technique based on the semi-inversion procedure for equation operators and the method of moments was used to yield the optimal solution. The essentials of the solution and its application to the wave scattering by polygonal cylinders and flat conducting strip structures are proposed by Veliev and Veremey [49]. The previous versions of this method were suggested by (Nomura and Katsura [36], Hongo [19] and Otsuki [37] (from Veliev, E. I. [49])) for completely conducting strip and slit configurations. This analytical-numerical method, which utilizes spectral approach, somehow solves the problem to a system of linear algebraic equations for the unknown Fourier coefficients of the current density function. Appropriate truncation of the infinite system of equations can obtain the results with any desired accuracy.

It should be realized that the applicability of the truncation method cannot always be modified, additionally, the matrix elements correlated with the system of linear algebraic equations usually collapse slowly with an increase of their index.

1.3. Aims and the Scope of the Study

Despite there are various powerful analytical techniques, the main influence of numerical techniques is that they may be applied to a scatterer of random shape and are generally only restricted by the size of the scatterer. But this limitation is a realistic problem. Apparently, a set of linear equations which denote the scattering issue can be generated but the obtained set may be too large to be solved. Fortunately, the developments in computer technology make the solution of many electromagnetic problems possible for a required degree of accuracy. In contrast, the asymptotic techniques work best when compared to the wavelength the scatterer size is large. However, the difficulty of the problem increases when the complex shaped bodies are of interest.

The use of analytical methods along with numerical methods may bypass these restrictions. The numerical methods are limited to the bodies having a maximum dimension of less than a few wavelengths, while the analytical methods produce accurate outcomes for the scatterer much larger than those of one wavelength. Thereby, these methods may be combined to overcome the scattering problems involving scatterers of intermediate size and size in the resonance region. Additionally by using analytical-numerical methods the computation time required may be decreased to an acceptable level.

In this study, diffraction by an impedance strip is researched by using the analytical-numerical technique proposed by Veliev and Veremey [50]. In Chapter 2, the formulation of the problem for H-polarized wave is given. By expressing the electric and magnetic currents as infinite series in terms of Gegenbauer polynomials, two integral equations in spectral domain for electric and

magnetic currents are derived. In Chapter 3, the integral equations are reduced to a system of linear algebraic equations for both currents with some unknown coefficients. In Chapter 4, some physical quantities are represented in terms of the unknown coefficients which will be denoted by solving the system of linear algebraic equations. In Chapter 5, the solution of branch-cut integrals are obtained and finally in Chapter 5, the curves for both currents, far field and RCS are represented. The results are reviewed and compared with some previously obtained results.

The aims of the current research are:

- 1 to employ a new analytical-numerical technique to solve a recognized diffraction problem that still does not have a proper solution,
- 2 to obtain an accurate solution for the impedance strip which can be used to simulate many practical obstacles,
- 3 to retrieve a solution which may work in a wide frequency range,
- 4 to set a base solution and write computer codes which may be used to analyze some complex structures that could be treated as a combination of multiple strips.

2. FORMULATION OF THE PROBLEM

The scatterer of the diffraction problem that will be formulated in this section is a strip of width $2a$ where the same impedance is assumed to be imposed on both sides. The geometry of the problem is illustrated in Figure 2.1 and η denotes the normalized impedance of the strip.

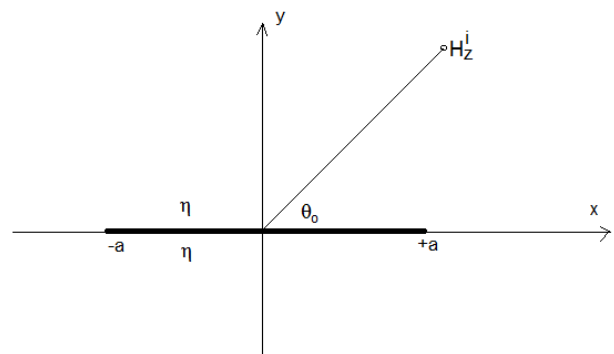


Figure 2.1. Geometry of the problem

Since the strip is uniform along the z -axis, the problem can be reduced to a two dimensional problem. The time dependence of the fields are assumed to be $\exp(-i\omega t)$ and suppressed throughout the analysis. The incident magnetic field is given as a linearly polarized plane wave

$$H_z^i(x, y) = e^{-ik(x\alpha_0 + y\sqrt{1-\alpha_0^2})} \quad (2.1)$$

where

$$\alpha_0 = \cos\theta_0. \quad (2.2)$$

The total field is

$$H_z(x, y) = H_z^i(x, y) + H_z^s(x, y) \quad (2.3)$$

where H_z^s is the scattered field.

On the strip, the total field must satisfy the Leontovich boundary condition which is frequently called as impedance boundary condition, given by,

$$\left\{ \frac{\partial H_z(x, y)}{\partial y} \pm ik\eta H_z(x, y) \right\} \Big|_{y=\pm 0} = 0. \quad (2.4)$$

So the total field can be expressed as [42]

$$H_z(x, y) = H_z^i(x, y) + \frac{1}{4} \int_{-a}^a \left\{ kY I_m(x') - iI_e(x') \frac{\partial}{\partial y} \right\} H_0^{(1)}(k\sqrt{(x-x')^2 + y^2}) dx \quad (2.5)$$

where I_m and I_e are the equivalent magnetic and electric current densities respectively. Expression of magnetic and electric current densities can be defined as follows respectively,

$$\bar{I}_e = \hat{a}_y \times [\bar{H}]^+ \quad (\bar{H} = H\hat{a}_z) \quad (2.6)$$

$$\bar{I}_e = \hat{a}_y \times [H_z(x, +0) - H_z(x, -0)] \Rightarrow \quad (2.7)$$

$$[H_z(x, +0) - H_z(x, -0)]\hat{a}_x = f_2(x)\hat{a}_x$$

and

$$\bar{I}_m = \hat{a}_y \times [\bar{E}]^+ \quad (2.8)$$

$$i\omega\epsilon_0\bar{E} = \nabla \times \bar{H} \quad \bar{E} = \frac{1}{i\omega\epsilon_0} \nabla \times \bar{H} \quad (2.9)$$

$$\bar{E} = \frac{1}{i\omega\epsilon_0} \begin{pmatrix} \hat{a}_x & \hat{a}_y & \hat{a}_z \\ \frac{\partial}{\partial x} & \frac{\partial}{\partial y} & \frac{\partial}{\partial z} \\ 0 & 0 & H_z \end{pmatrix} \quad (2.10)$$

$$\bar{E} = \frac{1}{i\omega\epsilon_0} \left\{ \frac{\partial H_z}{\partial y} \hat{a}_x - \frac{\partial H_z}{\partial x} \hat{a}_y \right\} \quad (2.11)$$

$$\bar{I}_m = \frac{1}{i\omega\epsilon_0} \left\{ \frac{\partial H_z}{\partial y} \hat{a}_x - \frac{\partial H_z}{\partial x} \hat{a}_y \right\} \times \hat{a}_y \quad (2.12)$$

$$\bar{I}_m = \frac{1}{i\omega\epsilon_0} \left\{ \frac{\partial H(x, +0)}{\partial y} - \frac{\partial H(x, -0)}{\partial y} \right\} \hat{a}_z \quad (2.13)$$

$$kY = \omega\sqrt{\epsilon_0\mu_0} \cdot \frac{1}{Z} = \frac{\omega\sqrt{\epsilon_0\mu_0}}{\sqrt{\frac{\mu_0}{\epsilon_0}}} = \omega\epsilon_0 \quad (2.14)$$

$$\begin{aligned} kY\bar{I}_m &= \cancel{\omega\epsilon_0} \left(\frac{1}{i\omega\epsilon_0} \left\{ \frac{\partial H(x, +0)}{\partial y} - \frac{\partial H(x, -0)}{\partial y} \right\} \right) \hat{a}_z \\ &= -i \left\{ \frac{\partial H(x, +0)}{\partial y} - \frac{\partial H(x, -0)}{\partial y} \right\} \\ &= -if_1(x)\hat{a}_z \end{aligned}$$

So Eq. 2.5 can be rearranged as

$$H_z(x, y) = H_z^i(x, y) - \frac{i}{4} \int_{-a}^{+a} \left\{ f_1(x') + f_2(x') \frac{\partial}{\partial y} \right\} H_0^{(1)}(k\sqrt{(x-x')^2 + y^2}) dx' \quad (2.16)$$

2.1. Application of Boundary Conditions

If we rewrite the Leontovich boundary condition for $y = +0$ and $y = -0$, and if we subtract and add these two equations we can obtain the following expressions:

$$\frac{\partial H_z(x, +0)}{\partial y} + ik\eta H_z(x, +0) = 0 \quad (2.17)$$

and

$$\frac{\partial H_z(x, -0)}{\partial y} - ik\eta H_z(x, -0) = 0 \quad (2.18)$$

The difference of Eq. (2.17) and Eq. (2.18) is

$$\begin{aligned} \frac{\partial H_z(x, +0)}{\partial y} - \frac{\partial H_z(x, -0)}{\partial y} + ik\eta \{H_z(x, +0) + H_z(x, -0)\} &= 0 \\ (2.19) \end{aligned}$$

And the sum is

$$\begin{aligned} \frac{\partial H_z(x, +0)}{\partial y} + \frac{\partial H_z(x, -0)}{\partial y} + ik\eta \{H_z(x, +0) - H_z(x, -0)\} &= 0 \\ (2.20) \end{aligned}$$

Using the expressions electric and magnetic current densities f_2 and f_1 in Eqs. (2.19) and (2.20)

$$f_1(x) + ik\eta \{H_z(x, +0) + H_z(x, -0)\} = 0 \quad (2.21)$$

$$\begin{aligned} f_2(x) + \frac{1}{ik\eta} \left\{ \frac{\partial H_z(x, +0)}{\partial y} + \frac{\partial H_z(x, -0)}{\partial y} \right\} &= 0 \\ (2.22) \end{aligned}$$

are derived.

The expressions of total field at $y = \pm 0$ can be obtained from Eqs. (2.3) and (2.16) as

$$\begin{aligned} H_z(x, +0) &= H_z^i(x, +0) \\ &- \lim_{y \rightarrow +0} \frac{i}{4} \int_{-a}^{+a} \left\{ f_1(x') + f_2(x') \frac{\partial}{\partial y} \right\} H_0^{(1)}(k|x-x'|) dx' \end{aligned} \quad (2.23)$$

and

$$\begin{aligned} H_z(x, -0) &= H_z^i(x, -0) \\ &- \lim_{y \rightarrow -0} \frac{i}{4} \int_{-a}^{+a} \left\{ f_1(x') + f_2(x') \frac{\partial}{\partial y} \right\} H_0^{(1)}(k|x-x'|) dx' \end{aligned} \quad (2.24)$$

$$H_0^{(1)}(k|x-x'|) dx' \quad (2.15)$$

In Eq.(2.20), we require the sum of these two expressions as

$$\begin{aligned}
 &H_z(x, +0) + H_z(x, -0) = \\
 &H_z^i(x, +0) + H_z^i(x, -0) \\
 &- \lim_{y \rightarrow +0} \frac{i}{4} \int_{-a}^{+a} \left\{ f_1(x') + f_2(x') \frac{\partial}{\partial y} \right\} H_0^{(1)}(k|x-x'|) dx' \quad (2.25) \\
 &- \lim_{y \rightarrow -0} \frac{i}{4} \int_{-a}^{+a} \left\{ f_1(x') + f_2(x') \frac{\partial}{\partial y} \right\} H_0^{(1)}(k|x-x'|) dx' .
 \end{aligned}$$

For the incident field we have that

$$\begin{aligned}
 H_z^i(x, 0) &= H_z^i(x, +0) = \\
 H_z^i(x, -0) &= e^{-ikx\alpha_0} \quad (2.26)
 \end{aligned}$$

and from Senior [42] we have that

$$(\lim_{y \rightarrow +0} + \lim_{y \rightarrow -0}) \int_{-a}^{+a} \left\{ f_2(x') \frac{\partial}{\partial y} \right\} H_0^{(1)}(k|x-x'|) dx' = 0 \quad (2.27)$$

and

$$\begin{aligned}
 &\lim_{y \rightarrow +0} \int_{-a}^{+a} f_1(x') H_0^{(1)}(k|x-x'|) dx' = \\
 &\lim_{y \rightarrow -0} \int_{-a}^{+a} f_1(x') H_0^{(1)}(k|x-x'|) dx' \quad (2.28) \\
 &= \int_{-a}^{+a} f_1(x') H_0^{(1)}(k|x-x'|) dx' .
 \end{aligned}$$

So by substituting Eq. (2.26) on Eq. (2.27) and Eq.(2.28) into Eq. (2.25) one can get that;

$$-\frac{1}{ik\eta} f_1(x) = 2H_z^i(x, 0) \quad (2.29)$$

$$-\frac{i}{2} \int_{-a}^{+a} f_1(x') H_0^{(1)}(k|x-x'|) dx'$$

or

$$\begin{aligned}
 &-\frac{1}{k\eta} f_1(x) = 2ie^{-ikx\alpha_0} \quad (2.30) \\
 &+ \frac{1}{2} \int_{-a}^{+a} f_1(x') H_0^{(1)}(k|x-x'|) dx'
 \end{aligned}$$

Eq. (2.30) is the integral equation for the magnetic current $f_1(x)$.

At this stage we will derive the integral equation for magnetic current in spectral domain using the integral representation of Hankel function given as;

$$H_0^{(1)}(k|x-x'|) = \frac{1}{\pi} \int_{-\infty}^{+\infty} \frac{e^{ik(x-x')t}}{\sqrt{1-t^2}} dt. \quad (2.31)$$

Using Eq. (2.31) in Eq. (2.30)

$$-\frac{1}{k\eta} f_1(x) = 2ie^{-ikx\alpha_0} + \frac{1}{2\pi} \int_{-a}^{+a} f_1(x') \int_{-\infty}^{+\infty} \frac{e^{ik(x-x')t}}{\sqrt{1-t^2}} dt dx' \quad (2.32)$$

and changing the order of integration

$$\begin{aligned}
 &-\frac{1}{k\eta} f_1(x) = 2ie^{-ikx\alpha_0} \\
 &+ \frac{1}{2\pi} \int_{-\infty}^{+\infty} \left\{ \int_{-a}^{+a} f_1(x') e^{-ikx't} dx' \right\} \frac{e^{ikxt}}{\sqrt{1-t^2}} dt \quad (2.33)
 \end{aligned}$$

is obtained. Where

$$F_1(t) = \int_{-a}^{+a} f_1(x') e^{-ikx't} dx' \quad (2.34)$$

is the Fourier transform of the magnetic current density $f_1(x)$. So

$$-\frac{1}{k\eta} f_1(x) = 2ie^{-ikx\alpha_0} \quad (2.35)$$

$$+ \frac{1}{2\pi} \int_{-\infty}^{+\infty} F_m(t) \frac{e^{ikxt}}{\sqrt{1-t^2}} dt$$

is derived.

The following variable changes are required to be able to express the current density functions in terms of Gegenbauer polynomials.

Since $-a \leq x \leq a$, if we use the variable change $x = a\zeta$, $x' = a\zeta'$, $\xi = ka$

$$F_1(t) = \int_{-1}^{+1} f_1(a\zeta') e^{-i(\xi/a)(a\zeta')} (ad\zeta') \quad (2.36)$$

$$F_1(t) = \int_{-1}^{+1} af_1(a\zeta') e^{-i\xi t \zeta'} d\zeta'$$

and let

$$\tilde{f}_1(\zeta') = af_1(a\zeta'). \quad (2.37)$$

So,

$$F_1(t) = \int_{-1}^{+1} \tilde{f}_1(\zeta') e^{-i\xi t \zeta'} d\zeta' \quad (2.38)$$

is obtained. Means that Eq. (2.35) can be arranged as;

$$-\frac{1}{\left(\frac{\xi}{a}\right)\eta} f_1(x) = 2ie^{-i\left(\frac{\xi}{a}\right)\alpha_0(a\zeta)} \quad (2.39)$$

$$+ \frac{1}{2\pi} \int_{-\infty}^{+\infty} F_m(t) \frac{e^{i\left(\frac{\xi}{a}\right)(a\zeta)t}}{\sqrt{1-t^2}} dt$$

or

$$-\frac{1}{\xi\eta} af_1(x) = 2ie^{-i\xi\alpha_0\zeta} \quad (2.40)$$

$$+ \frac{1}{2\pi} \int_{-\infty}^{+\infty} F_m(t) \frac{e^{i\xi t \zeta}}{\sqrt{1-t^2}} dt$$

and

$$-\frac{1}{\xi\eta} \tilde{f}_1(\zeta) = 2ie^{-i\xi\alpha_0\zeta} \quad (2.41)$$

$$+ \frac{1}{2\pi} \int_{-\infty}^{+\infty} F_m(t) \frac{e^{i\xi t \zeta}}{\sqrt{1-t^2}} dt.$$

If we multiply both side of the equation by $e^{-i\xi\beta\zeta}$ and integrate between -1 and $+1$

$$-\frac{1}{\xi\eta} \int_{-1}^{+1} \tilde{f}_1(\zeta) e^{-i\xi\beta\zeta} d\zeta = 2i \int_{-1}^{+1} e^{-i\xi\alpha_0\zeta} e^{-i\xi\beta\zeta} d\zeta \quad (2.42)$$

$$+ \frac{1}{2\pi} \int_{-1}^{+1} e^{-i\xi\beta\zeta} \int_{-\infty}^{+\infty} F_m(t) e^{i\xi t \zeta} \frac{dt}{\sqrt{1-t^2}} d\zeta$$

is derived. From Eq. (2.33) it is obvious that the form on the left hand side can be expressed as

$$F_m(\beta) = \int_{-1}^{+1} \tilde{f}_1(\zeta) e^{-i\xi\beta\zeta} d\zeta. \tag{2.43}$$

The first term on the right hand side is

$$\int_{-1}^{+1} e^{-i\xi\alpha_0\zeta} e^{-i\xi\beta\zeta} d\zeta = 2 \frac{\sin \xi(\beta + \alpha_0)}{\xi(\beta + \alpha_0)} \tag{2.44}$$

and the second term on the right hand side by changing the order of integration;

$$\begin{aligned} & \int_{-\infty}^{+\infty} \frac{F_m(t)}{\sqrt{1-t^2}} \int_{-1}^1 e^{i\xi(t-\beta)\zeta} d\zeta dt = \\ & \int_{-\infty}^{+\infty} \frac{F_m(t)}{\sqrt{1-t^2}} \left(\frac{e^{i\xi(t-\beta)\zeta}}{i(t-\beta)\xi} \right) \Big|_{-1}^1 dt \\ & = \frac{2}{\xi} \int_{-\infty}^{+\infty} \frac{F_m(t)}{\sqrt{1-t^2}} \frac{\sin \xi(t-\beta)}{(t-\beta)} dt \end{aligned} \tag{2.45}$$

is obtained. So Eq. (2.41) can be rearranged as

$$\begin{aligned} -\frac{1}{\xi\eta} F_m(\beta) &= 4i \frac{\sin \xi(\beta + \alpha_0)}{\xi(\beta + \alpha_0)} \\ &+ \frac{1}{\xi\pi} \int_{-\infty}^{+\infty} \frac{F_m(t)}{\sqrt{1-t^2}} \frac{\sin \xi(t-\beta)}{t-\beta} dt. \end{aligned} \tag{2.46}$$

This equation is the integral equation for the magnetic current density in spectral domain. In a similar way, the integral equation for the electric current density in spectral domain is obtained. This equation can be expressed as

$$\begin{aligned} F_e(\beta) &= \frac{4}{\eta} \sqrt{1-\alpha_0^2} \frac{\sin \xi(\beta + \alpha_0)}{\xi(\beta + \alpha_0)} \\ &- \frac{1}{\pi\eta} \int_{-\infty}^{+\infty} F_e(t) \sqrt{1-t^2} \frac{\sin \xi(t-\beta)}{t-\beta} dt \end{aligned} \tag{2.47}$$

3. REDUCTION OF LINEAR EQUATIONS TO THE SYSTEM OF LINEAR ALGEBRAIC EQUATIONS

In this section, the solution of the integral for electric $F_e(\beta)$ and magnetic $F_m(\beta)$ current densities will be reduced to the solution of two uncoupled system of linear algebraic equations. The first step of the reduction process is to express the current densities in Fourier transform domain and obtain a general spectral expression for currents. Then by using the constraints implied by edge conditions, electric and magnetic current density expressions will be obtained in transform domain. Finally, they will be written in the form of infinite system of linear algebraic equations involving Gegenbauer polynomial coefficients as unknowns.

3.1. General Expressions for the Current Density Functions in the Transform Domain

Since it is necessary to express the current functions in spectral domain, the Fourier transform $F(\beta)$ of the current density function $\tilde{f}(\zeta)$ must be found as

$$F(\beta) = \int_{-1}^{+1} \tilde{f}(\zeta) e^{-i\xi\beta\zeta} d\zeta. \tag{3.1}$$

The current density function $\tilde{f}(\zeta)$ is defined for $|\zeta| \leq 1$ and it is zero elsewhere. Let $\tilde{f}(\zeta)$ be represented by a uniformly convergent series, such as,

$$\tilde{f}(\zeta) = (1-\zeta^2)^\nu \sum_{n=0}^{\infty} f_n C_n^{\nu+\frac{1}{2}}(\zeta) \tag{3.2}$$

where $C_n^{\nu+\frac{1}{2}}(\zeta)$ denote the Gegenbauer polynomials and ν is a constant related to the edge condition. The value of ν in Eq. (3.2) will be determined by enforcing the functions such as to satisfy the edge conditions for electric and magnetic current densities separately.

For the electric current density function $\tilde{f}_e(\zeta)$, and the magnetic current density function $\tilde{f}_m(\zeta)$, from Meixner's (1972) edge conditions, ν can be determined for $\zeta \rightarrow 0$ as,

$$\tilde{f}_e(\zeta) = O(\zeta^{-1/2}) \text{ and } \tilde{f}_m(\zeta) = O(\zeta^{1/2}). \tag{3.3}$$

The order relations given above for electric and magnetic current densities can be obtained respectively as $\nu = -1/2$ and $\nu = 1/2$ by considering the asymptotic behavior of Gegenbauer polynomials together with Eq. (3.2). The integration in Eq. (3.1) is divided into two parts, as follows

$$F(\beta) = \int_{-1}^0 \tilde{f}(\zeta) e^{-i\xi\beta\zeta} d\zeta + \int_0^{+1} \tilde{f}(\zeta) e^{-i\xi\beta\zeta} d\zeta \tag{3.4}$$

By replacing ζ with $-\zeta$ and by changing the order of upper and lower limits in the first term on the right-hand-side, Eq. (3.4) will be written as:

$$F(\beta) = \int_0^1 \tilde{f}(-\zeta) e^{-i\xi\beta\zeta} d\zeta + \int_0^1 \tilde{f}(\zeta) e^{-i\xi\beta\zeta} d\zeta. \tag{3.5}$$

Now to determine $\tilde{f}(-\zeta)$ the following formula (Prodnikov, A. P., 1983, p. 732) will be used

$$C_n^\lambda(-z) = (-1)^n C_n^\lambda(z) \tag{3.6}$$

and, $\tilde{f}(-\zeta)$ can be expressed as:

$$\tilde{f}(-\zeta) = (1-\zeta^2)^\nu \sum_{n=0}^{\infty} (-1)^n f_n C_n^{\nu+\frac{1}{2}}(\zeta). \tag{3.7}$$

By substituting Eqs. (3.7) and (3.2) into Eq. (3.5),

$$\begin{aligned} F(\beta) &= \int_0^1 (1-\zeta^2)^\nu \sum_{n=0}^{\infty} f_n C_n^{\nu+\frac{1}{2}}(\zeta) \\ &\cdot \{ e^{-i\xi\beta\zeta} + (-1)^n e^{i\xi\beta\zeta} \} d\zeta \end{aligned} \tag{3.8}$$

is obtained. If n is even, i.e. $n = 2p$, then Eq. (3.8) takes the form of,

$$F_{ev}(\beta) = 2 \int_0^{+1} (1 - \zeta^2)^\nu \sum_{p=0}^{\infty} f_{2p} \cdot C_{2p}^{\nu+\frac{1}{2}}(\zeta) \left\{ \frac{e^{-i\xi\beta\zeta} + e^{i\xi\beta\zeta}}{2} \right\} d\zeta \quad (3.9)$$

or

$$F_{ev}(\beta) = 2 \int_0^{+1} (1 - \zeta^2)^\nu \sum_{p=0}^{\infty} f_{2p} \cdot C_{2p}^{\nu+\frac{1}{2}}(\zeta) \cos(\xi\beta\zeta) d\zeta. \quad (3.10)$$

By changing the order of integration and summation

$$F_{ev}(\beta) = 2 \sum_{p=0}^{\infty} f_{2p} K_{2p} \quad (3.11)$$

is written with

$$K_{2p} = \int_0^{+1} (1 - \zeta^2)^\nu C_{2p}^{\nu+\frac{1}{2}}(\zeta) \cos(\xi\beta\zeta) d\zeta. \quad (3.12)$$

On the other hand, if n is odd, i.e. $n = 2p+1$ then Eq. (3.8) takes the form of,

$$F_{od}(\beta) = \int_0^{+1} (1 - \zeta^2)^\nu \sum_{p=0}^{\infty} f_{2p+1} \cdot C_{2p+1}^{\nu+\frac{1}{2}}(\zeta) 2i \left\{ \frac{e^{-i\xi\beta\zeta} - e^{i\xi\beta\zeta}}{2i} \right\} d\zeta \quad (3.13)$$

or

$$F_{od}(\beta) = -2i \int_0^{+1} (1 - \zeta^2)^\nu \sum_{p=0}^{\infty} f_{2p+1} \cdot C_{2p+1}^{\nu+\frac{1}{2}}(\zeta) \sin(\xi\beta\zeta) d\zeta. \quad (3.14)$$

Again by changing the order of integration and summation, it yields

$$F_{od}(\beta) = -2i \sum_{p=0}^{\infty} f_{2p+1} K_{2p+1} \quad (3.15)$$

with

$$K_{2p+1} = \int_0^{+1} (1 - \zeta^2)^\nu C_{2p+1}^{\nu+\frac{1}{2}}(\zeta) \sin(\xi\beta\zeta) d\zeta. \quad (3.16)$$

It can easily be seen from Eq. (3.8) that,

$$F(\beta) = F_{ev}(\beta) + F_{od}(\beta) \quad (3.17)$$

Now, in order to express K_{2p} and K_{2p+1} in a form convenient for numerical calculations, the following expressions [38] are being used:

$$\int_0^1 (1 - x^2)^{\frac{z-1}{2}} C_{2n+1}^z(x) \sin(ax) dx = (-1)^n \pi \frac{\Gamma(2n+2z+1) J_{2n+2z+1}(a)}{(2n+1)! \Gamma(z) (2a)^z} \quad (3.18)$$

$$\int_0^1 (1 - x^2)^{\frac{z-1}{2}} C_{2n}^z(x) \cos(ax) dx = (-1)^n \pi \frac{\Gamma(2n+2z) J_{2n+2z}(a)}{(2n)! \Gamma(z) (2a)^z}. \quad (3.19)$$

As usual, $\Gamma(\cdot)$ denotes the Gamma functions and $J_n(\cdot)$ denotes the well-known Bessel function of the first kind.

In Eqs. (3.18) and (3.19), by setting $x = \zeta, z = \nu + \frac{1}{2}$

and $a = \xi\beta$, the followings can be written

$$K_{2p} = \int_0^{+1} (1 - \zeta^2)^\nu C_{2p}^{\nu+\frac{1}{2}}(\zeta) \cos(\xi\beta\zeta) d\zeta = \Gamma(2p+2\nu+1) J_{2p+\nu+\frac{1}{2}}(\xi\beta) (-1)^p \frac{\Gamma(\nu+\frac{1}{2})}{(2p)! \Gamma(\nu+\frac{1}{2}) (2\xi\beta)^{\nu+\frac{1}{2}}} \quad (3.20)$$

and

$$K_{2p+1} = \int_0^{+1} (1 - \zeta^2)^\nu C_{2p+1}^{\nu+\frac{1}{2}}(\zeta) \sin(\xi\beta\zeta) d\zeta = \Gamma(2p+2\nu+2) J_{2p+\nu+\frac{3}{2}}(\xi\beta) (-1)^p \pi \frac{\Gamma(\nu+\frac{1}{2})}{(2p+1)! \Gamma(\nu+\frac{1}{2}) (2\xi\beta)^{\nu+\frac{1}{2}}}. \quad (3.21)$$

From Eq. (3.11), Eq. (3.15) and Eq. (3.17) $F(\beta)$ is

$$F(\beta) = 2 \sum_{p=0}^{\infty} f_{2p} K_{2p} - 2i \sum_{p=0}^{\infty} f_{2p+1} K_{2p+1} \quad (3.22)$$

and from Eqs. (3.20) and (3.21), it can be written as

$$F(\beta) = 2 \sum_{p=0}^{\infty} f_{2p} (-1)^p \pi \frac{\Gamma(2p+2\nu+1)}{\Gamma(2p+1)} \frac{J_{\nu+\frac{1}{2}+2p}(\xi\beta)}{\Gamma(\nu+\frac{1}{2}) (2\xi\beta)^{\nu+\frac{1}{2}}} - 2i \sum_{p=0}^{\infty} f_{2p+1} (-1)^p \pi \frac{\Gamma(2p+2\nu+2)}{\Gamma(2p+2)} \frac{J_{\nu+\frac{3}{2}+2p}(\xi\beta)}{\Gamma(\nu+\frac{1}{2}) (2\xi\beta)^{\nu+\frac{1}{2}}} \quad (3.23)$$

or

$$F(\beta) = \frac{2\pi}{\Gamma(\nu+\frac{1}{2})} \sum_{p=0}^{\infty} (-1)^p \left\{ f_{2p} \frac{\Gamma(2p+2\nu+1)}{\Gamma(2p+1)} \frac{J_{\nu+\frac{1}{2}+2p}(\xi\beta)}{(2\xi\beta)^{\nu+\frac{1}{2}}} - i f_{2p+1} \frac{\Gamma(2p+2\nu+2)}{\Gamma(2p+2)} \frac{J_{\nu+\frac{3}{2}+2p}(\xi\beta)}{(2\xi\beta)^{\nu+\frac{1}{2}}} \right\}. \quad (3.24)$$

By rearranging the last equation, the Fourier transform of the current density function can be obtained as follows:

$$F(\beta) = \frac{2\pi}{\Gamma(\nu + \frac{1}{2})} \sum_{n=0}^{\infty} (-i)^n f_n \tag{3.25}$$

$$\frac{\Gamma(n+2\nu+1)}{\Gamma(n+1)} \frac{J_{n+\nu+\frac{1}{2}}(\xi\beta)}{(2\xi\beta)^{\nu+\frac{1}{2}}}$$

This completes the calculation for the Fourier transform of a current element represented in terms of Gegenbauer polynomials given by Eq. (3.2). Since no restriction is imposed on the current series expression during the derivation, it is obvious that this representation is valid for both electric and magnetic currents.

Now considering the edge conditions separately for electric and magnetic current components, the corresponding spectral expressions in the Fourier domain can easily be obtained. First, the magnetic current density will be obtained simply by substituting $\nu = 1/2$ which yields

$$F_m(\beta) = \pi \sum_{n=0}^{\infty} (-i)^n (n+1) f_n^m \frac{J_{n+1}}{\xi\beta} \tag{3.26}$$

Similarly, by inserting $\nu = -1/2$ in Eq. (3.25) it is possible to obtain the Fourier transform of the electric current density. But, it is obviously seen that due to the presence of $[\Gamma(\nu+1/2)]^{-1}$ term in the expression, the current density will have a singularity in this case. Therefore, in order to remove this singularity the series expansion given by Eq. (3.2) will be used for $\nu = -1/2$:

$$\tilde{f}_e(\zeta) = (1-\zeta^2)^{-\frac{1}{2}} \sum_{n=0}^{\infty} f_n^e C_n^0(\zeta) \tag{3.27}$$

In [38] it is given that,

$$C_n^0(\zeta) = \frac{2}{n} T_n(\zeta) \tag{3.28}$$

where $T_n(\cdot)$ denotes the well-known Chebyshev polynomials which is valid for $n \neq 0$; therefore, Eq. (3.27) can be written as,

$$\tilde{f}_e(\zeta) = (1-\zeta^2)^{-\frac{1}{2}} \sum_{n=0}^{\infty} f_n^e \frac{2}{n} T_n(\zeta) \tag{3.29}$$

From Eq. (3.1), the Fourier transform of $\tilde{f}(\zeta)$ for $\nu = -\frac{1}{2}$ is,

$$F_e(\beta) = \int_{-1}^{+1} (1-\zeta^2)^{-\frac{1}{2}} \sum_{n=1}^{\infty} f_n^e \frac{2}{n} T_n(\zeta) e^{-i\xi\beta\zeta} d\zeta \tag{3.30}$$

or

$$F_e(\beta) = \sum_{n=1}^{\infty} \frac{2}{n} f_n^e \int_{-1}^{+1} (1-\zeta^2)^{-\frac{1}{2}} T_n(\zeta) e^{-i\xi\beta\zeta} d\zeta \tag{3.31}$$

The following equality is given for $n \neq 0$ in [38]

$$\int_{-a}^a \frac{1}{\sqrt{a^2-x^2}} T_n\left(\frac{x}{a}\right) e^{ipx} dx = i^n \pi J_n(ap) \tag{3.32}$$

so the integral in Eq. (3.31) can be calculated as,

$$\int_{-1}^{+1} (1-\zeta^2)^{-\frac{1}{2}} T_n(\zeta) e^{-i\xi\beta\zeta} d\zeta = \pi (-i)^n J_n(\xi\beta) \tag{3.33}$$

and by substituting Eq. (3.33) into Eq. (3.31),

$$F_e(\beta) = \pi \sum_{n=1}^{\infty} (-i)^n \frac{2}{n} f_n^e J_n(\xi\beta) \tag{3.34}$$

is obtained.

Now, in order to calculate the contribution for $n = 0$, let the analysis start with the series expansion for the Fourier transform of the current given by Eq. (3.25):

$$F(\beta) = \frac{2\pi}{\Gamma(\nu + \frac{1}{2})} \sum_{n=0}^{\infty} (-i)^n f_n$$

$$\frac{\Gamma(n+2\nu+1)}{\Gamma(n+1)} \frac{J_{n+\nu+\frac{1}{2}}(\xi\beta)}{(2\xi\beta)^{\nu+\frac{1}{2}}}$$

The term $\Gamma(n+2\nu+1)$ can be written in a more convenient form:

$$\Gamma(n+2\nu+1) = \Gamma(n+2(\nu+\frac{1}{2})) \tag{3.35}$$

which gives (Prudnikov, A. P., 1983, p. 720)

$$\Gamma(n+2\nu+1) = (2(\nu+\frac{1}{2}))_n \Gamma(2(\nu+\frac{1}{2})) \tag{3.36}$$

where $(\cdot)_n$ denotes that

$$(2(\nu+\frac{1}{2}))_n = \frac{\Gamma(n+2\nu+1)}{\Gamma(2\nu+1)} \tag{3.37}$$

The following identify [38]

$$\Gamma(2z) = \frac{2^{2z-1}}{\sqrt{\pi}} \Gamma(z) \Gamma(z+\frac{1}{2}) \tag{3.38}$$

is used with Eq. (3.36) and

$$\Gamma(n+2\nu+1) = (2(\nu+\frac{1}{2}))_n \Gamma(\nu+\frac{1}{2}) \tag{3.39}$$

$$\Gamma(\nu+1) \frac{2^{2(\nu+\frac{1}{2})-1}}{\sqrt{\pi}}$$

is obtained. By substituting Eq. (3.39) into Eq. (3.25) and considering that $n = 0$ with $\nu = -1/2$ for the electric current

$$F_e(\beta) \Big|_{n=0} = \pi f_0^e J_0(\xi\beta) \tag{3.40}$$

is derived. Here, the following equality is being taken into account

$$\Gamma(n+2\nu+1) \Big|_{n=0} = \Gamma(\nu+\frac{1}{2}) \tag{3.41}$$

$$\Gamma(\nu+1) \frac{2^{2(\nu+\frac{1}{2})-1}}{\sqrt{\pi}}$$

and the analysis gives the complete expression for the electric current density

$$F_e(\beta) = \pi f_0^e J_0(\xi\beta) + 2\pi \sum_{n=1}^{\infty} \frac{f_n^e}{n} (-i)^n J_n(\xi\beta) \tag{3.42}$$

for any value of n .

3.2. System of Linear Algebraic Equations for f_n^e

In the previous section, the Fourier transform of $\tilde{f}_e(\zeta)$ for $\nu = -\frac{1}{2}$ was obtained as

$$F_e(\beta) = \pi \sum_{n=0}^{\infty} X_n J_n(\xi\beta) \tag{3.43}$$

where

$$X_n = f_0^e \quad \text{for } n = 0 \tag{3.44}$$

and

$$X_n = 2(-i)^n \frac{f_n^e}{n} \quad \text{for } n \neq 0. \tag{3.45}$$

If Eq. (3.43) is substituted into Eq. (2.47), the problem is reduced to that of finding the unknowns f_n^e with $n = 0, 1, 2, \dots$ as follows:

$$\eta\pi \sum_{n=0}^{\infty} X_n J_n(\xi\beta) = 4\sqrt{1-\cos^2\theta_0} \frac{\sin \xi(\beta + \cos \theta_0)}{\xi(\beta + \cos \theta_0)} - \frac{1}{\pi} \int_{-\infty}^{\infty} \frac{\sqrt{1-t^2} \sin \xi(t-\beta)}{t-\beta} \left\{ \pi \sum_{n=0}^{\infty} X_n J_n(\xi t) \right\} dt. \tag{3.46}$$

By rearranging Eq. (3.46)

$$\eta\pi \sum_{n=0}^{\infty} X_n J_n(\xi\beta) = +4\sqrt{1-\cos^2\theta_0} \frac{\sin \xi(\beta + \cos \theta_0)}{\xi(\beta + \cos \theta_0)} - \sum_{n=0}^{\infty} X_n \int_{-\infty}^{\infty} \frac{\sqrt{1-t^2} \sin \xi(t-\beta)}{t-\beta} J_n(\xi t) dt \tag{3.47}$$

is obtained. In order to be able to express Eq. (3.47) in a more convenient form for numerical calculations, both sides of the equations will be multiplied by

$$\frac{J_{l+\tau}(\xi\beta)}{\beta^\tau} \quad \text{for } l = 0, 1, 2, \dots$$

and by integrating each term with respect to β from $-\infty$ to ∞

$$\eta\pi \int_{-\infty}^{\infty} \frac{J_{l+\tau}(\xi\beta)}{\beta^\tau} \sum_{n=0}^{\infty} X_n J_n(\xi\beta) d\beta = 4 \int_{-\infty}^{\infty} \sqrt{1-\cos^2\theta_0} \frac{\sin \xi(\beta + \cos \theta_0)}{\xi(\beta + \cos \theta_0)} \frac{J_{l+\tau}(\xi\beta)}{\beta^\tau} d\beta - \int_{-\infty}^{\infty} \frac{J_{l+\tau}(\xi\beta)}{\beta^\tau} \sum_{n=0}^{\infty} X_n \int_{-\infty}^{\infty} \frac{\sqrt{1-t^2} \sin \xi(t-\beta)}{t-\beta} J_n(\xi t) dt d\beta \tag{3.48}$$

is written. If Eq. **Pogreška! Izvor reference nije pronađen.** is rearranged by changing the order of integration and summation, it yields

$$\eta\pi \sum_{n=0}^{\infty} X_n \int_{-\infty}^{\infty} \frac{J_{l+\tau}(\xi\beta) J_n(\xi\beta)}{\beta^\tau} d\beta = 4 \int_{-\infty}^{\infty} \frac{\sqrt{1-\cos^2\theta_0}}{\xi} \frac{\sin \xi(\beta + \cos \theta_0)}{\beta + \cos \theta_0} \frac{J_{l+\tau}(\xi\beta)}{\beta^\tau} d\beta - \sum_{n=0}^{\infty} X_n \int_{-\infty}^{\infty} \frac{\sqrt{1-t^2} J_n(\xi t)}{t-\beta} \left\{ \int_{-\infty}^{\infty} \frac{\sin \xi(t-\beta)}{t-\beta} \frac{J_{l+\tau}(\xi\beta)}{\beta^\tau} d\beta \right\} dt. \tag{3.49}$$

The integrals in the first and second terms on the right-hand side of Eq. (3.49) can be calculated as follows from the equality given in [38]:

$$\frac{1}{\pi} \int_{-\infty}^{\infty} \frac{J_{l+\tau}(\xi\beta)}{\beta^\tau} \frac{\sin \xi(t-\beta)}{t-\beta} d\beta = \frac{J_{l+\tau}(\xi t)}{t^\tau}. \tag{3.50}$$

This equality will give the value of the first integral on the right-hand side of Eq. (3.49) by setting $t = -\cos \theta_0$ which yields

$$\frac{1}{\pi} \int_{-\infty}^{\infty} \frac{J_{l+\tau}(\xi\beta)}{\beta^\tau} \frac{\sin \xi(\beta + \cos \theta_0)}{\beta + \cos \theta_0} d\beta = \frac{J_{l+\tau}(-\xi \cos \theta_0)}{(-\cos \theta_0)^\tau}. \tag{3.51}$$

By using the series representation of Bessel functions, the negative argument functions can be expressed as follows in terms of Bessel functions with positive arguments:

$$\frac{1}{\pi} \int_{-\infty}^{\infty} \frac{J_{l+\tau}(\xi\beta)}{\beta^\tau} \frac{\sin \xi(\beta + \cos \theta_0)}{\beta + \cos \theta_0} d\beta = (-1)^l \frac{J_{l+\tau}(\xi \cos \theta_0)}{\cos^\tau \theta_0}. \tag{3.52}$$

Now, substitution of Eq. (3.50), Eq. (3.51) into Eq. (3.49) yields that,

$$\eta \sum_{n=0}^{\infty} X_n \int_{-\infty}^{\infty} \frac{J_{l+\tau}(\xi\beta) J_n(\xi\beta)}{\beta^\tau} d\beta = \frac{4\sqrt{1-\cos^2\theta_0}}{\xi} (-1)^l \frac{J_{l+\tau}(\xi \cos \theta_0)}{\cos^\tau \theta_0} - \sum_{n=0}^{\infty} X_n \int_{-\infty}^{\infty} \frac{J_{l+\tau}(\xi t)}{t^\tau} J_n(\xi t) \sqrt{1-t^2} dt. \tag{3.53}$$

The integral on the left-hand side of Eq. (3.53) is denoted as

$$d_{\ln}^{E1} = \int_{-\infty}^{\infty} \frac{J_{l+\tau}(\xi\beta) J_n(\xi\beta)}{\beta^\tau} d\beta \tag{3.54}$$

and the integral on the right hand side is named as

$$D_{\ln}^{E1} = \int_{-\infty}^{\infty} \frac{J_{l+\tau}(\xi t) J_n(\xi t)}{t^\tau} \sqrt{1-t^2} dt \tag{3.55}$$

So, by substituting these two equations into Eq. (3.53)

$$\eta \sum_{n=0}^{\infty} X_n d_{\ln}^{E1} = \lambda^{E1} - \sum_{n=0}^{\infty} X_n D_{\ln}^{E1} \tag{3.56}$$

is obtained with

$$\lambda^{E1} = -\frac{4\sqrt{1-\cos^2\theta_0}}{\xi} (-1)^l \frac{J_{l+\tau}(\xi \cos \theta_0)}{\cos^\tau \theta_0}. \tag{3.57}$$

Now Eq. (3.56) can be arranged simply as

$$\tilde{\lambda}^{E1} = \sum_{n=0}^{\infty} X_n (\eta d_{ln}^{E1} + D_{ln}^{E1}) \tag{3.58}$$

which gives an infinite system of linear algebraic equations for f_n^e . The details of the numerical computation will be shown in the following sections which requires to manipulate analytically the integral seen above.

3.3. System of Linear Algebraic Equations for f_n^m

In the previous section, the Fourier transform of

$\tilde{f}_m(\zeta)$ for $\nu = \frac{1}{2}$ was obtained as,

$$F_m(\beta) = \pi \sum_{n=0}^{\infty} Y_n \frac{J_{n+1}(\xi\beta)}{\xi\beta} \tag{3.59}$$

where

$$Y_n = (-i)^n (n+1) f_n^m. \tag{3.60}$$

If this equation is substituted into Eq. (2.46)

$$-\frac{1}{\xi\eta} \pi \sum_{n=0}^{\infty} Y_n \frac{J_{n+1}(\xi\beta)}{\xi\beta} = 4i \frac{\sin \xi(\beta + \cos \theta_0)}{\xi(\beta + \cos \theta_0)} \tag{3.61}$$

$$+ \frac{1}{\xi\pi} \int_{-\infty}^{\infty} \frac{\sin \xi(t-\beta)}{(t-\beta)\sqrt{1-t^2}} \left\{ \pi \sum_{n=0}^{\infty} Y_n \frac{J_{n+1}(\xi t)}{\xi t} \right\} dt$$

is obtained. By changing the order of integration and summation and by rearranging the equation

$$-\frac{\pi}{\eta} \sum_{n=0}^{\infty} Y_n \frac{J_{n+1}(\xi\beta)}{\xi\beta} = 4i \frac{\sin \xi(\beta + \cos \theta_0)}{(\beta + \cos \theta_0)} \tag{3.62}$$

$$+ \sum_{n=0}^{\infty} Y_n \left\{ \int_{-\infty}^{\infty} \frac{\sin \xi(t-\beta)}{(t-\beta)\sqrt{1-t^2}} \frac{J_{n+1}(\xi t)}{\xi t} dt \right\}$$

is written. By multiplying both sides of Eq. (3.62) by $\beta^{-1} J_{l+1}(\xi\beta)$ and integrating each term with respect to β from $-\infty$ to ∞

$$-\frac{\pi}{\eta} \int_{-\infty}^{\infty} \left\{ \frac{J_{l+1}(\xi\beta)}{\beta} \sum_{n=0}^{\infty} Y_n \frac{J_{n+1}(\xi\beta)}{\xi\beta} \right\} d\beta = \tag{3.63}$$

$$4i \int_{-\infty}^{\infty} \frac{\sin \xi(\beta + \cos \theta_0)}{(\beta + \cos \theta_0)} \frac{J_{l+1}(\xi\beta)}{\beta} d\beta$$

$$+ \int_{-\infty}^{\infty} \frac{J_{l+1}(\xi\beta)}{\beta} \sum_{n=0}^{\infty} Y_n \left\{ \int_{-\infty}^{\infty} \frac{\sin \xi(t-\beta)}{(t-\beta)\sqrt{1-t^2}} \frac{J_{n+1}(\xi t)}{\xi t} dt \right\} d\beta$$

is found. Or

$$-\frac{\pi}{\eta} \sum_{n=0}^{\infty} Y_n \int_{-\infty}^{\infty} \frac{1}{\xi} \frac{1}{\beta^2} J_{l+1}(\xi\beta) J_{n+1}(\xi\beta) d\beta = \tag{3.64}$$

$$4i \int_{-\infty}^{\infty} \frac{\sin \xi(\beta + \cos \theta_0)}{(\beta + \cos \theta_0)} \frac{J_{l+1}(\xi\beta)}{\beta} d\beta$$

$$+ \sum_{n=0}^{\infty} Y_n \int_{-\infty}^{\infty} \left\{ \frac{J_{n+1}(\xi t)}{\xi t} \frac{1}{\sqrt{1-t^2}} \int_{-\infty}^{\infty} \frac{\sin \xi(t-\beta)}{(t-\beta)} \frac{J_{l+1}(\xi\beta)}{\beta} d\beta \right\} dt.$$

Each term in Eq. (3.64) will be written later in a form more convenient for numerical calculations. For using similar notations with the previous section

$$d_{ln}^{E2} = \int_{-\infty}^{\infty} \frac{J_{n+1}(\xi\beta) J_{l+1}(\xi\beta)}{\beta^2} d\beta \tag{3.65}$$

is written. Now to evaluate the integral on the right-hand side of Eq.(3.64), Eq. (3.50) is used with $\tau=1$, and $t = -\cos \theta_0$ which gives

$$\frac{1}{\pi} \int_{-\infty}^{\infty} \frac{J_{l+1}(\xi\beta)}{\beta} \frac{\sin \xi(\beta + \cos \theta_0)}{\beta + \cos \theta_0} d\beta = \frac{J_{l+1}(-\xi \cos \theta_0)}{-\cos \theta_0}. \tag{3.66}$$

By substituting, Eq. (3.66) into Eq. (3.64)

$$-\frac{\pi}{\eta \xi} \sum_{n=0}^{\infty} d_{ln}^{E2} Y_n = 4i \frac{J_{l+1}(-\xi \cos \theta_0)}{-\cos \theta_0} \pi \tag{3.67}$$

$$+ \sum_{n=0}^{\infty} Y_n \int_{-\infty}^{\infty} \frac{J_{n+1}(\xi t) J_{l+1}(\xi t) \pi}{\xi t \sqrt{1-t^2} t} dt$$

is obtained, or

$$-\frac{1}{\eta} \sum_{n=0}^{\infty} d_{ln}^{E2} Y_n = \tilde{\lambda}^{E2} + \sum_{n=0}^{\infty} Y_n D_{ln}^{E2} \tag{3.68}$$

is written, where

$$D_{ln}^{E2} = \int_{-\infty}^{\infty} J_{n+1}(\xi t) J_{l+1}(\xi t) \frac{1}{t^2 \sqrt{1-t^2}} dt \tag{3.69}$$

$$\tilde{\lambda}^{E2} = 4i(-1)^l \xi \frac{J_{l+1}(\xi \cos \theta_0)}{\cos \theta_0}. \tag{3.70}$$

Finally, Eq. (3.68) can be expressed as,

$$-\tilde{\lambda}^{E2} = \sum_{n=0}^{\infty} Y_n \left(\frac{1}{\eta} d_{ln}^{E2} + D_{ln}^{E2} \right) \tag{3.71}$$

which is the system of linear algebraic equations for f_n^m

4. FIELD ANALYSIS

The total field expression Eq. (2.16) involving the electric and magnetic current densities as unknowns is the fundamental formula for field analysis. In the present section, first the field analysis will be presented in a formal way by assuming that the current densities are known. Then, the steps for numerical determination of the unknowns will be given.

4.1. Scattered Far Field and Total Scattering Cross Section

As stated in Eq. (2.5), the scattered field expression was given as

$$H_z(x, y) = H_z^i(x, y) + \frac{1}{4} \int_{-a}^a \left\{ k Y I_m(x') - i I_e(x') \frac{\partial}{\partial y} \right\}.$$

$$H_0^{(1)} \left(k \sqrt{(x-x')^2 + y^2} \right) dx.$$

In order to obtain the scattered far field, the first step is to substitute the asymptotic expression of Hankel for large argument. Which is given as [5, p.337]

$$H_n^{(1)}(z) \approx \sqrt{\frac{2}{\pi z}} e^{i(z - \frac{2n+1}{4}\pi)}. \tag{4.1}$$

Using

$$x = r \cos \varphi, \quad y = r \sin \varphi \quad (4.2)$$

in the following expression which is a part of the argument of the Hankel function:

$$\begin{aligned} (x-x')^2 + y^2 &= r^2 \cos^2 \varphi - 2rx' \cos \varphi + x'^2 + r^2 \sin^2 \varphi \\ &= r^2 - 2rx' \cos \varphi + x'^2 \end{aligned} \quad (4.3)$$

or

$$(x-x')^2 + y^2 = r^2 \left(1 - 2 \frac{x'}{r} \cos \varphi + \left(\frac{x'}{r}\right)^2\right),$$

is written. Then, by inserting it into the argument

$$k\sqrt{(x-x')^2 + y^2} = kr \sqrt{1 - 2 \frac{x'}{r} \cos \varphi + \left(\frac{x'}{r}\right)^2} \quad (4.4)$$

$$= kr \sqrt{1 - 2 \frac{kx'}{kr} \cos \varphi + \left(\frac{kx'}{kr}\right)^2}$$

and by using the binomial expansion formula

$$k\sqrt{(x-x')^2 + y^2} = kr \left\{1 - \frac{kx'}{kr} \cos \varphi + O\left(\frac{1}{(kr)^2}\right)\right\} \quad (4.5)$$

$$= kr \left(1 - \frac{x'}{r} \cos \varphi\right) + O\left(\frac{1}{kr}\right).$$

is obtained. So as $kr \rightarrow \infty$ Eq. (3.2) can be expressed as,

$$H_0^{(1)}(k\sqrt{(x-x')^2 + y^2}) \approx H_0^{(1)}\left(kr\left(1 - \frac{x'}{r} \cos \varphi\right)\right) \quad (4.6)$$

$$= \sqrt{\frac{2}{\pi kr}} \left(1 - \frac{x'}{r} \cos \varphi\right)^{-\frac{1}{2}} e^{i\left\{kr\left(1 - \frac{x'}{r} \cos \varphi\right) - \frac{\pi}{4}\right\}} \left\{1 + O\left(\frac{1}{kr}\right)\right\}$$

and by rearranging simply

$$\begin{aligned} H_0^{(1)}(k\sqrt{(x-x')^2 + y^2}) &= \\ &= \sqrt{\frac{2}{i\pi kr}} e^{i(kr(1 - \frac{x'}{r} \cos \varphi))} \left\{1 + O\left(\frac{1}{kr}\right)\right\} \end{aligned} \quad (4.7)$$

is written. If Eq. (4.7) is substituted into the equation of scattered field the following is obtained

$$\begin{aligned} H_z^s(x, y) &= H_z^s(r, \varphi) = \\ &= -\frac{i}{4} \sqrt{\frac{2}{i\pi kr}} e^{ikr} \int_{-a}^{+a} \left\{f_1(x') + f_2(x') \frac{\partial}{\partial y}\right\} e^{-ikx' \cos \varphi} dx'. \end{aligned} \quad (4.8)$$

The following of the partial derivative in polar coordinates

$$\frac{\partial}{\partial y} = \frac{\partial r}{\partial y} \frac{\partial}{\partial r} + \frac{\partial \varphi}{\partial y} \frac{\partial}{\partial \varphi} \quad (4.9)$$

with Eq. (4.2)

$$\frac{\partial}{\partial y} = \sin \varphi \frac{\partial}{\partial r} + \frac{\cos \varphi}{r} \frac{\partial}{\partial \varphi} \quad (4.10)$$

and considering for large r , the second term on the right-hand side is obviously zero. So, Eq. (4.8) can be written as

$$H_z^s(r, \varphi) = -\frac{i}{4} \sqrt{\frac{2}{i\pi kr}} e^{ikr} \quad (4.11)$$

$$\cdot \int_{-1}^{+1} \left\{ \tilde{f}_1(\zeta') + \frac{\xi \sin \varphi}{4} \tilde{f}_2(\zeta') \right\} e^{-i\xi \zeta' \cos \varphi} d\zeta'.$$

Then, let the scattered field be expressed as

$$H_z^s(r, \varphi) = A(kr) \phi(\varphi) \quad (4.12)$$

where,

$$A(kr) = \sqrt{\frac{2}{\pi kr}} e^{i(kr - \frac{\pi}{4})} \quad (4.13)$$

and,

$$\phi(\varphi) = \phi_e(\varphi) + \phi_m(\varphi). \quad (4.14)$$

In this case $\phi(\varphi)$ represents the far field radiation pattern. The integrals in Eq. (4.11) are the Fourier transforms of the current density functions. By using Eq. (3.43) and Eq. (3.59) the $\phi_e(\varphi)$ and $\phi_m(\varphi)$ can be obtained as follows:

$$\phi_e(\varphi) = \frac{\pi}{4} \sum_{n=0}^{\infty} X_n J_n(\xi \cos \varphi) \quad (4.15)$$

and,

$$\phi_m(\varphi) = \frac{\xi \sin \varphi}{4} \pi \sum_{n=0}^{\infty} Y_n \frac{J_{n+1}(\xi \cos \varphi)}{\xi \cos \varphi}. \quad (4.16)$$

As known the total scattering cross section can be calculated as [5, p.102],

$$\frac{\sigma_s}{4a} = -\frac{1}{\xi} \operatorname{Re}\{\phi(\theta)\} \quad (4.17)$$

where θ is the incident angle. It is obvious that the calculation of the RCS requires to know the values of X_n and Y_n . From the analysis accomplished in the previous sections, it should be clear that the determination of X_n and Y_n is reduced to numerical evaluation of

$$D_{\ln}^{E1}, D_{\ln}^{E2}, d_{\ln}^{E1} \text{ and } d_{\ln}^{E2}.$$

5. NUMERICAL ANALYSIS

As shown in the previous section the analysis of the scattered field is reduced to the numerical evaluation of the functions $d_{\ln}^{E1,2}$ and $D_{\ln}^{E1,2}$. The integral expressions of these terms given by equations Eq. (3.54), Eq. (3.55), Eq. (3.65), and Eq. (3.69) are not convenient for numerical calculations. Therefore by using some analytical methods these integrals are evaluated as follows:

$$d_{\ln}^{E1} = \frac{1}{\xi} \left(\frac{\xi}{2}\right)^{\tau}. \quad (5.1)$$

$$\frac{\left[1 + (-1)^{l+n}\right] \Gamma(\tau) \Gamma\left(\frac{n+l+1}{2}\right)}{\Gamma\left(\frac{n-l+1}{2}\right) \Gamma\left(\frac{l-n+1+2\tau}{2}\right) \Gamma\left(\frac{n+l+2\tau+1}{2}\right)}$$

$$d_{ln}^{E_2} = \frac{8\xi(-1)^{\frac{n-l}{2}}}{\pi(n+l+3)(n+l+1)\{1-(n-l)^2\}} \tag{5.2}$$

$$D_{ln}^{E_1} = \left\{ 1 + (-1)^{l+n} \right\} \left\{ \frac{\xi^{l+n+\lambda+\tau}}{4} \sum_{k=0}^{\infty} h_{kln}^{\lambda,\tau} \xi^{2k} \frac{\Gamma\left(k + \frac{l+n+1}{2}\right)}{\Gamma\left(k + \frac{l+n}{2} + 2\right)} \right\}$$

$$i \left\{ \sum_{k=1}^{\frac{l+n}{2}} \frac{1}{4\pi} \frac{\Gamma\left(-k + \frac{l+n}{2}\right) \Gamma\left(k + \frac{1}{2}\right) \Gamma\left(k + \frac{\lambda+\tau+1}{2}\right)}{\Gamma(k+2) \Gamma\left(k - \frac{l+n}{2} + l + \tau + 1\right)} \right.$$

$$\left. \frac{\Gamma\left(k + \frac{\lambda+\tau}{2} + 1\right)}{\Gamma\left(k + \frac{l+n}{2} + \lambda + \tau + 1\right) \Gamma\left(k - \frac{l+n}{2} + n + \lambda + 1\right)} e^{2k+\lambda+\tau} \right.$$

$$\left. - \sum_{k=0}^{\infty} \frac{1}{4\pi} \frac{\Gamma\left(k + \frac{l+n+1}{2}\right)}{\Gamma\left(k + \frac{l+n}{2} + 2\right)} h_{kln}^{\lambda,\tau} e^{2k+l+n+\lambda+\tau} \times \left\{ 2 \ln \xi + \psi\left(k + \frac{l+n+1}{2}\right) \right. \right.$$

$$\left. + \psi\left(k + \frac{l+n+\lambda+\tau+1}{2}\right) + \psi\left(k + \frac{l+n+\lambda+\tau}{2} + 1\right) - \psi(k+1) \right.$$

$$\left. - \psi\left(k + \frac{l+n}{2} + 2\right) - \psi(k+l+\tau+1) \right.$$

$$\left. - \psi(k+n+\lambda+1) - \psi(k+l+n+\lambda+\tau+1) \right\} \tag{5.3}$$

$$D_{ln}^{E_2} = \left\{ 1 + (-1)^{l+n} \right\} \left\{ R_{ln1}^{E_2}(\tau, \lambda) = \right.$$

$$\left. \frac{\xi^{l+n+\lambda+\tau}}{2} \sum_{k=0}^{\infty} h_{kln}^{\lambda,\tau} \xi^{2k} \frac{\Gamma\left(k + \frac{l+n+1}{2}\right)}{\Gamma\left(k + \frac{l+n}{2} + 1\right)} \right\}$$

$$- i \left\{ \sum_{k=0}^{\frac{l+n}{2}-1} \frac{1}{2\pi} \frac{\Gamma\left(-k + \frac{l+n}{2}\right) \Gamma\left(k + \frac{1}{2}\right) \Gamma\left(k + \frac{\lambda+\tau+1}{2}\right)}{\Gamma(k+1) \Gamma\left(k - \frac{l+n}{2} + n + \lambda + 1\right)} \right.$$

$$\left. \frac{\Gamma\left(k + \frac{\lambda+\tau}{2} + 1\right)}{\Gamma\left(k + \frac{l+n}{2} + \lambda + \tau + 1\right) \Gamma\left(k - \frac{l+n}{2} + l + \tau + 1\right)} \right.$$

$$\left. \times \frac{e^{2k+\lambda+\tau} W_n}{\Gamma\left(k + \frac{l+n+1}{2}\right) h_{kln}^{\lambda,\tau} e^{2k+l+n+\lambda+\tau}} \right.$$

$$\left. - \sum_{k=0}^{\infty} \frac{2\pi}{\Gamma\left(k + \frac{l+n}{2} + 1\right)} \right.$$

$$\left. \times \left\{ 2 \ln \xi + \psi\left(k + \frac{l+n+1}{2}\right) \right. \right.$$

$$\left. + \psi\left(k + \frac{l+n+\lambda+\tau+1}{2}\right) + \psi\left(k + \frac{l+n+\lambda+\tau}{2} + 1\right) \right.$$

$$\left. - \psi(k+1) \right.$$

$$\left. - \psi\left(k + \frac{l+n}{2} + 1\right) - \psi(k+l+\tau+1) \right.$$

$$\left. - \psi(k+n+\lambda+1) - \psi(k+l+n+\lambda+\tau+1) \right\} \tag{5.4}$$

where,

$$W_n = 0, \quad l+n=0$$

$$W_n = 1, \quad l+n \neq 0.$$

$\Gamma(\cdot)$ denotes the Gamma function and,

$$h_{kln}^{\lambda,\tau} = (-1)^k \frac{\Gamma\left(k + \frac{l+n+\lambda+\tau+1}{2}\right) \Gamma\left(k + \frac{l+n+\lambda+\tau+2}{2}\right)}{\Gamma(k+1) \Gamma(k+l+n+\lambda+\tau+1) \Gamma(k+n+\lambda+1) \Gamma(k+l+\tau+1)} \tag{5.5}$$

6. RESULTS

The approach method used in this thesis is a hybrid method named as analytical-numerical method. In general, the aim of using hybrid methods is to eliminate the disadvantages of the analytical methods which operate well at high frequencies and of the numerical methods which operate well at low frequencies. Stated in other words its aim is, to obtain an accurate solution for a wide frequency range. By comparing the results obtained by Veliev et al. [51] and the ones obtained by using this method it can be easily concluded that our results are much close to results obtained by Veliev et al. [51]. Figure 6.1, Figure 6.2, Figure 6.3, and Figure 6.4 illustrate the monostatic RCS as a function of incidence angle for $ka = 5.0, 15.0$. In order to investigate the effect

of the surface impedance on the scattered far field, two different cases have been considered as in $\eta = 1.5$ and $\eta=3.0$. In view of the two RCS curves for the impedance strip, the backscattered field is not affected by the impedance of the strip surface in the shadow region. On the other hand, Figure 6.5, Figure 6.6, Figure 6.7, and Figure 6.8 illustrate the bistatic RCS as a function of observation angle for $\theta = 60^\circ$ and $ka = 5.0, 15.0$. It is seen from the figures that our RCS results agree quite well with the results of Veliev et al. [51]. In addition, there are different trials in Figure 6.9 - Figure 6.15.

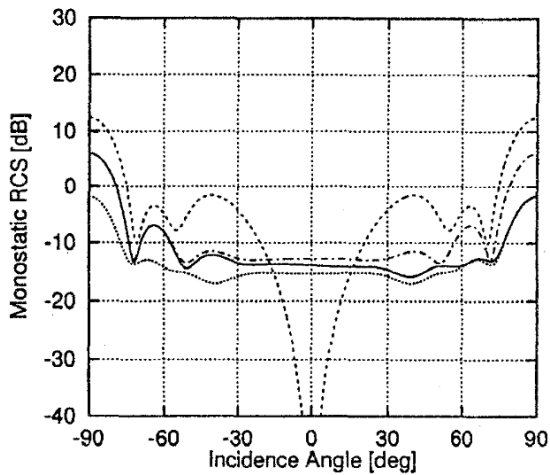


Figure 6.1. Monostatic RCS [dB], $\theta_0 = 60^\circ$, $ka = 5.0$.
 - - - - : $\eta_1 = \eta_2 = 0.0$; — : $\eta_1 = 1.5, \eta_2 = 3.0$;
 : $\eta_1 = \eta_2 = 1.5$; - . - . : $\eta_1 = \eta_2 = 3.0$
 (Veliev et al. [51])

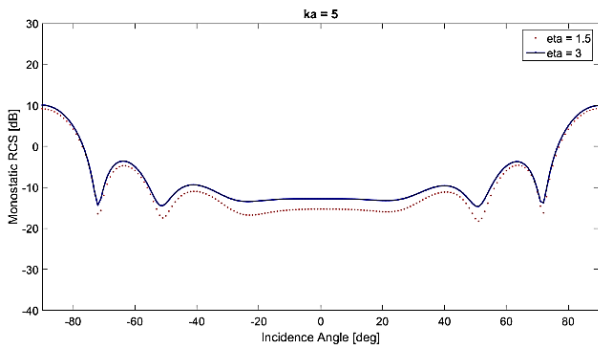


Figure 6.2. Monostatic RCS [dB], $ka=5.0$
 ($\eta = 1.5$ and $\eta = 3.0$)

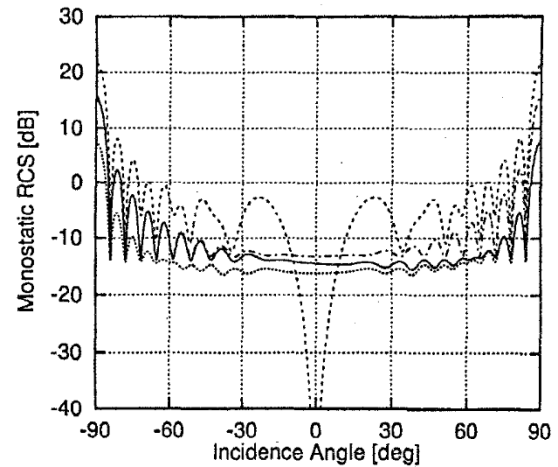


Figure 6.3. Monostatic RCS [dB], $\theta_0 = 60^\circ$, $ka=15.0$.
 - - - - : $\eta_1 = \eta_2 = 0.0$; — : $\eta_1 = 1.5, \eta_2 = 3.0$;
 : $\eta_1 = \eta_2 = 1.5$; - . - . : $\eta_1 = \eta_2 = 3.0$
 (Veliev et al. [51])

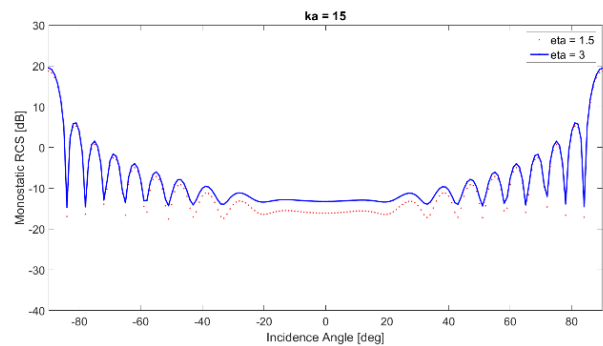


Figure 6.4. Monostatic RCS [dB], $ka=15.0$
 ($\eta = 1.5$ and $\eta = 3.0$)

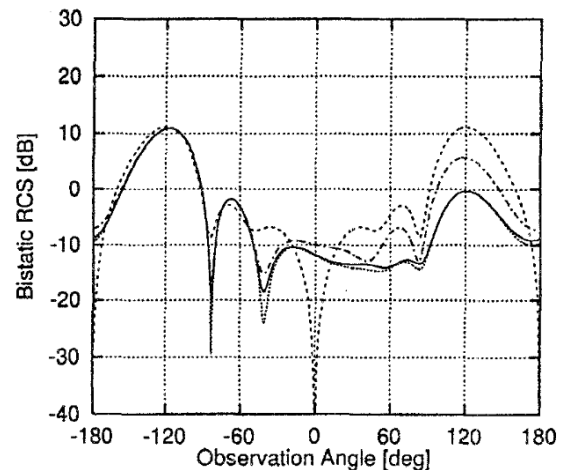


Figure 6.5. Bistatic RCS [dB], $\theta_0 = 60^\circ$, $ka=5.0$.
 - - - - : $\eta_1 = \eta_2 = 0.0$; — : $\eta_1 = 1.5, \eta_2 = 3.0$;
 : $\eta_1 = \eta_2 = 1.5$; - . - . : $\eta_1 = \eta_2 = 3.0$
 (Veliev et al. [51])

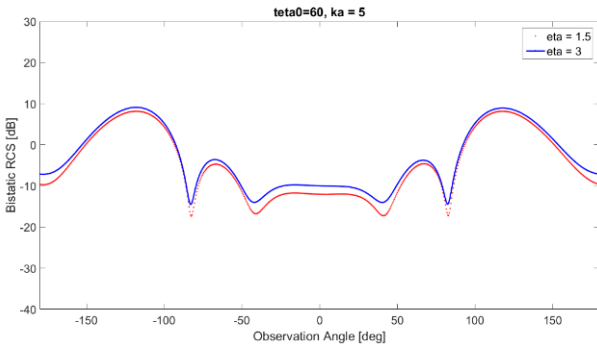


Figure 6.6. Bistatic RCS [dB], $ka=5.0$
($\eta = 1.5$ and $\eta = 3.0$)

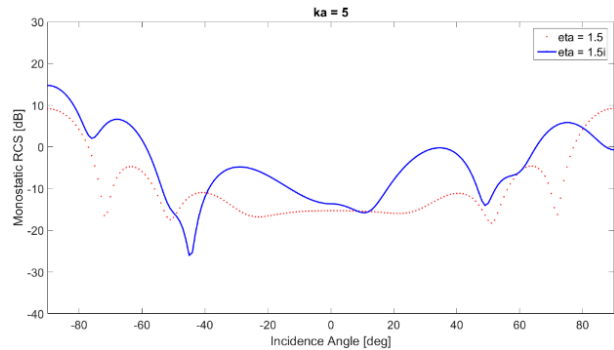


Figure 6.9. Monostatic RCS [dB], $ka=5.0$
($\eta = 1.5$ and $\eta = 1.5i$)

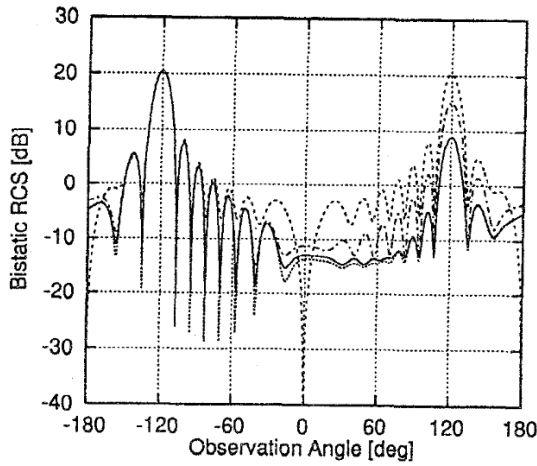


Figure 6.7. Bistatic RCS [dB], $\theta_0 = 60^\circ$, $ka=15.0$.
 - - - - : $\eta_1 = \eta_2 = 0.0$; — : $\eta_1 = 1.5, \eta_2 = 3.0$;
 : $\eta_1 = \eta_2 = 1.5$; - . - . : $\eta_1 = \eta_2 = 3.0$
 (Veliev et al. [51])

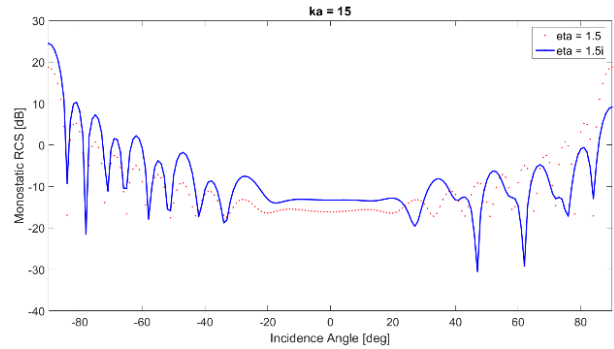


Figure 6.10. Monostatic RCS [dB], $ka=15.0$
($\eta = 1.5$ and $\eta = 1.5i$)

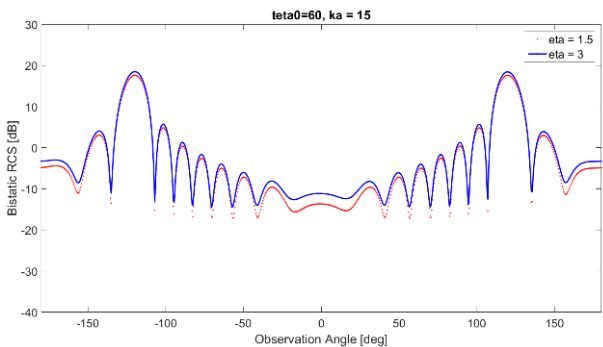


Figure 6.8. Bistatic RCS [dB], $ka=15.0$
($\eta = 1.5$ and $\eta = 3.0$)

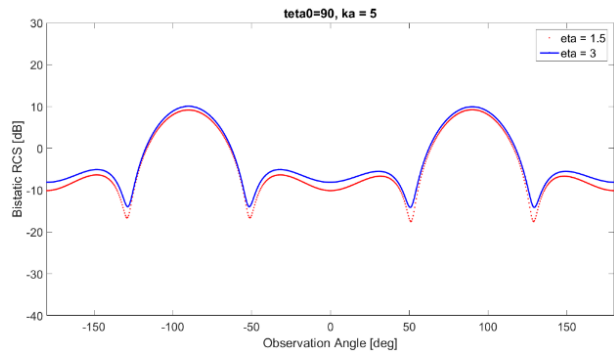


Figure 6.11. Bistatic RCS [dB], $\theta_0 = 90^\circ$, $ka=5.0$
($\eta = 1.5$ and $\eta = 3.0$)

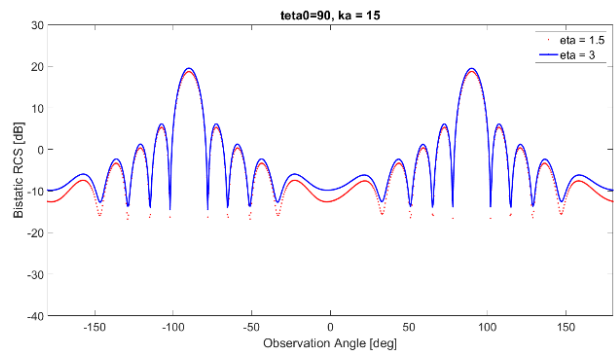


Figure 6.12. Bistatic RCS [dB], $\theta_0 = 90^\circ$, $ka=15.0$
($\eta = 1.5$ and $\eta = 3.0$)

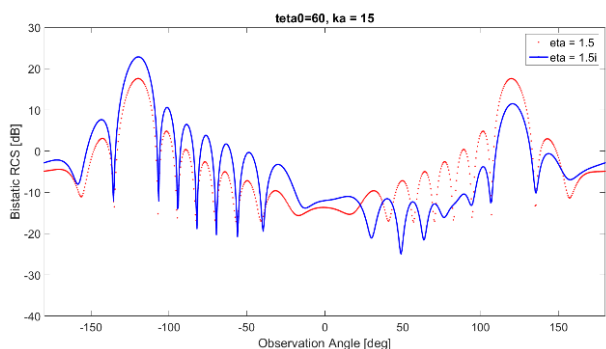


Figure 6.13. Bistatic RCS [dB], $\theta_0 = 60^\circ$, $ka=15.0$
($\eta = 1.5$ and $\eta = 1.5i$)

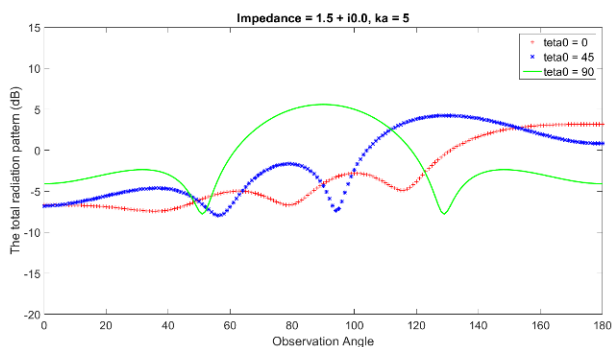


Figure 6.14. The total radiation pattern for $ka=5$

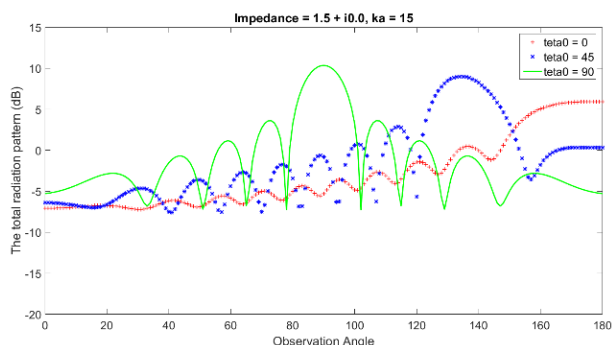


Figure 6.15. The total radiation pattern for $ka=15$

7. CONCLUSION

In this study, the diffraction of the H-polarized plane wave by an infinitely long strip, having the same impedance on both faces with a width of $2a$ is considered. Applying the boundary condition to an integral representation of the scattered field, the problem is formulated as simultaneous integral equations satisfied by the electric and magnetic current density functions. The integral equations are reduced to two uncoupled infinite systems of linear algebraic equations and physical quantities are obtained in terms of the solution of systems of linear algebraic equations. Numerical examples on the monostatic radar cross section (RCS), bistatic RCS, and the total scattering field radiation pattern are presented. Some obtained results are compared with the other existing results.

The system which is considered in this thesis is the simple impedance strip illuminated normally by a plane

wave. The canonical strip structure is chosen in terms of its conformity to many practical problems. This method is applicable for the analysis of more complicated structures which may be considered as a combination of different strip configurations. At that rate, the mathematical sense of the solution will not change. However, there will be some extra terms in the matrix equations. Because of this, the computer codes in this thesis must be modified for different strip configurations.

8. REFERENCES

- [1] Abramowitz, M.; Stegun, I. E., 1968. Handbook of Mathematical Functions. Dower Publications, New York, p. 1043.
- [2] Ahluwalia, D. S., 1970. Uniform Asymptotic Theory of Diffraction by the Edge of a Three-Dimensional Body. SIAM J. Appl. Math. Vol.18, No.2, pp. 287-301.
- [3] Apaydin, G.; Sevgi, L., 2015. Method of Moments Modeling of Backscattering By a Soft-Hard Strip. IEEE Trans. on Antennas and Propagation, Vol.63, No.12, pp. 5822-5826.
- [4] Bhattacharyya, A. K.; Sengupta, D. L., 1991. Radar Cross Section Analysis and Control. Artech House, London, p. 289. (Uffimtsev, P. I., 1958).
- [5] Born, M.; Wolf, E., 1965. Principles of Optics. Pergamon Press, Frankfurt, Germany, p.808. (Rayleigh, L., 1871).
- [6] Bowman, J. J., 1967. High-Frequency Backscattering from an Absorbing Infinite Strip with Arbitrary Face Impedance. Canadian Journal of Phys., Vol. 45, pp. 2409-2430.
- [7] Burnside, W. D.; Yu, C. L.; Marhefka, R. J., 1975. A Technique to Combine the Geometrical Theory of Diffraction and the Moment Method. IEEE Trans. On Ant. And Proc., Vol. AP-23, pp. 551-558.
- [8] Butler, C. M., 1985. General Solution of the Narrow Strip Integral Equations. IEEE Trans. on Ant. and Proc., Vol. AP-33, No. 10, pp. 1085-1090.
- [9] Büyükaksoy, A.; Serbest, A. H.; Uzgören, G., 1989. Secondary Diffraction of Plane Waves by an Impedance Strip. Radio Science, Vol. 24, pp. 455-464.
- [10] Castro, L. P.; Kapanadze, D., 2008. The impedance boundary value problem of diffraction by a strip. J. Math. Appl., Vol. 337, pp. 1031-1040.
- [11] Chakrabarti, A., 1977. Diffraction by a unidirectionally conducting strip. Ind. J. Pure Appl. Math., Vol. 8, pp. 702-717.
- [12] Copson, E. T., 1946. An integral-equation method of solving plane diffraction problems. Proceedings of the Royal Society A Mathematical, Physical and Engineering Sciences, pp. 100-118.
- [13] Emets, V.; Rogowski, J., 2015. Diffraction by a Strip with Different Boundary Conditions on Its Surfaces. 16th International Conference on Computational Problems of Electrical Engineering (CPEE), Lviv (Ukraine), pp. 39-42.
- [14] Faulkner, T. R., 1965. Diffraction of an Electromagnetic Plane-wave by a Metallic Strip.

- IMA Journal of Applied Mathematics, Vol. 1, pp. 149-163.
- [15] Felsen, L. B.; Marcuvitz, N., 1973. Radiation and Scattered of Waves. Prentice Hall, New Jersey, p. 883.
- [16] Grinberg, G. A., 1960. Diffraction of Electromagnetic Waves by Strip of Finite Width. Soviet Phys. Dokland. Vol. 4, No. 6, pp. 1222-1225.
- [17] Harrington, R. F., 1968. Field Computation by Moment Method. Macmillan, New York, p. 285.
- [18] Herman, M. I.; Volakis, J. L., 1987. High Frequency Scattering by a Resistive Strip and Extensions to Conductive and Impedance Strips. Radio Science, Vol. 22, No. 3, pp. 335-349.
- [19] Hongo, K., 1972. Diffraction of Electromagnetic Plane Wave by an Infinite Slit Embedded in an Anisotropic Plasma. Journal of Applied Physics, Vol. 43, No. 12, pp. 4996-5001.
- [20] Imran, A.; Naqvi, Q. A.; Hongo, K., 2009. Diffraction of electromagnetic plane wave by an infinitely long conducting strip on dielectric slab. Opt Comm, Vol. 282, pp. 443-450.
- [21] Imran, A.; Naqvi, Q. A.; Hongo, K., 2007. Diffraction of electromagnetic plane wave by an impedance strip. Prog In Elec Res., Vol. 75, pp. 303-318.
- [22] Jones, D. S., 1964. The Theory of Electromagnetism, Pergamon, London.
- [23] Keller, J. B., 1962. J. Opt. Soc. Of America, Vol. 52, No. 2, pp. 116-130. (Keller, J. B., 1953).
- [24] Kouyoumjian, R. G.; Pathak, P. H., 1974. A Uniform Geometrical Theory of Diffraction for Edge in a Perfect Conducting Surface. Proc. Of the IEEE, Vol. 62, No. 11, pp. 1448-1461.
- [25] Kobayashi, K., 1993. The Wiener-Hopf Technique and Its Applications to Diffraction problems Involving Two Dimensional Obstacles with Finite Cross-Section. Lecture Notes, p. 145.
- [26] Lawrie, J. B.; Abrahams, I. D., 2007. A brief historical perspective of the Wiener-Hopf technique. J. Eng. Math., Vol. 59, pp. 351-358.
- [27] Levine, H.; Schwinger, J., 1948. On the Theory of Electromagnetic Wave Diffraction by an Aperture in an Infinite Plane Conducting Screen. Comm. Pure and Appl. Math., Vol. 3, pp. 355-391.
- [28] Maliuzhinets, G. D., 1958. Excitation, Reflection and Emission of Surface Waves from a Wedge with given Face Impedance. Soviet Phys. Dokland, Vol. 3, No. 3, pp. 752-755.
- [29] Medgyesi, L. N.; Wang, D. S., 1989. Hybrid Solutions for Scattering from Perfectly Conducting Bodies of Revolution. IEEE Trans. on Antennas and Propagation, Vol. AP-31, No. 4, pp. 570-583.
- [30] Medgyesi, L. N.; Wang, D. S., 1989. Hybrid Methods for Analysis of Complex Scatterers. Proc. of the IEEE, Vol. 77, No. 5, pp. 770-779.
- [31] Meixner, J., 1972. The Behavior of Electromagnetic Fields at Edges. IEEE Trans. on Ant. and Prop. Vol. AP-20, No. 4, pp. 442-446. (Meixner, J., 1949).
- [32] Miles, J. W., 1949. On Certain Integral Equations in Diffraction Theory. Vol. 28, pp. 223-226.
- [33] Morse, P. M.; Rubenstein, P. J., 1938. The Diffraction of Waves by Ribbons and Slits. Phys. Rev., Vol. 54, pp. 895-898.
- [34] Nagasaka, T.; Kobayashi, K., 2015. Wiener-Hopf Analysis of the Plane Wave Diffraction by a Thin Material Strip: the Case of H-polarization. Electromagnetics in Advanced Applications (ICEAA) 2015 International Conference, Turin, pp. 626-628.
- [35] Noble, B., 1958. Methods Baesd on the Wiener-Hopf Technique. Pergamon, London.
- [36] Nomura, Y.; Katsura, S., 1957. Diffraction of Electromagnetic Waves by Circular Plate and Circular Hole. J. Phys. Soc. Japan, Vol. 10, No. 4, pp. 285-304.
- [37] Otsuki, T., 1978. Diffraction by two parallel slits in plane. J. Math. Phys., Vol. 46, pp. 911-915.
- [38] Prudnikov, A. P.; Brickov, Y. A.; Maricev, O. I., 1983. Integrals and Series of Special Functions. Nauka Press, Moskow, p. 785.
- [39] Rayleigh, L., 1871. On the scattering of light by small particles. Philosophical Magazine, series 4, Vol. 41, pp. 447-454.
- [40] Spiegel, M. R., 1968. Mathematical Handbook of Formulas and Tables. Mc-Graw Hill Company, New York, p. 271.
- [41] Sahalos, J. N.; Thiele, G. A., 1981. On the Application of the GTD-MM Technique and Its Limitations. IEEE Trans. on Ant. and Proc., Vol. AP-29, pp. 780-786.
- [42] Senior, T. B. A., 1951. Diffraction by a Semi-Infinite Metallic Sheet. Proc. of the Royal Society, Vol. 213, pp. 436-458.
- [43] Senior, T. B. A., 1979. Backscattering from Resistive Strips. IEEE Trans. on Ant. and Proc., Vol. AP-27, No. 6, pp. 808-813.
- [44] Serbest, A. H.; Büyükkaksoy, A., 1993. Some Approximate Methods Related to the Diffraction by Strips and Slits. Analytical and Numerical Methods in Electromagnetic Wave Theory, Science House, Japan, pp. 229-256.
- [45] Sommerfeld, A., 1896. Mathematische Theorie der Diffraction. Math. Ann. 47, pp. 317-374.
- [46] Thiele, G. A.; Newhouse, T. H., 1975. A Hybrid Technique for Combining Moment Method with the Geometrical Theory of Diffraction. IEEE Trans. on Ant. and Proc., Vol. AP-23, Jan., pp. 62-69.
- [47] Tiberio, R.; Kouyoumjian, R. G., 1979. A Uniform GTD Solution for the Diffraction by Strips Illuminated at Grazing Incidence. Radio Science, Vol. 14, No. 6, pp. 933-941.
- [48] Veliev, E. I.; Kobayashi, K.; Ogata, M.; Koshikawa, S., 1998. Diffraction by a Strip with Different Surface Impedances: The Case of H Polarization. VII International Conference on Mathematical Methods in Electromagnetic Theory, Vol. 2, pp. 727-729.
- [49] Veliev, E. I.; Veremey, V. V., 1993. Numerical-Analytical Approach for the Solution to the Wave Scattering by Polygonal Cylinders and Flat Strip Structures. M. Hashimoto, M. İdemen, O.A. Tretyakov. Analytical and Numerical Methods in

Electromagnetic Wave Theory, Science House, Japan, pp. 471-514.

- [50] Veliev, E. I.; Veremey, V. V.; Shestopalov, V. P., 1989. Electromagnetic Wave Diffraction on Polygonal Cylinders-New Approach. Proc. of 1989 URSI Int. Symp. on Electromagnetic Theory, p. 628.
- [51] Veliev, E. I.; Kobayashi, K.; Ogata, M., 1998. Diffraction by a strip with different surface impedances: the case of H polarization. Proceedings of 1998 International Conference on MMET, Kharkov, Ukraine, pp. 727-730.
- [52] Volakis, J. L.; Bindiganavale, S. S., 1996. Scattering by a Narrow Groove in an Impedance Plane. Radio Science, Vol. 31, No. 2, pp. 401-408.
- [53] Wandzura, S., 1992. Electrical Current Basis Functions for Curved Surfaces. Electromagnetics, Vol. 12, Np. 1, pp. 77-90.

Contact addresses

Emine Avşar Aydin, Assistant Professor

Adana Science and Technology University,
Department of Aeronautics Engineering
Seyhan/Adana-TURKEY
+90-05318436781
eaydin@adanabtu.edu.tr / rasvaenime@gmail.com

Turgut İköz, Professor

Çukurova University, Department of Electrical-
Electronic Engineering
Adana-TURKEY
+90-03223386868
tikiz@cu.edu.tr

THE EFFECT OF THE LOADING ORDER ON THE FORMATION OF THE STRESS-STRAIN STATE OF THE REINFORCED CONCRETE FRAME STRUCTURE

UTJECAJ PORETKA OPTEREĆENJA NA FORMIRANJE STANJA NAPREZANJA I ISTEZANJA OKVIRNE STRUKTURE KONSTRUKCIJE OD ARMIRANOG BETONA

Anatolij Vladimirovich Kovrov, Aleksei Vladimirovich Kovtunenko, Nina Konstantinovna Vysochan

Preliminary communication

Abstract: *The paper considers the influence of the physical and geometric nonlinearity of reinforced concrete frame structures on the formation of the stress-strain state in the phased construction of a building. The basic principles of a statically indeterminate reinforced concrete frame structure analysis with a consideration of the design scheme creation order and load application, as well as the cracking processes, are proposed. An example of the two steps of the analysis of the transversal frame of a three-storey and three-span building for administrative and production purposes in accordance with the proposed principles of the analysis is shown. The method of the analysis is based on the study of the fundamental technological scheme of the building construction with the partition of the analysis which is accomplished on the corresponding enlarged steps. With a consideration of the construction and loading order and processes of cracking in the elements, a comparison of the results of the implemented analysis in the elastic stage is done.*

Keywords: *cracking, numerical-analytical boundary element method, reinforced concrete frame structure, order of loading*

Prethodno priopćenje

Sažetak: *U radu se razmatra utjecaj fizičke i geometrijske nelinearnosti armiranobetonskih okvirnih konstrukcija na formiranje stanja naprezanja i istezanja u faznoj izgradnji zgrade. Predlažu se osnovna načela analize okvirne strukture statički neodređene armiranobetonske konstrukcije s obzirom na redoslijed oblikovanja i primjenu opterećenja, kao i proces pucanja. Primjer dva koraka analize poprečnog okvira iskazan je na zgradi trorasponske konstrukcije s tri kata za administrativne i proizvodne svrhe, u skladu s predloženim načelima analize. Metoda analize temelji se na proučavanju temeljne tehnološke sheme građevne konstrukcije s podjelom analize koja se postiže kroz odgovarajuće uvećane korake. Imajući u vidu izgradnju, redoslijed opterećenja i proces pucanja elemenata, uspoređeni su rezultati provedene analize u elastičnoj fazi.*

Ključne riječi: *pucanje, numeričko-analitička metoda graničnih elemenata, okvirna struktura armirano betonske konstrukcije, redoslijed opterećenja*

1. INTRODUCTION

It is known [4, 7] that cracking has a significant effect on the stress-strain state of reinforced concrete structures. It causes the development of displacements, falling of pre-stressing forces, change and redistribution of the internal forces.

In statically indeterminate reinforced concrete structures, due to their physical and geometric nonlinearity, the sequence of the creation of the design scheme and the application of the load affect the distribution of internal forces [9, 10, 11].

The simultaneous impact of the above-mentioned factors on the stress-strain state of statically indeterminate reinforced concrete frame structures has still not been sufficiently studied.

Thus, the development of the methods for determining the stress-strain state of reinforced concrete frame structures is based on the numerical-analytical boundary element method, which allows the inspection of the functioning of systems up to the limit state; and the respective physical nature of their work is the actual and necessary task for the subsequent development of the analysis theory of statically indeterminate reinforced concrete structures.

The aim is to study the effect of the construction and loading order, as well as the processes of cracking on the stress-strain state of reinforced concrete frame structures with the use of the numerically-analytical boundary element method [1, 2, 3].

2. THE PRINCIPLE OF THE MODELING OF THE DESIGN SCHEME WITH A CONSIDERATION OF THE LOADING ORDER

In design practice, including the frame structure, static analysis is made on the full design loads (a combination of permanent and temporary loads). Strength calculation and construction are made on the design forces, which were acquired as a result of this calculation.

In real terms, the construction of buildings is carried out in stages. The loading of the constructed parts is carried out in the respective stages. By the time of the subsequent stages of the erection of the building, the stiffness of the constructed parts can differ from the stiffness in the elastic phase.

Thus, a redistribution of the internal stresses in the real circumstances also occurs in stages, depending on the technology of the building construction.

Before performing the calculations, it is necessary to examine the fundamental technology of the building scheme erection and divide the analysis in the corresponding enlarged steps. The analysis results at each stage are the initial data for the realization of the following analysis.

The analysis method of reinforced concrete frame structures with a consideration of the cracking processes by using the numerically analytical method of boundary elements is proposed in the paper [4].

The partition of the rods of the frame structure (columns and beams) onto the elements with piecewise constant stiffness is carried out in determining the stress-strain state of reinforced concrete frame structures with a consideration of the cracking processes by using the numerical and analytical boundary element method.

The stiffness of elements is determined by using a practical method based on a simplified "bending moment - curvature" diagram, proposed in [5, 6].

The analysis is carried out with the assumption of the structure functioning in the elastic stage, which is why the bending stiffness is defined as the product $E_b I_{red}$ in the first stage.

Further, stiffness is determined by curvatures that are obtained on the basis of the bending moments.

Stiffness does not change in the elements where the bending moments do not exceed the cracking value. In reinforced concrete elements, cracking is taken into account in accordance with [5...7]. In the areas where the bending moments exceed the cracking value, the element stiffness is determined by a formula that is proposed by I. E. Prokopovich in [7]:

$$B_g = E_b A_b h_0^2 \sqrt{\mu n_1} b_1, \quad (1)$$

where, A_b – the cross-sectional area of the beam;

h_0 – the working height of the section;

$\mu = A_s / A_b$ – the sectional ratio of reinforcement;

A_s – the sectional area of the valve;

$n_1 = E_s / E_b$ – the ratio of the elastic modulus reinforcement and concrete.

Coefficient b_1 is defined as follows:

$$b_1 = \beta_1 + \beta_2 \left(\frac{M_{erc}}{M} \right)^2, \quad (2)$$

An element with a rectangular cross-section has the following values of coefficients: $\beta_1 = 0,159$, $\beta_2 = 0,074$.

At the limit value of the bending moment ($M=M_u$), the curvature may increase indefinitely at the constant bending moment (i.e. under the assumption that a plastic hinge formed in the cross-section).

An analysis of the frame structure with the new values of stiffness is accomplished after the determining of the stiffness of each element.

These operations are repeated until convergence is reached.

It is necessary to divide the analysis process on enlarged steps in order to reflect the real order of the application of loads on the building frame.

An analysis of a one-storey frame of the first floor is accomplished only through a constant load. As a result, in some elements, the process of cracking is observed, which sharply reduces their stiffness.

When considering the design scheme that represents a two-storey frame, the initial stiffness of the first floor elements is taken from the results of the first stage analysis, and the stiffness of the second floor elements is taken from the assumption of the work in the elastic stage.

At the subsequent stages of the analysis, the stiffness of the already erected elements is similarly received from the results of the previous stage.

3. AN ANALYSIS OF THE REINFORCED CONCRETE STRUCTURE WITH A CONSIDERATION OF THE LOADING ORDER

Consider the example of the first two stages of the analysis of the transversal reinforced concrete frame of a three-storey and three-span building for administrative and production purposes with a consideration of the load application order. The analysis was performed by using the program developed in the system of computer mathematics MATLAB, which allows the consideration of the processes of cracking [4].

The distance between transverse frames is assumed to be 6.0 m. The collection of permanent and temporary loads on each floor of the building and the analysis of the frame structure in the elastic stage are made with a consideration of the current regulations [8].

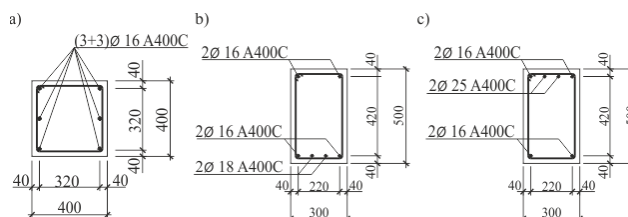


Figure 1. Cross-sections of the frame elements
a) columns; b) span sections of beams; c) support sections of beams.

The reinforcement of elements and the construction of the reinforced concrete frame are made according to the results of the frame structure analysis in relation to the action of the design loads (Fig. 1).

The design scheme of the building framework at the first step is applied as a one-storey frame loaded by a constant load (Fig. 2).

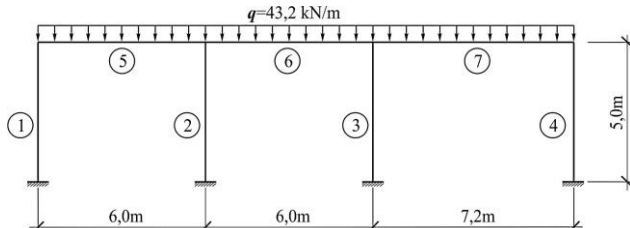


Figure 2. Estimated carcass scheme building on the first stage of the calculation

4. RESULTS OF THE ANALYSIS

The diagrams of the bending moments that occur in the structure at the first step of the analysis in the elastic stage and with a consideration of the cracking processes are shown in Fig. 3.

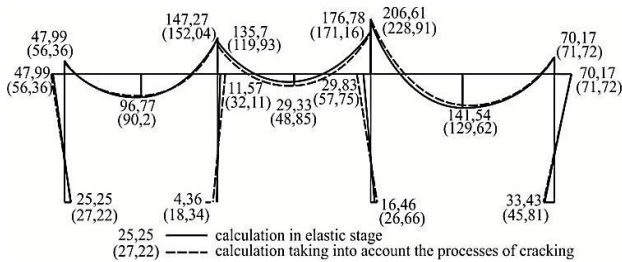


Figure 3. The diagram of the bending moments at the first stage of the calculation

Table 1. Comparison of the results at the first stage

№ of elements	№ of sections	Values of the bending moments M, kNm		Change of forces Δ, %
		analysis in the elastic stage	analysis with a consideration of cracking	
1	1	25.25	27.22	7.80
	3	-47.99	-56.36	17.44
4	1	-33.43	-45.81	37.03
	3	70.17	71.72	2.21
5	1	-47.99	-56.36	17.44
	2	96.77	90.2	-6.79
	3	-147.27	-152.04	3.24
6	1	-135.69	-119.93	-11.61
	2	29.33	48.85	66.55
	3	-176.78	-171.16	-3.18
7	1	-206.61	-228.91	10.79
	2	141.54	129.62	-8.42
	3	-70.17	-71.72	2.21

Note: Section 1 taken at the left end of the element;
Section 2 taken in the middle of the element;
Section 3 taken at the right end of the element.

Table 1 shows a comparison of the bending moment values that occur in some elements of the structure at the first stage of the construction obtained in the results of the

analysis in the elastic stage and with a consideration of the cracking processes.

Table 1 shows that the moments occurring in the outside columns increase. In the support sections of the outside beams the moments increase and decrease in the span sections. In the mid-span beam, moments decrease in the support sections and increase in the span at almost 67%.

The design scheme at the second step is applied as a two-storey frame (Fig. 4).

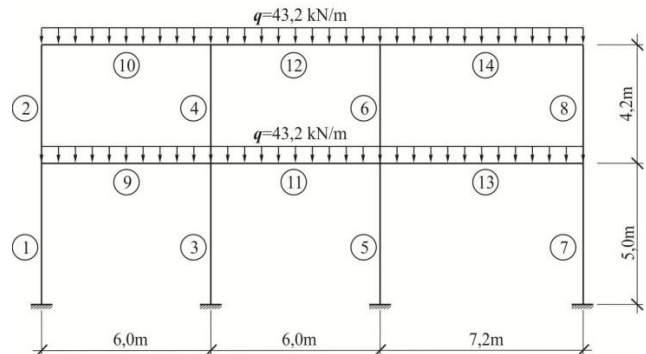


Figure 4. The estimated building framework scheme at the second stage of the calculation

The diagrams of the bending moments that occur in the structure at the second step of the analysis in the elastic stage and with a consideration of the cracking processes are shown in Fig. 5.

Table 2 shows a comparison of the bending moment values that occur in some elements of the structure at the first stage of the construction obtained in the results of the analysis in the elastic stage and with a consideration of the loading order and cracking processes.

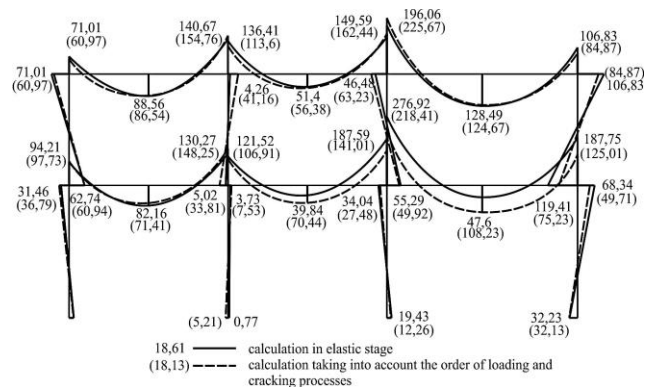


Figure 5. The diagram of the bending moments at the second stage of the calculation

As shown in Table 2, bending moments are the most reduced, in comparison with the elastic analysis in the columns of the right outside span. The largest redistribution, in comparison with the elastic analysis, occurred in the span sections of the middle and right span beams. Thus, in the mid-span the value of the bending moment increased by about 77%, and in the outside it increased by 127%.

Table 2. Comparison of the results of the calculation at the second step

№ of elements	№ of sections	Values of the bending moments M , kNm		Change of forces Δ , %
		analysis in the elastic stage	analysis with a consideration of the cracking and loading order	
1	1	18.61	18.13	-2.58
	3	-31.46	-36.79	16.94
2	1	62.74	60.94	-2.87
	3	-71.01	-60.97	-14.14
7	1	-32.23	-32.13	-0.31
	3	68.34	49.79	-27.14
8	1	-119.41	-75.22	-37.01
	3	106.83	84.87	-20.56
9	1	-94.21	-97.73	3.74
	2	82.16	71.41	-13.08
	3	-130.27	-148.25	13.80
10	1	-71.01	-60.97	-14.14
	2	88.56	86.54	-2.28
	3	-140.67	-154.76	10.02
11	1	-121.52	-106.91	-12.02
	2	39.84	70.44	76.81
	3	-187.59	-141.003	-24.83
12	1	-136.41	-113.6	-16.72
	2	51.4	56.38	9.69
	3	-149.59	-162.44	8.59
13	1	-276.92	-218.41	-21.13
	2	47.6	108.23	127.37
	3	-187.75	-125.01	-33.42
14	1	-196.06	-225.67	15.10
	2	128.49	124.67	-2.97
	3	-106.83	-84.87	-20.56

Note: Section 1 taken at the left end of the element;
Section 2 taken in the middle of the element;
Section 3 taken at the right end of the element

5. CONCLUSION

The results of the example of the first two stages of the analysis of the transversal frame of a three-storey and three-span building indicate that the consideration of the phasing of the construction (of the order of the application of loads) and cracking has a significant impact on the redistribution of internal forces.

The continuation of various investigations should be done for a detailed study of the examined effects.

6. REFERENCES

- [1] Bazhenov, V. A.; Kolomiets, L. V.; Orobie, V. F et al. Structural Mechanics. Special course. Application of boundary element method. – Odessa: Astroprint, 2003–p.288.
- [2] Dashchenko, A. V.; Kirilov, V. H.; Kolomiets, L. V.; Orobie, V. F. MATLAB for scientific and engineering calculations - Odessa: Astroprint, 2003, p. 216
- [3] Orobie, V. F.; Kovrov, A. V. The decision of problems of statics, dynamics and stability of bar systems. Application of boundary element method. – Odessa, 2004, p.122.
- [4] Dorofeev, V. S. Determination of stress-strain state of reinforced concrete frame structures, taking into account the processes of cracking / Dorofeev, V. S.; Kovrov A. V.; Kovtunenکو, A. V.; Kushnir, A. M. // Herald of the National University "Lviv Polytechnic". – Lviv, "Lviv Polytechnic", 2010. Herald № 662. pp. 169-174.
- [5] Kovrov, A. V. By the analysis of the deformation patterns of cross-sections of continuous reinforced concrete beams / Kovrov, A. V.; Chaykovsky, R. E.; Sinyukina, T. A. // Herald of ODABA. Odessa, 2007. № 27. pp. 178-183.
- [6] Yaremenko, A. F. On a practical method for determining the hardness of concrete beams / Yaremenko, A. F.; Kovrov, A. V.; Sinyukina, T. A. // Herald of Odessa, 2005. № 20. pp. 389-394.
- [7] Prokopovich, I. E.; Zedgenidze, V. A. Applied theory of creep. M.: Stroyizdat, 1980. p. 240.
- [8] DBN V.1.2–2: 2006. Loads and effects. – Kiev, Ukraine Ministry of Construction, 2006. p. 57
- [9] Shein, A. I.; Zav'yalova, O. B. The influence of physical nonlinearity of concrete on stress-deformed state of elements of monolithic reinforced concrete frames, calculated with account of the history of loading. Promyshlennoe i grazhdanskoe stroitel'stvo, 2012, no. 8, pp. 29–31. (In Russian).
- [10] Zav'yalova, O. B. Account history-load of the monolithic reinforced concrete plate-core systems in determining the stress state of their elements. Promyshlennoe i grazhdanskoe stroitel'stvo, 2012, no. 7, pp. 58–61. (In Russian).
- [11] Kabantsev, O. V.; Karpilovsky, V. S.; Kriksunov, E. Z.; Perelmutter, A. V. The technology of the design forecast of stressedly-deformed state of constructions with regard to the history of construction, loading and deformation. // International Journal for Computational Civil and Structural Engineering. 7, 3(2011), pp. 110-117.

Contact addresses

Kovrov Anatoliy Vladimirovich, PhD, Professor
Department "Strength of Materials"
Odessa State Academy of Civil Engineering and Architecture
Street Didrihsone 4, Odessa, Ukraine
E-mail: akovrov@inbox.ru

Kovtunenکو Aleksei Vladimirovich, PhD, Assistant Professor
Department "Strength of Materials"
Odessa State Academy of Civil Engineering and Architecture
Street Didrihsone 4, Odessa, Ukraine
E-mail: kovtunenکو.aleks@mail.ru

Vysochan Nina Konstantinovna, Research Assistant
Department "Strength of Materials"
Odessa State Academy of Civil Engineering and Architecture
Street Didrihsone 4, Odessa, Ukraine
E-mail: ninokli@mail.ru

AN ANALYSIS OF THE TECHNOLOGICAL PROPERTIES OF FACILITATED PLASTER SOLUTIONS MADE FROM DRY BUILDING MIXES

ANALIZA TEHNOLOŠKIH SVOJSTAVA OLAKŠANIH GIPSANIH RJEŠENJA IZ SUHIH GRAĐEVINSKIH MJEŠAVINA

Christina Moskalova, Oleg Popov

Preliminary communication

Abstract: *The paper deals with the development and optimization of the compositions of dry building mixes for heat-insulating plaster with improved technological properties and with the rational use of the modifying polymeric additives.*

Keywords: *dry building mixes, polymer, perlite sand*

Prethodno priopćenje

Sažetak: *U članku se razmatra razvoj i optimizacija sastava suhih građevinskih mješavina za toplinsko-izolacijske žbuke s poboljšanim tehnološkim svojstvima uz racionalno korištenje modificirajućih polimernih aditiva.*

Ključne riječi: *suhe građevinske mješavine, polimer, vulkanski pijesak*

1. INTRODUCTION

Nowadays the dry building mixes (DBM) are applied practically in all kinds of activities, but more often in the the external and internal finishing. Under the modern conditions, with the permanent increase of the cost of resources, the task is to reduce the operating costs of buildings at the expense of enriching the heat-protective characteristics of the enclosure walls. The reduction of heat loss through the walls of buildings can allow the reduction of the cost of the heating fuel and also of the emission of combustion products, which will cause a positive ecological effect. According to that, lightweight heat-insulation plaster solutions, the so-called warm plasters, are becoming more and more popular in the modern building market. The main objective of the research is to investigate the building mixes' rheological and mechanical behavior in their fresh state. As it will be discussed later, the mineral fillers and polymeric additives have a significant rheological influence on the building mixes, which over time becomes crucial to their durability behavior.

2. RESEARCH AND RESULTS

According to the State Standard (SS) 28013-98, lightweight plasters belong to the solutions with a density not more than 1500 kg/m^3 [1]. Literature [2] contains some information which indicates that in the case of lightweight plaster, it is right to consider that lightweight plaster whose density is not over 1300 kg/m^3 is the

solution. As a result, the heat-insulating plaster solutions are characterized by the low parameters of compression strength, in the range of 3 MPa. Heat-insulating plasters are used as solutions with lightweight fillers and a large part of them are perlite. Apart from the low density, the particles of perlite, at the expense of the surface roughness, promote a stress relaxation on the border between the plaster and the basis, which is an important factor of the spalling avoidance [3, 4]. When analyzing the multi-component solutions of heat-insulating plasters, it is concluded that finished dry mixes of industrial preparation are more often used for their preparation.

Modern DBMs are a multi-component organic mineral system [5] where a high-molecular organic component is presented in a variety of materials:

- water-soluble, for example, methylcellulose;
- re-dispersible in water, in particular the copolymers of vinyl ester;
- waterproof, in particular the polymeric and cellulose fibers.

The rheological behavior of mixtures and mechanical characteristics of the composites received from the dry mixes with the cement binder, and also the influence on the yielded properties introduced in a DBM of organic compounding (polymers) and mineral fillers has been studied. One of the primary goals of the research is the reduction in the composition of the dry mixes of an expensive perlite at the expense of the introduction of the limestone coquina. At the same time, the required physical-mechanical performance and technological properties of the plaster obtainable from the DBM should be saved.

The base structure of the investigated dry mixes includes binder, mineral fillers and polymeric additives. The experiment was conducted under the optimal 18 points plan [6]. The following components such as the four factors of structure (in relation to 1000 m.u. dry mix) were used:

X_1 - limestone powder to $S_{sv} = 400 \text{ m}^2/\text{kg}$,
 $80 \pm 20 \text{ m.u.}$;

X_2 - circulated perlite sand of mark 100,
 $40 \pm 10 \text{ m.u.}$;

X_3 - methylhydroxyethylcellulose Tylose 60010
 (water-soluble, nonionic ethers of cellulose),
 $1.15 \pm 0.15 \text{ m.u.}$;

X_4 - polymeric re-dispersible powder Vinnapas
 RE 5034N (copolymer vinylchloride, ethylene
 and vinylaurate), $1.5 \pm 0.5 \text{ m.u.}$

Each investigated mixture had an identical flowability of 16-17 cm of flow at the expense of the selection of the quantity of mixing water. This condition was accepted by taking into account the typical technological working conditions of manufactured dry blends and equipment parameters.

The flowability of mortar mixes was defined under the European standard DIN 18555-2 [7] on a jolt-table as such technique, from our point of view, is more correct for a DBM heat-insulating facing plaster compared to the technique of SS 5802-86 [8]. According to the diameter of flow, the plasters' mortar mixes are divided into: rigid <14 cm; plasticity - 14-20 cm and soft >20 cm. On the basis of this, all investigated blends refer to the plastic mix. Nevertheless, despite the equal flowability of all mixes, their rheological properties essentially differed.

3. RESULTS AND ANALYSIS

Rheological tests were performed on a rotary viscometer RPE-1M; the viscosity of mixes has been analyzed at a speed of deformation from 0.045 c^{-1} to 5.705 c^{-1} . According to the data obtained from the viscometer, the measured was plotted versus the applied rotational velocity ($\ln \gamma'$) from viscosity ($\ln \eta$). Figure 1 shows examples of the curves of deformations for compositions with 40 (a) and 20 (b) parts by mass units of perlite; curves represent a logarithmic dependence of the viscosity of the mixture of the speed of the deformations.

In each figure we can see two curves, one of them is on the top line and it describes the viscosity of a mix, and the second one, on the bottom line, shows the ability of a mix to restore the thixotropy of mixes. Firstly, it is important to note that the level of thixotropy of mixes at the structures with a considerable quantity of perlite is above the ones with a low content of perlite. This is evidenced by the differences of "straight" and "return" curved lines. The values of viscosity were obtained by using the Ostwald-de-Ville equation [9] $\eta = K \cdot (\ln \gamma')^m$, with the speed gradient $\ln \gamma' = 0 \text{ c}^{-1}$. For example, according to the curved lines in Fig. 1, it is possible to make the conclusion that the viscosity of mixes with the minimum quantity of perlite is equal to $\eta = 177 \text{ Pa}\cdot\text{s}$ or a little above, than in the mixes with the maximum

maintenance of the given filling material ($\eta = 124.9 \text{ Pa}\cdot\text{s}$), and with a lower ability of the structure for restoration. According to the 18 research data findings, an adequate experimental and statistical model was built, which describes the impact of variable factors on the viscosity of the mixture (an experimental error $S_e = 38.1$), see Eq. (1):

$$\eta \text{ (Pa}\cdot\text{s)} = 399.0 \pm 0x_1 - 89.3x_1^2 \pm 0x_1x_2 - 21.9x_1x_3 - 23.6x_1x_4 + 41.7x_2 - 57.3x_2^2 + 19.5x_2x_3 + 22.7x_2x_4 + 27.2x_3 - 114.5x_3^2 + 25.0x_3x_4 + 69.2x_4 \pm 0x_4^2 \quad (1)$$

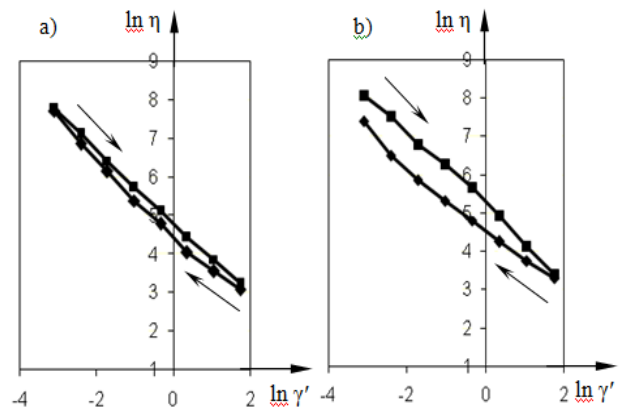


Figure 1. The curves of viscosity with an increasing and decreasing gradient of the speed of deformations for the compositions with the maximum (a) and minimum (b) contents of perlite

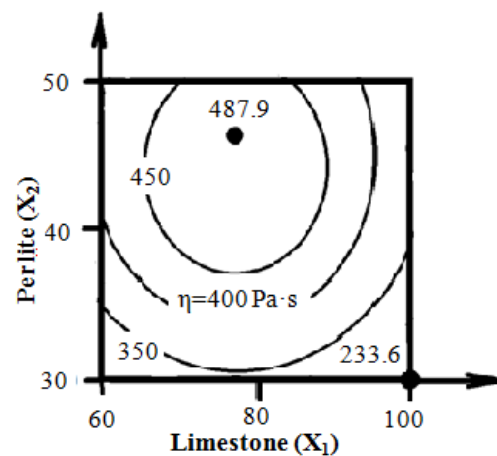


Figure 2. The influence of the powdered limestone and perlite on the viscosity of the mix

In accordance with this model, a diagram has been constructed. Fig. 2 illustrates the effect of the amount of the powdered limestone and perlite on the viscosity of the mix. The diagram is built for structures with an average quantity of methylhydroxyethylcellulose ($x_3=0$) and the maximum quantity of the re-dispersible powder Vinnapas ($x_4 = 1$). The analysis of the diagram allows us to say that the compositions with the average number of limestone (80 m.u.) and the amount of perlite about 45 m.u. are the most viscous. Therefore, at the observance of a constant flowability of a mix at the

expense of a change of the quantity of a small filling material, it is possible to essentially change the viscosity of a mix.

Durability cannot be considered a basic property for lightweight mortars, however, this figure should be provided at a sufficient level for this material. On the base of a similar model (1), a diagram shown in Fig. 3 has been built. It shows the influence of the quantity of the limestone and perlite by the amount of the compressive strength for structures, which is identical by quantity to the methylhydroxyethylcellulose and Vinnapas that are presented in Fig. 2.

As it is possible to notice from the diagram, more viscous structures also show more durability. Generally, within the factorial space of the experiment, under the influence of a variation of factors of the structure, the durability of a plaster mix changes two times from 2.4 to 4.3 MPa. Thus, the structures with an average quantity of a limestone demonstrate the strongest character (about 80 m.u.). At the same time, the quantity of perlite at which the material reaches its maximum strength depends on the dosage of Tylose. Therefore, with a higher level of the factor x_3 , and a larger number of perlite (x_2), we can observe the maximum strength.

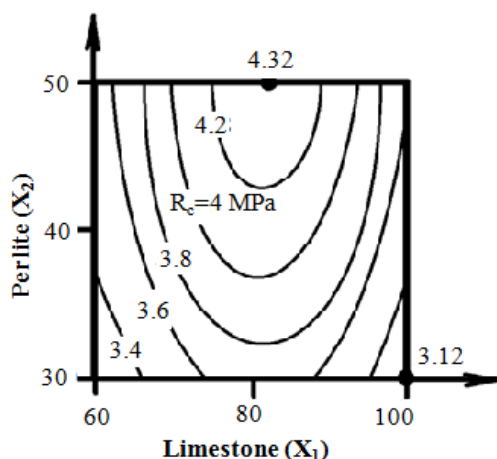


Figure 3. The influence of a ground limestone and perlite on the compressive strength

The frost resistance of a lightweight plaster mix is also included in the complex of the investigated properties within the limits of a given work. The results of research have shown that the compositions with an equal or above average quantity of methylhydroxyethylcellulose and Vinnapas (1.15 and 1.5 m.u.) respectively show frost resistance not below 50 cycles, which is a sufficient level for the given type of material.

Density can be considered as the most important property of lightweight plaster mixes because this indicator defines their heat-protection ability. The analysis of hardened composites has shown that at equal or above average quantity of methylhydroxyethylcellulose and Vinnapas, the values of the density of facing plasters do not exceed 1200 kg/m^3 , which is more preferable in comparison with the 1500 kg/m^3 described as the standard, and even 1300 kg/m^3 which has been recommended. Moreover, it is possible to notice that with the increase of the quantity

of the ground limestone from 60 to 80 m.u., the density of plaster mixes did not raise practically in any of the experimental factor space.

4. SUMMARY AND CONCLUSIONS

The above described effects can be explained as the changes of the mineral framing of packing particles; however, it cannot be assumed that the composites durability is provided by the low-strength perlite and limestone. The indirect proof of this is that the strongest solutions (above 4.2 MPa) turn out in the area with the maximum quantity of the re-dispersible powder Vinnapas and methylhydroxyethylcellulose, which are in a greater degree the factors that influence the cement matrix.

Thereby, the carried out analysis of the influence of the composition of the lightweight plaster mix on their indicators of quality - viscosity, durability, frost resistance and density, allows for the recommendation to use dry building mixes with a higher quantity of methylhydroxyethylcellulose and Vinnapas at up to 80 m.u. of the powdered limestone. Thus, the quantity of perlite as a part of a plaster mix can be lowered from 50 to 40 m.u. without any deterioration of the basic quality indicators.

5. REFERENCES

- [1] SS 28013-98. Mortars. General technical specifications, 1982.
- [2] Runova, R. F.; Nosovsky, Y. L. The technology of the modified building mortars, Textbook, Publisher KNUBiA, 2007, 53-54.
- [3] Karapuzov, E. K.; Soha, V. G. Insulation of facades, Higher Education, 2007.
- [4] Meisel, I. L. Effective insulation of expanded perlite, Building materials, No. 6 (1996), 6-7.
- [5] Karapuzov, E. K.; Soha, V. G.; Ostapenko, T. E. Materials and technology in modern construction, Higher Education, 2004.
- [6] Voznesensky, V. A.; Lyashenko, T. V.; Ivanov, Y. P.; Nikolov, I. I. Computers and optimization composite materials, 1989.
- [7] DIN 18555-2. Testing of mortars containing mineral binders; freshly mixed mortars containing aggregates of dense structure (heavy aggregates); determination of consistence, bulk density and air content, 1982.
- [8] SS 5802-86. Mortars. Test methods, 1986.
- [9] Shram, G. Practical Fundamentals of rheology and reometry, Colossus, 2003.

Contact addresses

Popov Oleg, Phd, Vice-rector

Odessa State Academy of Civil Engineering and
Architecture
Didrihsona str. 4
Odessa 65029
Ukraine
e-mail: prorector_npr@ogasa.org.ua

Moskalova Christina, Phd

Odessa State Academy of Civil Engineering and
Architecture
Department of International Relations
Didrihsona str. 4
Odessa 65029
Ukraine
e-mail: intercom@ogasa.org.ua

FREE-VIBRATION OF BERNOULLI-EULER BEAM USING THE SPECTRAL ELEMENT METHOD

SLOBODNA VIBRACIJA BERNOULLI-EULEROVE ZRAKE KORIŠTENJEM METODE SPEKTRALNOG ELEMENTA

Saida Hamioud, Salah Khalfallah

Preliminary communication

Abstract: *The present work describes the spectral finite element formulation and the solution of Bernoulli-Euler free vibrations beams. The formulation including the partial differential equations of motion, the spectral displacement field and the dynamic stiffness matrix, is established in the scope of the spectral element method. The development is recognized for the general case without considering boundary conditions. The work describes the solution of the problem using three distinct methods: (1) the finite element method, (2) the analytical method and (3) the spectral element method. Particularly, natural frequencies for clamped-free vibration of Bernoulli-Euler beams are established. In the finite element approach, the element number varied in order to improve the accurate solution. Contrary, the spectral element method requires only one to two elements. Results using this method are compared with the finite element method and analytical procedure ones. The spectral element method shows notable advantages compared to the finite element method reducing the number of elements as well as increasing the accuracy.*

Keywords: *Analytical solution, Bernoulli- Euler beam, finite element method, free vibration, Spectral element method, spectral stiffness matrix.*

Prethodno priopćenje

Sažetak: *Rad opisuje formulaciju konačnog spektralnog elementa i rješenje slobodnih vibracija Bernoulli-Eulerovih zraka. Uključujući i parcijalne diferencijalne jednačbe gibanja, spektralna polja pomaka i matricu dinamičke krutosti, uspostavljena je formulacija u okviru metode spektralnog elementa. Razvoj se promatra za općenite slučajeve, bez uzimanja rubnih uvjeta u obzir. Rad opisuje rješenje problema pomoću tri različite metode: (1) metoda konačnih elemenata, (2) analitička metoda i (3) metoda spektralnog elementa. Ustanovljene su prirodne slobodne vibracije Bernoulli-Eulerovih zraka. U metodi konačnog elementa, broj elementa mijenjao se s ciljem poboljšanja ispravnog rješenja. Nasuprot tome, metoda spektralnog elementa zahtijeva samo jedna do dva elementa. Rezultati koji koriste ovu metodu uspoređeni su s metodom konačnog elementa i metodom analitičkog pristupa. Metoda spektralnog elementa pokazala je značajnu prednost u odnosu na metodu konačnog elementa u smanjenju broja elemenata i povećanju točnosti.*

Ključne riječi: *analitičko rješenje, Bernoulli-Eulerova traka, metoda konačnog elementa, slobodna vibracija, metoda spektralnog elementa, matrica spektralne krutosti*

1. INTRODUCTION

Beam members are the basic structural components widely used in mechanical, aeronautical, automobile and civil engineering fields. For these reasons, important researchers have made efforts to deal with the static and dynamic analyses. In the Bernoulli-Euler's theory, the shear force is neglected in the formulation of the spectral and finite element methods, indifferently.

In structural mechanics, the finite element method (FEM) becomes a popular tool largely used in many areas of engineering and science. In this scope, the FE technique is chosen to analyze a crane under a moving

load [1]. The FEM and the boundary element method (BEM) are combined in order to analyze a 2D domain [2] and the Euler-Bernoulli nano-beam responses are studied by using the FEM [3]. However, the solutions using FEM become inaccurate in the higher frequency range. Vibration shapes of a structure vary with the frequencies. The FEM subdivides the structure into finite elements to accurate solutions and a large number of finite elements should be used to obtain reliable solutions.

Recently, the spectral finite element method (SFEM) based on the fast Fourier transform (FFT) has widely been used in the structural dynamic analysis. SFEM is an efficient tool for the treatment of vibration problems in

the higher frequency domain. SFEM leads to the exact solution of partial differential equations in the frequency-domain by using just one to two elements. The dynamic stiffness matrix (DSM) is formulated from the frequency-dependent shape functions that are obtained from the exact solutions of governed partial differential equations. In addition to that, the method using DSM does not require a subdivision of the structure into a larger number of elements. It can be able to predict eigen-solutions by using a minimum number of the degrees of freedom.

In this field, the basic concepts of SFEM are developed in [4]. During the last decades, SFEM is applied to the wave propagation in structures [5]. Doyle [6] and Doyle and Farris later [7] formulated SFEM for elementary isotropic waveguides. Furthermore, SFEM is developed for higher-order waveguides [8]. In general, many researchers applied SFEM to analyze the dynamic problems of beams, plates, trusses and other complex structures [9-11]. In the same context, the spectral element models are applied to the study of free vibrations and wave propagation analysis of uniform and tapered rotating beams [12].

In the present work, the SFEM formulation is developed to analyze the free vibration of the Euler-Bernoulli beams. By using dynamic shape functions and the dynamic stiffness method of beams, the natural frequencies of clamped-free boundary conditions are evaluated. The study can be easily applied to other boundary conditions. The SFEM results compared with the FEM ones show a notable accuracy by using a reduced finite element number. Practically, SFEM leads to the exact solution and needs less computational effort and time computing.

2. MATHEMATICAL FORMULATIONS

This section illustrates the formulation of clamped-free vibration beams with the finite element method, the spectral element method, and finally with the conventional analytical solution.

2.1. Finite element method

A prismatic beam having the length L , a cross section Ω , a moment of inertia I , Young's modulus E and a density ρ , is selected (Figure 1).

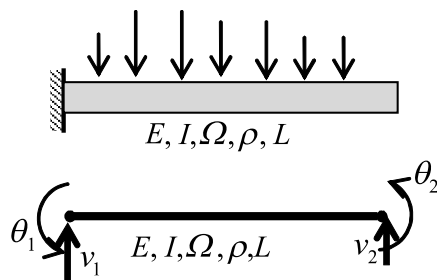


Figure 1. Geometrical and mechanical characteristics of the beam

Each node is defined by two degrees of freedom; the vertical displacement v and the slope $\theta = \frac{dv(x)}{dx}$.

Therefore, the element shown in Figure (1) using the free-body diagram then has four degrees of freedom. The displacement expression can be expressed by a polynomial function by using four constants.

$$v(x) = a_1 + a_2x + a_3x^2 + a_4x^3 = \langle \phi(x) \rangle \{a\} \quad (1)$$

The slope expression is

$$\theta(x) = \frac{dv(x)}{dx} = \langle \phi'(x) \rangle \{a\} \quad (2)$$

At the level of the element nodes, we can write

$$\{q_e\} = \begin{Bmatrix} v_1 \\ \theta_1 \\ v_2 \\ \theta_2 \end{Bmatrix} = \begin{bmatrix} 1 & 0 & 0 & 0 \\ 0 & 1 & 0 & 0 \\ 1 & L & L^2 & L^3 \\ 0 & 1 & 2L & 3L^2 \end{bmatrix} \{a\} = [A] \{a\} \quad (3)$$

In the compacted form, the relation (3) can be written as

$$\{a\} = [A]^{-1} \{q_e\} \quad (4)$$

The substitution of equation (4) into (1), the displacement field becomes

$$v(x) = \langle \phi(x) \rangle [A]^{-1} \{q_e\} \quad (5)$$

or,

$$v(x) = \langle N(x) \rangle \{q_e\} \quad (6)$$

Where,

$$\langle N(x) \rangle = \langle \phi(x) \rangle [A]^{-1} \quad (7)$$

The shape functions (7) can be derived as

$$N_1(x) = (1 - \frac{3}{L^2}x^2 + \frac{2}{L^3}x^3) \quad (8.1)$$

$$N_2(x) = (x - \frac{2}{L}x^2 + \frac{1}{L^2}x^3) \quad (8.2)$$

$$N_3(x) = (\frac{3}{L^2}x^2 - \frac{2}{L^3}x^3) \quad (8.3)$$

$$N_4(x) = (-\frac{1}{L}x^2 + \frac{1}{L^2}x^3) \quad (8.4)$$

The strain energy of the element can be developed as

$$U_e = \frac{1}{2} \int_L \frac{M^2(x)}{EI} dx = \frac{1}{2} \int_L EI \left(\frac{d^2v(x)}{dx^2} \right) dx \quad (9)$$

The substitution of the displacement expression (6) in the relationship (9) gives

$$U_e = \frac{1}{2} \langle q_e \rangle EI \int_0^L \left\{ \frac{d^2N_i}{dx^2} \right\} \left\langle \frac{d^2N_i}{dx^2} \right\rangle dx \{q_e\} \quad (10)$$

The stiffness matrix of the finite element is therefore

$$[K_e] = EI \int_0^L \left\{ \frac{\partial^2 N_i}{\partial x^2} \right\} \left\langle \frac{\partial^2 N_i}{\partial x^2} \right\rangle dx \quad (11)$$

The parameters of the stiffness matrix (11) are

$$[K_e] = \begin{bmatrix} \frac{12EI}{L^3} & \frac{6EI}{L^2} & -\frac{12EI}{L^3} & \frac{6EI}{L^2} \\ \frac{6EI}{L^2} & \frac{4EI}{L} & -\frac{6EI}{L^2} & \frac{2EI}{L} \\ -\frac{12EI}{L^3} & -\frac{6EI}{L^2} & \frac{12EI}{L^3} & -\frac{6EI}{L^2} \\ \frac{6EI}{L^2} & \frac{2EI}{L} & -\frac{6EI}{L^2} & \frac{4EI}{L} \end{bmatrix} \quad (12)$$

In the same manner, the mass matrix can be deduced by

$$[M_e] = \rho\Omega \int_0^L \{N_i(x)\} \langle N_i(x) \rangle dx \quad (13)$$

The introduction of the relation (8) into (13), the consistent mass matrix can be derived

$$[M_e] = \frac{\rho\Omega L}{420} \begin{bmatrix} 156 & 22L & 54 & -13L \\ 22L & 4L^2 & 13L & -3L^2 \\ 54 & 13L & 156 & -22L \\ -13L & -3L^2 & -22L & 4L^2 \end{bmatrix} \quad (14)$$

If a lumped mass hypothesis is considered, the mass matrix can be written as

$$[M_e] = \frac{\rho\Omega L}{2} \begin{bmatrix} 1 & 0 & 0 & 0 \\ 0 & 0 & 0 & 0 \\ 0 & 0 & 1 & 0 \\ 0 & 0 & 0 & 0 \end{bmatrix} \quad (15)$$

Applying boundary conditions $v(0) = 0$ and

$\frac{\partial v(0)}{\partial x} = 0$, the Lagrange's equations becomes

$$[K_e] \{q_e\} = \omega^2 [M_e] \{q_e\} \quad (16)$$

Case 1: Lumped mass hypothesis

$$\begin{bmatrix} \frac{12}{L^3} & -\frac{6}{L^2} \\ -\frac{6}{L^2} & \frac{4}{L} \end{bmatrix} - \frac{\omega^2 \rho\Omega L}{2EI} \begin{bmatrix} 1 & 0 \\ 0 & 0 \end{bmatrix} = 0. \quad (17)$$

The free vibration pulsation is then

$$\omega = \frac{\sqrt{6}}{L^2} \sqrt{\frac{EI}{\rho\Omega}} = \frac{2.4495}{L^2} \sqrt{\frac{EI}{\rho\Omega}} \quad (18)$$

Case 2: Consistent mass hypothesis

$$\begin{bmatrix} 12 & -6L \\ -6L & 4L^2 \end{bmatrix} - \frac{\omega^2 \rho\Omega L^4}{210EI} \begin{bmatrix} 78 & -11L \\ -11L & 4L^2 \end{bmatrix} = 0. \quad (19)$$

Set $\lambda = \frac{\omega^2 \rho\Omega L^4}{210EI}$, the solutions of the previous equation are

$$\lambda_1 = 0.0594295 \quad (20.1)$$

$$\lambda_2 = 5.76914 \quad (20.2)$$

The corresponding circular frequencies can be computed as

$$\omega_{c1} = \frac{3.533}{L^2} \sqrt{\frac{EI}{\rho\Omega}} \quad (21.1)$$

$$\omega_{c2} = \frac{34.807}{L^2} \sqrt{\frac{EI}{\rho\Omega}} \quad (21.2)$$

When comparing the obtained pulsations (18) and (21), it is necessary to adopt the consistent mass hypothesis in the study.

2.2. Analytical method

In the Bernoulli-Euler's beam theory, shear strains are neglected. These mean that the plane section before loading remains plane after loading.

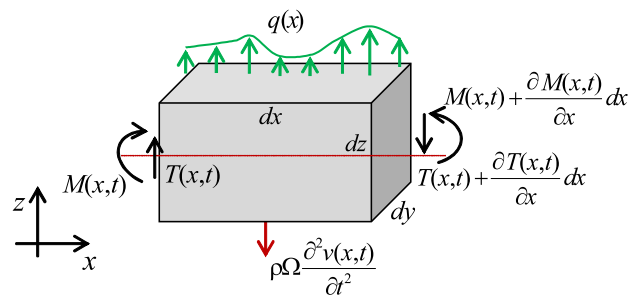


Figure 2. Free body diagram of the element dx

2.2.1. Equation of motion

Consider a free body diagram of a beam element (Figure 2) where $M(x, t)$ and $T(x, t)$ are the bending moment and the shear force at x and time t , respectively.

$q(x)$ is the external loading and $\rho\Omega \frac{\partial^2 v(x, t)}{\partial t^2}$ is the inertia force acting on the beam element.

The equilibrium equation according to the vertical axis is

$$T(x, t) - \left(T(x, t) + \frac{\partial T(x, t)}{\partial x} dx \right) - q(x) dx - \rho\Omega \frac{\partial^2 v(x, t)}{\partial t^2} dx = 0 \quad (22)$$

or,

$$\frac{\partial T(x, t)}{\partial x} = q(x) dx - \rho\Omega \frac{\partial^2 v(x, t)}{\partial t^2} \quad (23)$$

Since $T(x, t) = \frac{\partial M(x, t)}{\partial x}$ and $M(x, t) = EI \frac{\partial^2 v(x, t)}{\partial x^2}$,

the equation (23) can be written in the general partial differential equation as

$$\frac{\partial^4 v(x, t)}{\partial x^4} + \frac{\rho\Omega}{EI} \frac{\partial^2 v(x, t)}{\partial t^2} = \frac{q(x)}{EI}. \quad (24)$$

For a free vibration, the external loads are not considered in the analysis and the equation (24) becomes

$$\frac{\partial^4 v(x,t)}{\partial x^4} + \frac{\rho\Omega}{EI} \frac{\partial^2 v(x,t)}{\partial t^2} = 0. \tag{25}$$

The general solution of the equation (25) by using a separated variable method can be introduced.

$$v(x,t) = X(x) \cdot Y(t) \tag{26}$$

The relationships (25) and (26) deal to

$$\frac{EI}{\rho\Omega} \frac{d^4 X(x)}{dx^4} = - \frac{d^2 Y(t)}{dt^2} = \omega^2 = cste \tag{27}$$

The equation (27) can be written as

$$\frac{d^4 v(x)}{dx^4} = \frac{\omega^2 \rho\Omega}{EI} X(x) \tag{28.1}$$

$$\frac{d^2 Y(t)}{dt^2} = \omega^2 Y(t) \tag{28.2}$$

Set $\alpha^4 = \frac{\omega^2 \rho\Omega}{EI}$, the first differential equation (28.1) can be written

$$\frac{d^4 X(x)}{dx^4} - \alpha^4 X(x) = 0. \tag{29}$$

The spatial solution of the equation (29) is

$$X(x) = C e^{\beta x} \tag{30}$$

Substituting the equation (30) in the equation (29)

$$(\beta^4 - \alpha^4) C e^{\beta x} = 0. \tag{31}$$

The spatial solution of the equation (31) can be deduced as

$$X(x) = c_1 e^{i\alpha x} + c_2 e^{-i\alpha x} + c_3 e^{\alpha x} + c_4 e^{-\alpha x} \tag{32}$$

Thus, the general displacement field is

$$v(x,t) = [c_1 e^{i\alpha x} + c_2 e^{-i\alpha x} + c_3 e^{\alpha x} + c_4 e^{-\alpha x}] \cdot e^{i\omega t} \tag{33}$$

This spatial solution (32) can be written as

$$X(x,\omega) = A_1 \cos \alpha x + A_2 e^{-\alpha x} + A_3 \sin \alpha x + A_4 e^{\alpha x} \tag{34}$$

The application of the boundary conditions of a clamped-free beam are

$$X(x=0, \omega) = 0 \tag{35.1}$$

$$\frac{dX}{dx}(x=0, \omega) = 0 \tag{35.2}$$

$$\frac{dX}{dx}(x=L, \omega) = 0 \tag{35.2}$$

$$\frac{d^2 X}{dx^2}(x=L, \omega) = 0 \tag{35.3}$$

$$\frac{d^3 X}{dx^3}(x=L, \omega) = 0 \tag{35.4}$$

By applying the boundary conditions, we can build the following matrix.

$$[A(\lambda)] = \begin{bmatrix} 1 & 1 & 0 & 1 \\ 0 & -1 & 1 & 1 \\ -\cos \lambda & e^{-\lambda} & -\sin \lambda & e^\lambda \\ \sin \lambda & -e^{-\lambda} & -\cos \lambda & e^\lambda \end{bmatrix} \tag{36}$$

With $\lambda = \alpha L$

The determinant of the matrix $A(\lambda)$ must be null.

$$-4(1 + \cos \lambda \cdot \cosh(\lambda)) = 0 \tag{37}$$

The first five solutions of the equation (37) are regrouped in the table (1).

Table 1. First five eigen-values

Solution	1	2	3	4	5
$\lambda = \alpha L$	1.8751	4.69409	7.85476	10.9955	14.1372

2.3. Spectral element method

The partial differential equation (25) can be solved by using the Fourier decomposition of the displacement field into the sum of the harmonic vibration as

$$v(x,t) = \frac{1}{N} \sum_{n=0}^{N-1} W_n(x) \cdot e^{i\omega_n t} \tag{38}$$

By substituting the equation (38) into the relationship (25), we get the eigen-values of the problem for $\omega = \omega_n$.

$$\frac{d^4 W(x)}{dx^4} - \alpha^4 W(x) = 0 \tag{39}$$

Then the solution of the equation (39) is

$$W(x,\omega) = c_1 \cos \alpha x + c_2 \sin \alpha x + c_3 \cosh \alpha x + c_4 \sinh \alpha x \tag{40}$$

The nodal displacement and the slope at both ends can be expressed as

$$\{q_e\} = \begin{Bmatrix} v_1 \\ \theta_1 \\ v_2 \\ \theta_2 \end{Bmatrix} \begin{bmatrix} 1 & 0 & 1 & 0 \\ 0 & \alpha & 0 & \alpha \\ \cos \alpha L & \sin \alpha L & \cosh \alpha L & \sinh \alpha L \\ -\alpha \cos \alpha L & \alpha \cos \alpha L & \alpha \sinh \alpha L & \alpha \cosh \alpha L \end{bmatrix} \tag{41}$$

or,

$$\{q_e\} = [B(\omega)] \{c\} \tag{42}$$

When using the equation (40), transverse shear forces and bending moments at element node level are

$$\{F_e\} = \begin{Bmatrix} T_1 \\ M_1 \\ -T_2 \\ -M_2 \end{Bmatrix} = EI \begin{bmatrix} 0 & -\alpha^3 & 0 & \alpha^3 \\ \alpha^2 & 0 & -\alpha^2 & 0 \\ -\alpha^3 \cdot \sin \alpha L & \alpha^3 \cdot \cos \alpha L & -\alpha^3 \cdot \sinh \alpha L & -\alpha^3 \cdot \cosh \alpha L \\ -\alpha^2 \cdot \cos \alpha L & -\alpha^2 \cdot \sin \alpha L & \alpha^2 \cdot \cosh \alpha L & \alpha^2 \cdot \sinh \alpha L \end{bmatrix} \begin{Bmatrix} c_1 \\ c_2 \\ c_3 \\ c_4 \end{Bmatrix} \tag{43}$$

or,

$$\{F_e\} = EI [F(\omega)] \{c\} = EI [F(\omega)] \cdot [B(\omega)]^{-1} \{q_e\} \tag{44}$$

The quantity $(EI \cdot [F(\omega)] \cdot [B(\omega)]^{-1})$ is called the spectral stiffness matrix.

Finally, the parameters of the spectral element matrix of the Euler-Bernoulli beam are given by

$$K_{11} = K_{33} = \eta(\alpha L)^3 [\cos \alpha L \sinh \alpha L + \sin \alpha L \cosh \alpha L] \quad (45.1)$$

$$K_{22} = K_{44} = \eta \alpha L^3 [-\cos \alpha L \sinh \alpha L + \sin \alpha L \cosh \alpha L] \quad (45.2)$$

$$K_{12} = -K_{34} = \eta \alpha^2 L^3 \cdot \sin \alpha L \sinh \alpha L \quad (45.3)$$

$$K_{13} = -\eta(\alpha L)^3 [\sin \alpha L + \sinh \alpha L] \quad (45.4)$$

$$K_{14} = -K_{23} = \eta \alpha^2 L^3 [-\cos \alpha L + \cosh \alpha L] \quad (45.5)$$

$$K_{24} = \eta \alpha L^3 [-\sin \alpha L + \sinh \alpha L] \quad (45.6)$$

$$\text{With, } h = \frac{1}{1 - \cos \alpha L \cosh \alpha L}$$

After obtaining the spectral element matrix and applying the boundary conditions, the determinant of the spectral element matrix is zero.

$$|K| = K_{33} \cdot K_{44} - K_{34}^2 = 0 \quad (46)$$

The equation (46) leads to compute pulsations of free vibration.

$$\tanh^2(\alpha L) - \sin^2(\alpha L) = 0 \quad (47)$$

The solutions of the previous equation are, sequentially

$$\alpha_1 = 1.8751, \alpha_2 = 4.69409, \alpha_3 = 7.85475,$$

$$\alpha_4 = 10.9955, \alpha_5 = 14.1372, \dots$$

They are the exact solutions of the partial differential equation (39).

3. OBTAINED RESULTS

In this section, a clamped-free beam (Figure 3) is considered. Mechanical and geometrical data are regrouped in Table 3.

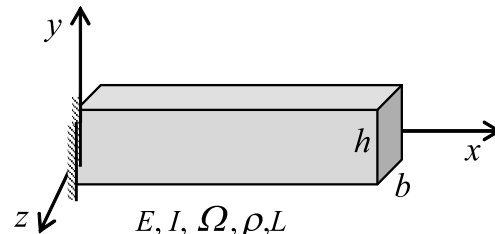


Figure 3. Studied beam

Table 3. Properties of the beam used

b (cm)	h (cm)	L (m)	E (N/m ²)	ρ (kg/m ³)
20	20	1	10^{11}	1000

Table 4. First five modes of vibration (rad/s)

Mode	1	2	3	4	5	Ratio
2 elements (SFEM)	203	1272.156	3565.087	6980.219	-	0.0%
20 elements (FEM)	203	1272.16	3562.03	6980.22	11540.73	0.155%
Exact Solution	203	1272.156	3565.087	6980.219	11538.940	-

3.1. Finite element method

The obtained results by using the finite element method are regrouped in Table (4). The first five modes of the clamped-free vibration beam are regrouped. The beam is meshed of different meshes as: 2, 5, 10, 15 and 20 elements.

Table (4) shows that the convergence towards the exact results is validated when 20 finite beam elements are used. Moreover, higher-order modes of vibration have a notable influence on the cantilever beam vibration. To accurate the dynamic results, it's necessary to use an important number of elements and a higher order of modes of vibration simultaneously.

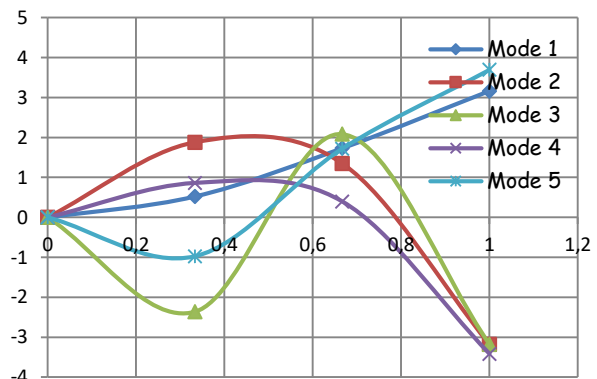


Figure 4. Transversal vibration of the first five modes

Figures (4-5) illustrate the shape modes of the vibration for the first five modes of the vibration. Figures (4-5) show the transversal and rotational shape modes of the vibration.

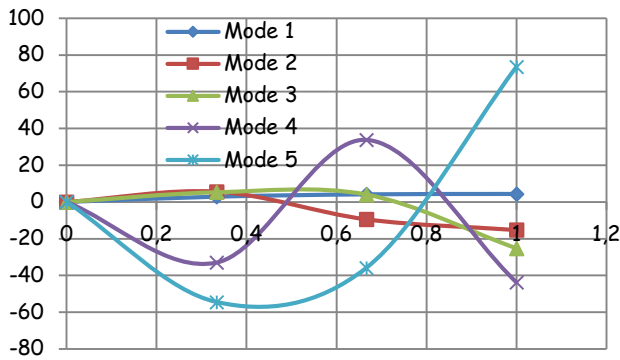


Figure 5. Rotational vibration of the first five modes

3.2. Spectral finite element method

Table (5) shows a comparison between the results obtained by the spectral element method (2 elements), the finite element method (20 elements) and the analytical solution. The analysis shows that the numerical computing can be achieved in the spectral element results and analytical method when the number of elements must be superior then 20.

Figure 6 shows the comparison between the diagonal stiffness parameters evaluated by using the FEM and SFEM. The finite element diagonal parameters are under-estimated compared to the SFEM ones.

Table 5. Comparison between the results of the methods used

Mode	1	2	3	4	5	Ratio
1 element	204	2009.60				57.96%
2 elements	203	1283	4339	12594		80.42%
5 elements	203	1273	3575	7062	11721	1.577%
10 elements	203	1272.20	3563	6986.90	11568	0.251%
15 elements	203	1272.18	3562.50	6983.20	11560.35	0.185%
20 elements	203	1272.16	3562.03	6980.22	11540.73	0.155%
Exact Solution (rad/s)	203	1272.156	3565.087	6980.219	11538.940	-

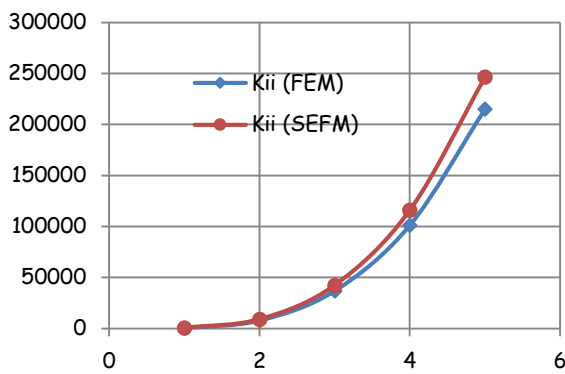


Figure 6. Diagonal stiffness parameters

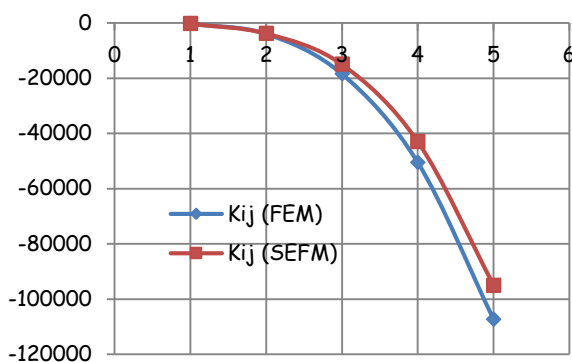


Figure 7. Non-diagonal stiffness parameters

In the same context, Figure 7 shows the comparison between the non-diagonal stiffness parameters computed with the FEM and SFEM. The figure illustrates that the finite element non-diagonal parameters are over-estimated compared to the SFEM ones. Rods and Euler-Bernoulli beams behave in the same manner corresponding to the diagonal and non-diagonal stiffness parameter variations evaluated with FEM and SFEM

[13]. Finally, what can bring the effect of shear forces on the free vibration of beam responses [14]?

4. CONCLUSIONS

In this work, the spectral finite element method (SFEM) is described as a numerical approach to predict the free-vibration of the Euler-Bernoulli beam responses. The exactness of the SFEM is validated by using only one to two elements. On the contrary, the finite element method requires important finite elements to reach an accurate solution. In this case, to predict the solution by using the FEM it is necessary to incorporate higher modes of vibration in the analysis.

The comparison is performed by the calculation of circular frequencies. The study shows that the proposed method is practical, efficient and can be used as a reference for the convergence criteria of structural dynamics via the finite element method.

The convergence of SFEM is principally due to the fact that the diagonal finite element method parameters are under-estimated, but the non-diagonal ones are over-estimated compared to the SFEM stiffness parameters.

5. REFERENCES

[1] Wu, J. J.; Whittaker, A. R.; Cartmell, M. P. (2000), The use of finite element techniques for calculating the dynamic response of structures to moving load, Computers and Structures, 78, pp. 789–799.
 [2] Anderson, L.; Nielsen, S. R. K.; Krenk, S. (2007), Numerical methods for analysis of structure and

ground vibration from moving loads, *Computers and Structures*, 85, pp. 43–58.

- [3] Eltahir, M. A.; Alshorbagy, A. E.; Mahmoud, F. F. (2013), Vibration analysis of Euler-Bernoulli nanobeams by using finite element method, *Applied mathematical modeling*, 37, pp. 4787-4797.
- [4] Narayanan, G. V.; Beskos, D. E. (1978), Use of dynamic influence coefficients in forced vibration problems with the aid of fast Fourier transform, *Computers and structures*, Vol. 9, pp. 145-150.
- [5] Doyle, J. F. (1988), A spectrally formulated finite elements for longitudinal wave propagation. *International Journal of Analytical and Experimental Modal Analysis*, 3, 1–5.
- [7] Doyle, J. F.; Farris, T. N. (1990), A spectrally formulated finite element for flexural wave propagation in beams. *International Journal of Analytical and Experimental Modal Analysis*, 5, pp. 13-23.
- [8] Gonçalves, P. J. P.; Brenner, M. J.; Elliott, S. J. (2007), Numerical evaluation of high-order modes of vibration in uniform Euler-Bernoulli beams, *Journal of sound and vibration*, 301, pp. 1035-1039.
- [10] Choi, J.; Inman, D. J. (2014), Spectrally formulated modeling of cable-harnessed structures, *Journal of sound and vibration*, 333 (14), pp. 3286-3304.
- [11] El Baroudi, A.; Razafirmahery, F. (2015), Transverse vibration analysis of Euler- Bernoulli beam carrying masse submerged in fluid, *Inter. Journal of Engineering and Technology*, 4(2), pp. 369-380.
- [12] Vinod, K. G.; Gopalakrishnan, S.; Ganguli, R. (2007), Free vibration and wave propagation analysis of uniform and tapered rotating beams using spectrally formulated finite elements. *International Journal of Solides and Structures*, 44, pp. 5875-5893.
- [13] Hamioud, S.; Khalfallah, S. (2016), Analyse des vibrations libres d'une barre par la méthode des éléments spectraux, *Algérie & Equipement*, accepté.
- [14] Hamioud, S.; Khalfallah, S. Free vibrations of Timoshenko beam by the spectral element method, in preparation.
- [6] Doyle, J. F. (1997), *Wave Propagation in Structures: Spectral Analysis Using Fast Discrete Fourier Transforms*, 2nd edition, Springer New York.
- [9] Ranjan, R. (2010), Hp spectral method for structural mechanics and fluid dynamic problems, Ph. D. thesis, Texas University, 222 p.

Contact addresses

M. Khalfallah Salah

Institution : National Polytechnic School of Constantine, Algeria
 Adress : B. P 75, A, Nouvelle ville RP, 25000 Constantine, Algérie.
 khalfallah_s25@yahoo.com

Ms. Hamioud Saida

Institution : University of Jijel, Algeria.
 Adress : HAMILOUD SAIDA
 Civil Engineering Departement
 B. P 98, Ouled Aissa, 18000 Jijel, Algérie.
 hamioud.saida@yahoo.com

THE QUANTITATIVE CHARACTERISTICS OF THE MICROSTRUCTURE OF BUILDING COMPOSITES

KVANTITATIVNE KARAKTERISTIKE MIKROSTRUKTURE GRAĐEVINSKIH KOMPOZITA

Irina Dovgan, Andrey Kolesnikov, Svetlana Semenova, Olga Zaitseva

Preliminary communication

Abstract: The article deals with the algorithm of the building material structure based on its photomicrographs by means of point images statistical analysis. The obtained values allow the defining of the basic characteristics of the material structure.

Keywords: building materials, image processing, Nih Image, point images, statistical geometry

Prethodno priopćenje

Sažetak: U radu se razmatra algoritam strukture građevinskog materijala na temelju njegove fotomikrografije pomoću statističke analize točkastih slika. Dobivene vrijednosti omogućavaju definiranje osnovnih karakteristika strukture materijala.

Ključne riječi: građevinski materijali, obrada slika, Nih Image, točkaste slike, statistička geometrija

1. INTRODUCTION

One of the directions of materials science that has significantly developed in the last decade is a structure-based research of the modeling and optimization of building composites [1,2]. The success of this research area is largely due to the possibility of a more effective control of the desired performance formation based on structural information, the evolving theory of the self-organization of dispersed systems [3] and the overall technical level of the improvement in the field of the research of composite materials. The qualitative results about the self-organizing processes in the materials and their models have been obtained in a number of studies [4]. A transition to the quantitative values and their correlations is more productive in choosing the optimal control actions on the composite properties by using the statistical procedures. In relation to that, it is necessary to analyze the possibility of obtaining such characteristics by simple means, by considering their content component and the possibility of building the "structure-properties" of statistical models. Such models, in comparison to the traditional "composition-properties" for material science models, have a number of advantages, i.e. a clear quantitative and qualitative interpretation, the possibility of considering the received dependences of the materials' broad classes, the possibility of their use to express the estimation of properties, and an easy transition to the physical models.

In composite materials, the interaction between their components – □ binder, filler and additives, is complex [5]. This, in particular, can appear in the tendency to form the distributions of components' particles, as well

as the pores and internal separation boundary in accordance with the laws that differ from the purely random ones, given by the Poisson law. At each fixed scale level, such a deviation can belong to two types (Fig. 1).

If the attraction force between the particles dominates, they form clusters. At the opposite tendency, quasi-regular structures are formed based on the maximum repulsion principle. This distribution is easy to acquire by giving the same charges to the movable particles.

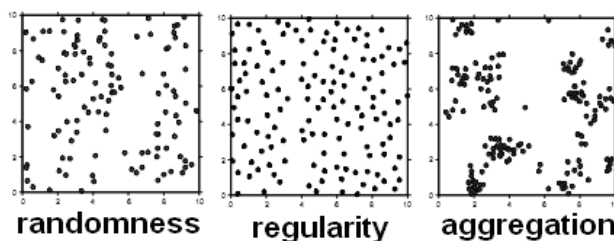


Figure 1. The nature of point distribution on a plane.

As a "reference point" for the complexity degree, it is possible to accept the DLVO theory that takes into account the only van-der-Waals and coulomb interactions. Particles obeying this theory are already characterized by structure organization and the complex interactions, i.e. periodic colloidal structures [5], long and short coagulation contacts are formed. The transition to the particles of complex nature, the possibility of structural and mechanical barriers formation, and other causes significantly complicate the accurate examination of the particles interaction in the composite binder test.

2. MAIN SECTION

One way to solve the problems arising in the study of the composite particles interaction is the transition to a simplified system - the original model. The distribution of macroscopic particles on the surface and in the bulk liquid phase [4] can be used particularly in such a model. In such systems, despite their relative simplicity and the ease of the experimental methods, processes of structure formation occur. Due to the capillary forces between particulates (2 to 5 mm), there is a preferential attraction; and what should additionally be taken into account at close range is their electrostatic, van der Waals and other types of interactions. The considered method of the processes of physical modeling in composites by using a particulate was used [4], and the introduction of a quantitative description increases its productivity.

One of the easiest ways to study the macrostructure of composites and their models based on the optical methods of studying at a relatively low increase (10x-1000x), for which a microscopic investigation in the reflected light is used which has not lost its relevance in spite of the emergence and development of more advanced techniques [6]. Enhanced with the corresponding means of fixing images (CCD-camera and the associated equipment, together with the software), the conventional microscopic study is transformed into computer microscopy techniques.

For a variety of materials, the structures observed by using the optical methods are characterized as small particles, pores, and other objects, and their spatial distribution can be examined.

Consider the possible options of the point objects of this type:

1. The particle components of the composite – the research is released if they are painted in different colors or vary in the gray scale.
2. The pores – there is no need for a stereological reconstruction of the observed object porous structure with the point approach.
3. Projections of cracks and internal borders' phase boundary on the chips or grinding – the point approach is possible to use in such objects only after the machine image segmentation of these lines and surfaces.
4. Mineral growths processed with a special treatment (e.g. phenolphthalein for lime in the cement stone, tannin for cracks).

The process of the investigation of these structures is as follows:

1. With the help of an electronic microscope eyepiece, converted to macro mode webcams and similar equipment, micrographs of a thin section or a smooth flat cleavage of the material are obtained. Further, it will be assumed that a preparation produced by appropriate means if necessary (such as a cement stone processed by a phenolphthalein developer). As an example, consider the implementation of the algorithm processing the micrographs of a plastering material based on gypsum and perlite [7] (Fig.2).

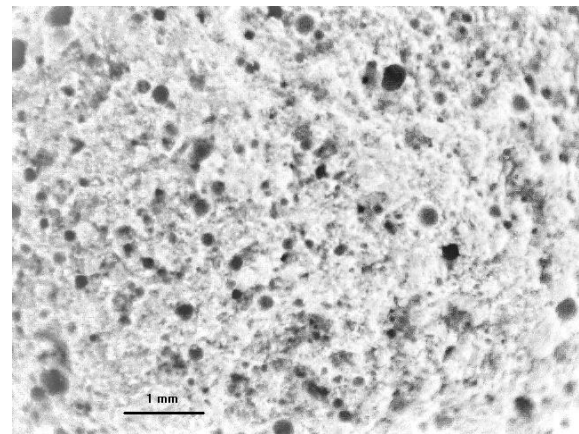


Figure 2. A photomicrograph of a material by subtracting the background light level (Scale mark - 1mm)

2. Further processing may be carried out by using a free software such as Nih Image, ImageJ and its derivatives, Image Tools and many commercial ones (e.g. Optimas). The Nih Image 1.62 Fat software [8], which has become a classic in the field of medicine and biology, was used in the emulator Executor 2.0 environment. The macro batch file for micrograph processing was written. After a background subtraction, a threshold separation image (Threshold) was carried out. Next, the filtering, which allows to remove the noise image produced by unrelated pixels was conducted. Furthermore, after the transfer to a binary image, the ultimate point of erosion (ultimate eroded point) was built. After the threshold separation and binarization, small clusters of pixels appear on the screen corresponding to the most central area of the original objects (Fig. 3).

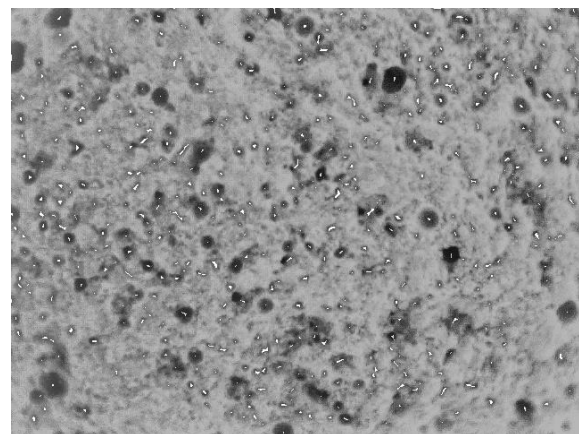


Figure 3. The ultimate erosion points imposed on the original image

Such objects may be analyzed automatically and display the values of their origin (their other parameters in the considered approach is not required) to the file (Fig. 4).

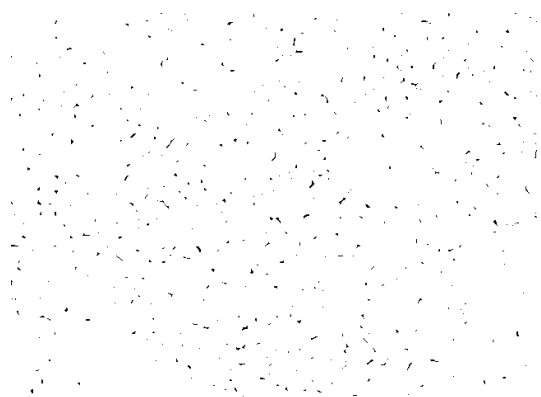


Figure 4. The ultimate erosion points of which the coordinates are determined

The third phase of the structure analysis is carried out by using the points' location on the plane and in the space analysis software (PPA (DOS), Past – Paleontological software, Ppa (mac) and others. The latter is activated as accessible on the same emulator. Consider the results of its work; they are displayed graphically.

The analysis of the distribution point can be made by a square grid (squares analysis). The square grid with side a (1) is imposed on the dot pattern.

$$a = \sqrt{\frac{\text{Preparation area}}{2 \times \text{Number of points}}} \quad (1)$$

Figure 5 shows an example of such a construction:

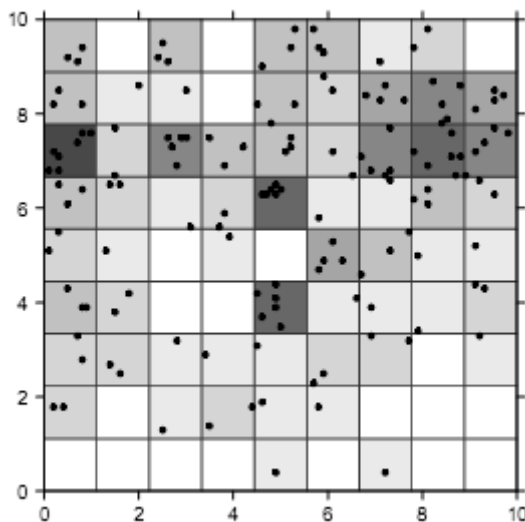


Figure 5. An analysis of the statistical characteristics of a point image by the square method

Furthermore, the number of events (in this case - of the particles or pores) in each square is calculated and the considered frequencies are processed statistically (Fig. 6).

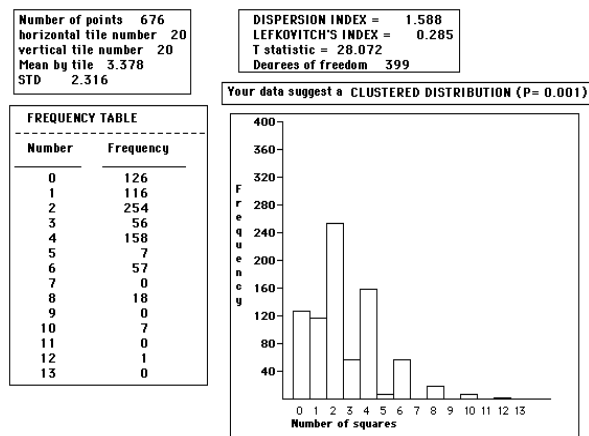


Figure 6. The results of the statistical analysis by the squares method

The essential data to decision making can be the output of the analysis results (Fig.7)

1) General data

Number of points 676
Density 18 cells/mm2

2) Indices

		Random	Meaning Regular	Clustered
Dispersion Index	2.389	=1	<1	>1
Lefkovitch's Index	0.495	=0	-1	+1
Packing Factor	0.067	=0	+1	
Eberdhart Index	1.185	1.27	<1.27	>1.27
Means/STD Index	2.323	close to 0	>0	
Equilateral Index	----	close to 1	close to 0	

Figure 7. The results and the boundary values of the point image statistical analysis

The dispersion index [9] or Fano factor is defined as the ratio of the variance σ^2 to the mean frequency μ (2)

$$D = \frac{\sigma^2}{\mu} \quad (2)$$

If $D = 1$, the image is random. This means that the set data has no dominant trend for clustering or dispersion. If $D < 1$, the point image has a regular structure, i.e. the point spread in the observed region is more or less regular. The dispersion index depends on the values of the mean values, which is why an additional criterion, the Lefkovitch index is used [10] (3) (in radians):

$$\Delta = \frac{4}{\pi} \arctg \frac{s^2}{\sigma^2} - 1 \quad (3)$$

Here s^2 - the variation of the frequency in this sample, σ^2 - the variation of random distributions, the Poisson distribution is substituted for the value of the average, $\sigma^2 = m$. As the dispersion index, $\Delta = 0$ corresponds to a random distribution, $\Delta = -1$ - regular and $\Delta = 1$ - cluster.

The Eberharda Index [11] (4) also allows on the test the assessment of the grouping of the object degree, S - the standard deviation and \bar{x} the average evaluation of the distance from a random point to the test.

$$I_E = \left(\frac{S}{\bar{x}} \right)^2 + 1 \quad (4)$$

The corresponding limit values are shown in Fig. 7. All major statistical characteristics indicate a high probability of a cluster formation in this sample.

The nature of the particles' mutual arrangement can be detected from the distribution diagram of the distance between the particles (Fig. 8). What can be found on the values of the density maxima are the approximate location of the coordination spheres (approximately 100 and 150 microns) and the mean value of the effective radius [12], characterizing the size of the "dead" space around the object under the study.

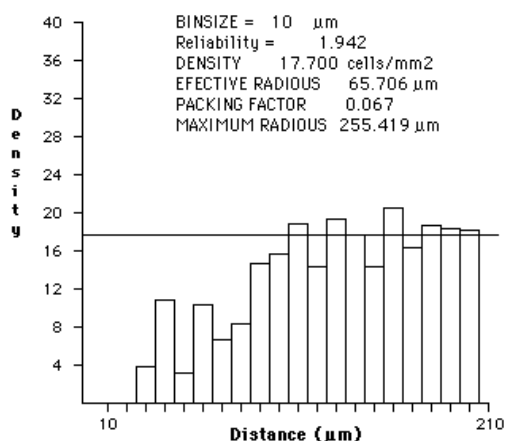


Figure 8. The distribution of distance between the particles and derivative values.

3. CONCLUSION

Thus, a consistent application of computer image and statistical processing of the micrographs and similar material structure images reveal the characteristic structure of the material and specify the conditions of their non-random distribution. This, in turn, may be interpreted as the evidence of the material self-organization process of the spatial structure that occurs at different time stages. The processes of space-time self-organization of composite materials are a significant influencing factor determining their performance.

4. REFERENCES

- [1] Bentz, D. P. Three-dimensional computer simulation of Portland cement hydration and microstructure development. *J. of the American Ceramic Society*, 80, 1997, 3-21
- [2] Bentz, D. P. Modelling cement microstructure: Pixels, particles, and property prediction. *Materials and Structures*, 32, 1999, 187-195
- [3] Bobryshev, A. H.; Kozomazov, V. N.; Babin, L. O.; Solomatov, V. I. *Sinergetika kompozitnyh materialov*. Lipeck, NPO ORIUS, 1994. 152 p.
- [4] Vyrovoy, V. N.; Dovgan', I. V.; Semenova, S. V. *Osobnosti strukturoobrazovaniya i formirovaniya svoystv polimernykh kompozitnyh materialov*, Odessa, TJeS, 2004, 168 p.
- [5] Frolov Ju.G. *Kurs kolloidnoj himii*, M., Himija, 1982, 400 p.
- [6] Sarid, D. *Exploring scanning probe microscopy with "Mathematica"*, John Wiley & Sons, Inc., New York, 1997, 262 p.
- [7] Kersh, V.; Kolesnikov, A.; Lyashenko, T.; Pidkapka, M. Structurally-oriented design of the heat insulation plastering material, *Proc. Of International conference of Advanced HVAC & Natural Gas Technology*, May 6-9, 2015, Riga, Latvia, 4p.
- [8] Schneider, C. A.; Rasband, W. S.; Eliceiri, K.W. NIH Image to ImageJ: 25 years of image analysis. *Nature Methods* 9, 671-675, 2012.
- [9] Hoel, P. G. On Indices of Dispersion. *Annals of Mathematical Statistics* 14 (2): (1943), 155-162.
- [10] Duncan, K. W. A modification to Lefkovich's index of spatial distribution, *Proceedings of the New Zealand Ecological Society*, 1972, v. 19, 158-162 pp.
- [11] Krebs, C. J. *Ecological Methodology*, 1999, 2nd ed., Addison-Welsey Educational Publishers, Inc., Menlo Park, 620 pp.
- [12] Rodiek, R. W. The density recovery profile: A method for the analysis of points in the plane applicable to retinal studies, *Visual Neuroscience*, 1995, v. 6, 95-111 pp.

Contact addresses

Svetlana Semenova, PhD, Assistant Professor
 Odessa State Academy of Civil Engineering and Architecture
 65059, Didrikhsona str. 4, Odessa, Ukraine
 Tel. +380503366911
 e-mail: svetasa@inbox.ru

THE DEVELOPMENT OF A FREQUENCY CONVERTER FOR HIGH SPEED PERMANENT MAGNET GENERATORS IN COGENERATION PLANTS

RAZVOJ PRETVARAČA FREKVENCije ZA VISOKOBRZINSKE GENERATORE S PERMANENTNIM MAGNETIMA U KOGENERACIJSKIM POSTROJENJIMA

Božo Terzić, Marin Despalatović, Goran Majić, Marijan Stergulc, Ante Kriletić, Krste Šormaz

Professional paper

Abstract: This paper describes the development of a frequency converter for high speed generators with permanent magnets that are used in cogeneration plants. A specific requirement of the converter is a transformable high frequency of the fundamental voltage harmonic. Therefore, two variants of the frequency converter in which the grid converter is the same for both structures are considered; while on the generator side of one variant, the converter based on a diode rectifier and step-up DC converter is used. On the generator side of the second variant, there is a three-phase inverter with IGBT transistors which have the same structure as the grid converter. The paper first describes the structure of power and control circuits of the frequency inverter, then the basic characteristics of the mechanical design of the power circuit of the three-phase IGBT inverter, as well as the control electronic boards that have been developed and tested. Furthermore, the paper also describes the basic features of the high speed motor generator group that serves to test the developed frequency converters. Finally, the results of the measurements on the laboratory model of the frequency converter with a diode bridge and a step-up DC / DC converter are presented.

Key words: frequency converter, permanent magnet generator, high speed electric machines

Stručni članak

Sažetak: U ovom radu opisan je razvoj pretvarača frekvencije za visokobrzinske generatore s permanentnim magnetima koji se koriste u kogeneracijskim postrojenjima. Specifičan zahtjev pretvarača je promjenljiva visoka frekvencija osnovnog harmonika napona. Stoga su razmatrane dvije varijante pretvarača u kojima je mrežni pretvarač potpuno isti za obje strukture, dok se na generatorskoj strani jedne varijante primjenjuje pretvarač temeljen na diodnom ispravljaču i uzlaznom istosmjernom pretvaraču, a u drugoj varijanti je na generatorskoj strani trofazni izmjenjivač s IGBT tranzistorima jednake strukture kao i mrežni izmjenjivač. U radu su prvo opisane strukture energetskih i upravljačkih krugova pretvarača frekvencije, a nakon toga i osnovne značajke konstrukcije energetskog dijela trofaznog IGBT izmjenjivača, kao i upravljačke elektroničke pločice koje su razvijene i testirane. Također, dane su osnovne značajke visokobrzinske motor generator grupe koja služi za testiranje razvijenih pretvarača frekvencije. Na kraju su prikazani rezultati mjerenja na laboratorijskoj maketi pretvarača frekvencije s diodnim mostom i uzlaznim DC/DC pretvaračem.

Ključne riječi: pretvarač frekvencije, generator s permanentnim magnetima, visokobrzinski električni strojevi

1. INTRODUCTION

The project “Safer and more efficient cogeneration/trigeneration plants” is carried out within the framework of the European Fund for Regional Growth (2007-2013). The Faculty of Electrical Engineering, Mechanical Engineering and Naval Architecture is the project applicant, while the company Banko d.o.o. from Split is the project partner.

Cogeneration plants transform heat from different sources into electrical energy and exploitative thermal energy through a unique thermodynamic and power

engineering process, while trigeneration plants also include production of cooling energy. Today, high-speed turbines with generators mounted on common shafts and frequency converters connected between the generator and the electrical grid are preferred for the conversion of thermal energy into electrical energy. As a consequence of generator high speeds (above 10000 min⁻¹), its voltage fundamental frequency is several times greater than the grid frequency, which requires the use of a frequency converter capable of generating voltages with high fundamental frequencies (up to 1000 Hz) in order to interface generators to the 50 Hz electrical grid.

One of the project objectives is to develop a frequency converter that will enable the connection of high speed permanent-magnet generators (PM generator) to the grid. Due to the high output frequency of the PM generator, two frequency converter structures are considered. These structures share an identical grid module while the generator module includes two variants: (1) converter consisting of a diode rectifier and a step-up DC/DC converter, (2) a three-phase converter with IGBT transistors identical to the grid converter.

In this paper, both converter structures are presented and their characteristics are explained, as well as the basic features considering the construction of power and control circuits of the three-phase converter with IGBT transistors which are an integral part of both converter structures. Furthermore, the high speed motor-generator group used for converter testing is described and the measurements results obtained on the laboratory setup of a step-up DC/DC converter based on the frequency converter are presented at the end of this paper.

2. BASIC STRUCTURES OF THE FREQUENCY CONVERTER POWER AND CONTROL CIRCUITS

A block diagram of a frequency converter with a generator module consisting of a diode rectifier and a step-up DC/DC converter is presented in Fig. 1, while Fig. 2 presents the structure of a frequency converter with identical generator and grid converters, both realized by a three-phase IGBT converter. In both structures, the grid module consists of a three-phase IGBT converter and an LCL filter. Along with its basic function of transferring energy from the DC link to the AC grid, the grid module provides an almost ideal sine waveform of the grid current ($THD_i < 5\%$) and the possibility to adjust the power factor ($\cos \varphi$) depending on the grid voltage and reactive power demand at the point of common coupling.

The advantages of the converter structure with a diode rectifier on the generator side are a less complex control structure and a DC/DC converter that is invariant to the frequency of the PM generator voltage. Therefore, the generator maximum speed is not limited by the converter structure. The basic drawback of this structure is a high amount of generator current harmonic distortion which produces additional generator losses, temperature increase and leads to lower generator efficiency. On the other hand, the structure with a three-phase IGBT converter and a sine filter on the generator side is characterized by an almost ideal sine waveform of the current and a significantly more complex vector control structure of the PM generator with different limitations due to the high frequencies of the generator voltage and the presence of a sine filter between the generator and the converter. The PM generator control structure is that of a well-known vector control implemented in the dq -rotating frame with the d -axis aligned to the rotor magnetic axis, which has been used in almost all servo drives dominated by motors with permanent magnets. Therefore, this control structure will not be presented in this paper. Instead, this paper will present the control

structure of the frequency converter based on a diode rectifier and a step-up DC/DC converter, which represents a unique solution that can be implemented in systems which include generators with a permanent magnet as well as classic synchronous generators with field windings.

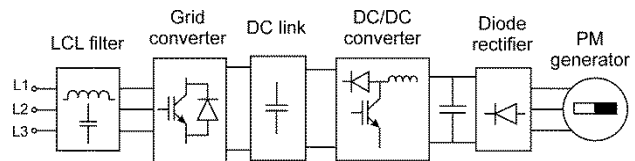


Figure 1. Block diagram of a frequency converter with a generator module consisting of a diode rectifier and a step-up DC/DC converter

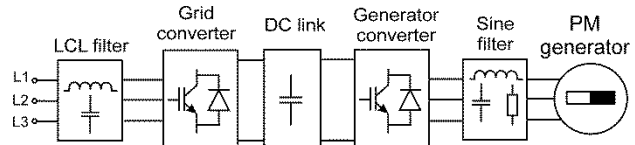


Figure 2. Block diagram of a frequency converter with an identical generator and grid converters

Fig. 3 presents a block diagram of the control structure for the frequency converter given in Fig. 1. The control of the grid converter and the step-up DC/DC converter is separated. The control structure of the grid converter provides a constant DC link voltage while the energy is transferred from the PM generator through the step-up DC/DC converter, the DC link and the grid converter to the grid. The control structure of the step-up DC/DC converter ensures the transfer of energy for a wide range of PM generator speeds, i.e. for the variable output voltage of the diode rectifier which is proportional to the generator speed.

The control structure of the grid converter is based on the vector control method implemented in the synchronous dq -rotating frame with the d -axis aligned to the grid voltage space vector [3]. This provides the control of the d - and q - current components which are proportional to the active and reactive power, respectively. The control structure is cascaded with two current feedbacks. The d - current control loop is an inner loop for which the referent value (i_d^*) is generated by the PI regulator of the DC link voltage (u_{DC}), which indicates that the outer control loop is used to control the DC link voltage measured on the capacitors. The DC link voltage is 10-15% greater than the maximum value of the grid line-to-line voltage which can be achieved as a result of the LCL filter connected in the circuit. In other words, this three-phase converter can be considered a boost converter.

The q - current control loop is independent of the DC link voltage control and its referent value (i_q^*) is set according to the desired power factor. The d - and q - voltages and currents needed for the control are obtained by measuring the instant values of phase voltages and currents, and afterwards a two-step transformation of the variables is used. First, three-phase values are transformed into a two-phase ($\alpha\beta$) stationary reference frame which is then transformed into the synchronously

rotating dq -reference frame by using the rotational angle $\theta = \omega t$.

In order to control the three-phase IGBT converter, inverse transformation is used, i.e. the referent values of the converter voltage components in the dq -reference frame (u_d^* , u_q^*) are transformed to the $\alpha\beta$ -reference frame (u_α^* , u_β^*) by using the same rotational angle θ as for the transformation of the measured quantities. The space vector modulation method is used to generate grid converter AC voltages.

The control structure of the step-up DC/DC converter is also cascaded with the inner loop controlling the generator current ($i_{G=}$) and the outer control loop controlling the generator voltage ($u_{G=}$). However, the generator voltage and current are AC quantities, and the

measuring sensors are located on the DC side of the diode rectifier since the mean values of the voltage and current on the DC side are proportional to the corresponding RMS values on the AC side. The pulse width modulation method is used to control the IGBT transistor of the DC/DC converter. During operation, the output voltage of the DC capacitors is constant (controlled by the grid converter), while the output voltage of the diode rectifier varies. This voltage is proportional to the generator voltage, which is proportional to the rotor speed for PM generators, and the presented control structure can be used to control the generator speed, which is the final objective considering the cogeneration plant operation.

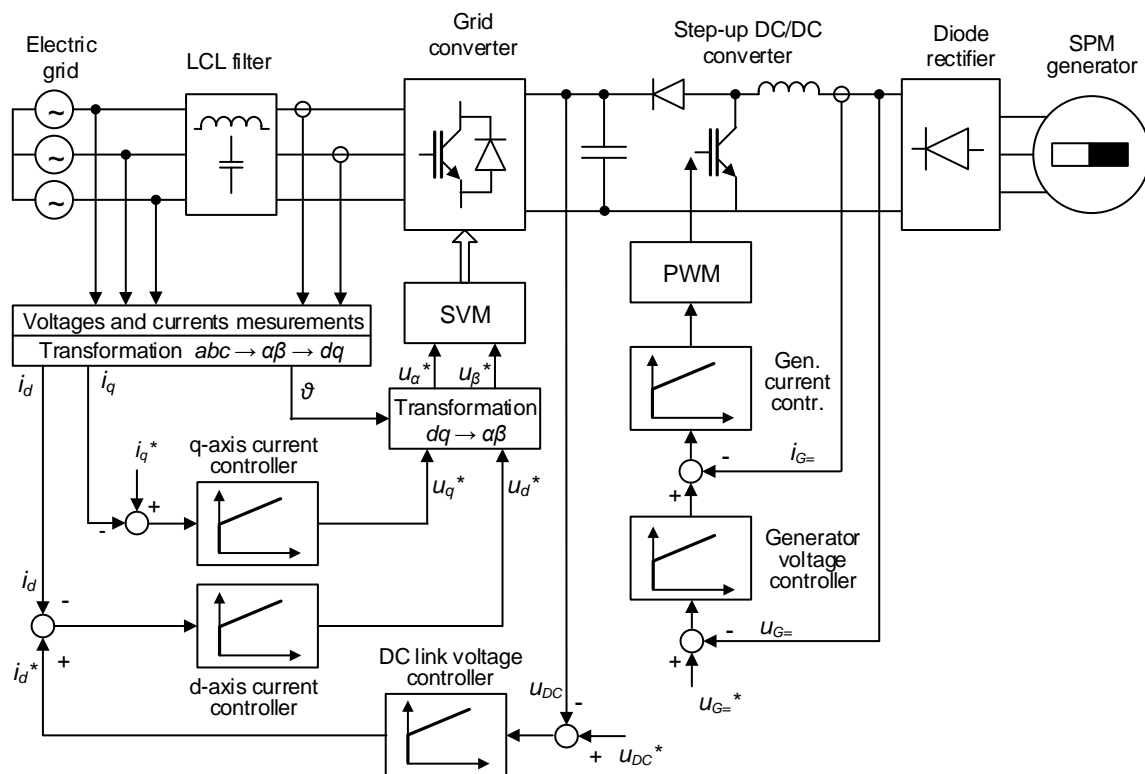


Figure 3. Block diagram of a grid converter and step-up DC/DC converter control structure

3. DEVELOPMENT OF THE FREQUENCY CONVERTER PROTOTYPE

Prototypes of both frequency converter structures are being developed within the project framework and the following section presents the basic characteristics and construction of a three-phase IGBT converter power circuit, as well as its control circuits.

Fig. 4 presents the basic structure of the power circuit and the block representation of units needed to control the frequency converter with a diode rectifier and step-up DC/DC converter. In comparison with the structure presented in Fig. 3, the DC link includes a braking circuit consisting of a resistor connected in a series with an IGBT transistor. This IGBT is turned on only when the DC link voltage exceeds the allowed limit which can occur if the converter is cut off from the grid, and in this case power needs to be dissipated on the resistor during a

short period of time to avoid an uncontrolled increase of the DC link voltage.

The three-phase IGBT converter, consisting of six IGBT transistors with freewheeling diodes, is based on FF900R12IE4 IGBT modules, manufactured by Infineon, with maximum ratings of 1200 V and 900 A. The aforementioned module presents the one phase leg of a three-phase converter with two IGBT transistors and two diodes (see Fig. 4), which suggests that the three-phase converter includes three IGBT modules mounted on a bonded fin heat sink air-cooled by a ventilator. An electronic board with six-channel driver circuits (driver unit in Fig. 4) is mounted directly on three IGBT modules and is used to transmit control signals generated by the microcontroller-based control unit. The driver unit is also used to shape control signals and to decouple the control unit from IGBT modules. It includes a short-circuit protection of IGBT modules which is

implemented by measuring the collector-emitter voltage during the conduction stage. Positive and negative DC buses consisting of 3mm wide copper sheets are mounted above the driver unit and 3mm wide isolation material is inserted between them. DC buses are connected to the capacitor block which consists of a series-parallel combination of electrolytic capacitors and resistors used to distribute the DC link voltage evenly among the series combinations of capacitors. DC buses construction requirements include a large surface area, minimal thickness and minimal space between the positive and

negative buses which is needed in order to minimize stray inductances between the capacitors and IGBT modules. In fact, sudden changes in IGBT currents can lead to overvoltage on stray inductances that are transferred onto IGBT modules and can cause the destruction of modules. In addition to the minimization of stray inductances, protective block capacitors are mounted with the identical purpose. Fig. 5 shows the three-phase IGBT converter with three HAT600 current transducers used to measure the current through the AC connections of IGBT modules.

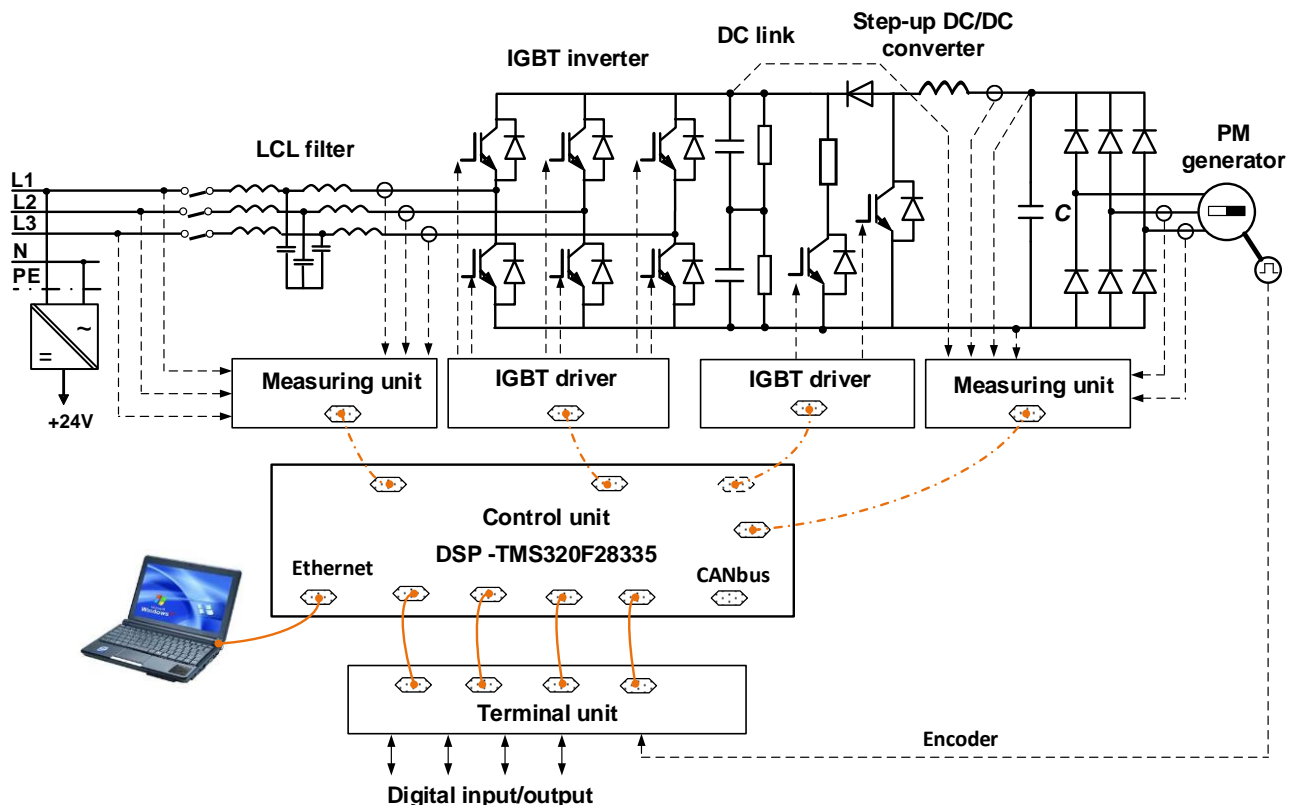


Figure 4. Structure of the power circuit and block representation of units needed to control the frequency converter with a diode rectifier and step-up DC/DC converter

Apart from the driver unit, three additional electronic boards were developed and constructed for the purpose of frequency converter control and are shown in Fig. 5:

- **Control unit** is a six-layered SMD electronic board based on the TMS320F28335 microcontroller, manufactured by Texas Instruments. Besides the microcontroller, used to implement control algorithms, the control unit is used to process analogue measurement signals (16 AI), as well as the input/output digital signals (8 DI, 8 DO, 12 PWM), and the unit itself houses several communication channels (CANbus, RS485, RS232, Ethernet ...).
- **Measuring unit** processes analogue signals for four-channel voltage measurements, three-channel current measurements and the one-channel measurement of the IGBT module temperature. For voltage measurement, LV25 voltage transducers are used and mounted on the unit while the three aforementioned

current transducers (see Fig. 4) are connected to the measuring unit by four-wire cables. Within each of the IGBT modules there is a resistive temperature sensor (NTC thermistor). The electronic circuit within the measuring unit processes temperature signals of all three IGBT modules and forms a single analogue output signal proportional to the highest temperature signal.

- **Terminal unit** represents the classical wire interface between the converter and the process, as well as with the superior control system, and it is used to connect the encoder for the PM generator's rotor speed and position measurements.



Figure 5. Power circuit of the three-phase IGBT converter



Figure 6. Control, measuring and terminal units

4. HIGH-SPEED MOTOR-GENERATOR GROUP

The motor-generator group consisting of a squirrel-cage induction motor and a surface permanent magnet machine (SPM machine) was acquired in order to test the constructed frequency converters. The nominal data of both machines are basically the same, and are defined for the sine waveform currents: $P = 100 \text{ kW}$, $U = 400\text{V}$, $I = 166 \text{ A}$, $n=20000 \text{ min}^{-1}$, $M = 48 \text{ Nm}$. A 3D model of the squirrel-cage induction machine with visible cooling channels is shown in Fig. 7, while Fig. 8 shows the motor-generator group. Machines are designed and constructed by the company HSTec from Zadar and their core business is the design and construction of high-speed motor spindles for tool machines. Machines of the motor-generator group are designed and constructed in such a manner that the stator frames with windings and rotors are obtained from the foreign manufacturer of high-speed machines, while the HSTec manufactured or acquired all other integral components such as the rotor shaft, cast iron stator casing with water cooling channels, incremental encoder for the rotor speed and position measurement, two temperature sensors for the stator windings and the terminal box. After a demanding and precise assembly of components, machines were tested in HSTec facilities, at no load conditions and nominal speed, during which the temperatures and vibrations were measured. Afterwards, machines were mounted on a common base and their shafts were mechanically

coupled by using a flexible clutch. Both machines are fitted with incremental encoders that generate 256 pulses per revolution. One encoder has 5V TTL output signals while other has sine/cosine output signals with $1 V_{pp}$ amplitude.

For the purpose of the lubrication of ceramic bearings, an oil + air lubrication system, manufactured by SKF, was installed. This unit lubricates eight bearings in total by injecting approx. 20 mm^3 of oil into the plastic tubes of the system by using compressed air (6 bar). The lubrication of bearings is repeated every six minutes. The air flow generates an additional cooling effect for each bearing.

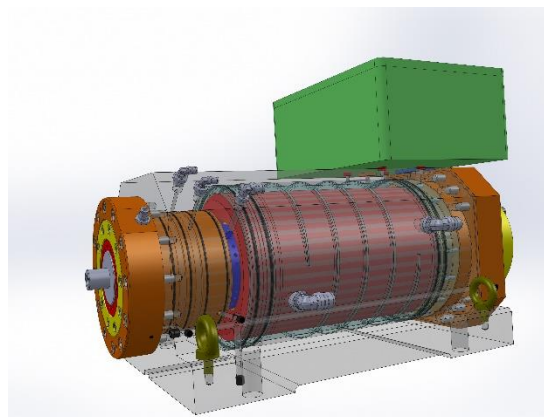


Figure 7. 3D model of a squirrel-cage induction machine



Figure 8. High-speed motor-generator group with a lubricating oil unit and cooling system

In order to cool the machines by using water, a hydraulic system was installed and it ensures a constant flow of coolant comprised of water and anticorrosive additives. This system requires a flow of 16 l/min , input coolant temperature between 10 and 40°C with a

maximum temperature increase of 10°C at the machine's nominal load.

5. EXPERIMENTAL RESULTS

Measurements were carried out by using the laboratory setup of the frequency converter with a diode rectifier and step-up DC/DC converter on the generator side (structure shown in Fig. 4). This laboratory setup is shown in Fig. 9 and it was constructed before the final prototype of the frequency converter with three-phase IGBT converters on both the grid and generator side. Apart from testing the operation of the frequency converter with a step-up DC/DC converter, the motor-generator group was tested for the first time at 50% of the motor nominal current and speed of approx. 13000 min^{-1} . During testing, the induction machine was used as a motor and it was connected to the 1Q VACON NXP0300 frequency converter, while the SPM machine was used as a generator connected to the abovementioned frequency converter.

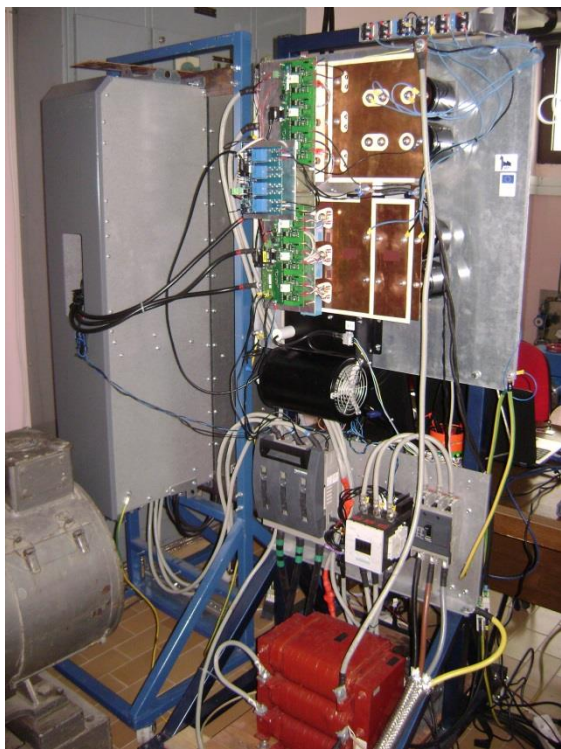


Figure 9. Laboratory setup of the frequency converter with a diode rectifier and step-up DC/DC converter

Fig. 10 presents the steady-state waveforms of the SPM generator current (red line) and current through the step-up DC/DC converter's inductor (blue line). Due to the operation of the diode rectifier, the generator current exhibits a non-sine waveform which presents a problem considering the additional heating and pulsating torque components of the SPM generator. The current through the inductor, besides the DC component (approx. 100A), contains a pulsating AC component generated due to the switching operations of the step-up DC/DC converter's IGBT transistor. The AC component frequency is determined by the transistor switching frequency which

is equal to 10 kHz. For the same operating point, Fig. 11 presents the grid current (red line) and the DC link voltage (blue line). The grid current exhibits a sine waveform with low pulsations around the peak values, while the DC link voltage is constant and equal to 630 V, which is approx. 12% higher than the grid line-to-line voltage maximum value ($\sqrt{2}\cdot 400\text{V}$).

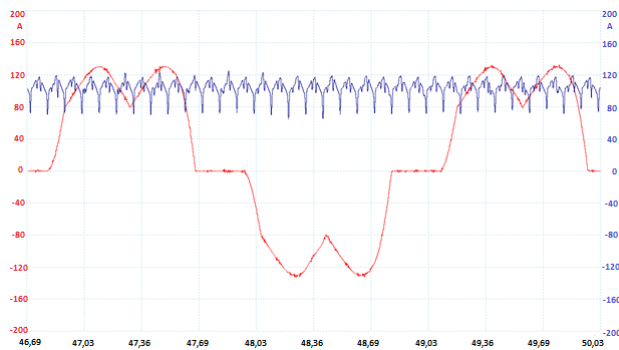


Figure 10. Measured SPM generator's current (red line) and current through the step-up DC/DC converter's inductor (blue line)

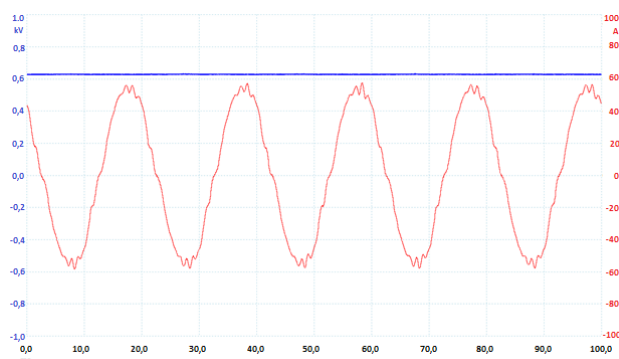


Figure 11. Measured grid current (red line) and the DC link voltage (blue line)

6. CONCLUSION

The development of frequency converters for high-speed permanent magnet generators used in cogeneration plants is specific in terms of the high frequencies of the generator's voltage fundamental harmonic. This enables the implementation of well-known frequency converters used in 4Q electrical drives consisting of two three-phase IGBT converters with the main issue being the high switching frequency of the generator converter due to the high frequency of the generator's voltage fundamental harmonic. On the other hand, a simpler solution involving a diode rectifier and step-up DC/DC converter is not affected by the high frequencies of the generator's voltage fundamental harmonic, but the additional heating and additional pulsating torque components are generated due to the non-sine waveform of the generator current.

7. REFERENCES

- [1] Muhammad H. Rashid: Power Electronics – circuits, devices and applications, Pearson Prentice Hall, USA, 2004.
- [2] Flegar, I.: Elektronički energetska pretvarači, Kigen, Zagreb, 2010.
- [3] Terzić, B.; Majić, G.; Slutej, A.: Stability Analysis of Three-Phase PWM Converter with LCL Filter by Means of Nonlinear Model, *Automatika - Journal for Control, Measurement, Electronics, Computing and Communications*, 51 (2010) , 3; 221-231
- [4] Jadrić, M.; Terzić, B.; Despalatović, M.; Majić, G.; Slutej, A.; Šimić, T.: Identification of Rotor Resistance and Transient Inductance of Induction Motors Using Frequency Selection Criterion // *Proceedings of the 2012 XXth International Conference on Electrical Machines / Marseille, Francuska, 2012.*, 978-984.
- [5] Terzić, B.; Jadrić, M.: Design and Implementation of the Extended Kalman Filter for the Speed and Rotor Position Estimation of Brushless DC Motor. // *IEEE Transactions on Industrial Electronics*. 48 (2001) , 6; 1065-1073.
- [6] <http://www.infineon.com/cms/en/product/power/igbt/igbt-module/igbt-module-1200v/channel.html>
- [7] <https://www.ti.com/product/tms320f28335>
- [8] User manual Motor spindle HSE130SE-B05-LC70-00, HSTec d.d., Zadar, 2015.
- [9] Application Manual Power Semiconductors, published by SEMIKRON International GmbH, 2011.

Contact addresses

Božo Terzić, Prof. Dr. Sc.

Faculty of Electrical Engineering, Mechanical Engineering and Naval Architecture,
University of Split
Ruđera Boškovića 32
21000 Split
Tel.: 021 305609
e-mail: bterzic@fesb.hr

AN EXPERIMENTAL RESEARCH OF THE COMBINED JOINTS OF WALL PANELS FROM THE NATURAL HARDENING FOAM CONCRETE

EKSPERIMENTALNA ISTRAŽIVANJA KOMBINIRANIH SPOJEVA ZIDNIH PLOČA OD PRIRODNO OTVRDNUTE BETONSKE PJENE

Anatoliy Kostyuk, Dariya Kovtunenka

Professional paper

Abstract: The article is dedicated to the investigation of a fracture behavior of combined horizontal joints of wallboards from natural hardening foam concrete and the influence of some factors on the ultimate loads for joints. Two of the most valuable factors that influence the ultimate loads for wallboard joints were allocated while planning the experiment: load eccentricity and indirect reinforcement. The samples consisting of three elements (top wallboard, bottom wallboard and floor slab) were made for the experiment. The typical scheme of destruction for the combined joints of wallboards with and without an indirect reinforcement was identified as a result of testing. The table of comparison of the analysis values of the ultimate loads for combined joints by the existing methods and obtained as a result of the analysis by SP "LIRA" with the received experimental data is shown in the article. Moreover, the diagrams of ultimate load relation with load eccentricity and indirect reinforcement are shown in the paper.

Keywords: ultimate load, combined joint, indirect reinforcement, natural hardening foam concrete, wall panels.

Stručni članak

Sažetak: Rad se bavi proučavanjem lomljivog ponašanja kombiniranih horizontalnih spojeva zidnih ploča od prirodno otvrdnute betonske pjene i utjecajem određenih faktora na krajnje opterećenje za spojeve. Dva najvrjednija faktora koja utječu na krajnja opterećenja za zglobove zidnih ploča dodijeljena su prilikom planiranja eksperimenta: ekscentričnost opterećenja i neizravno pojačanje. Uzorci koji se sastoje od tri elementa (vrh, dno i sredina zidne ploče) izrađeni su za eksperiment. Tipična shema uništenja kombiniranih spojeva zidnih ploča s i bez indirektnog pojačanja identificirana je kao rezultat proučavanja. Tablica usporedbe analiziranih vrijednosti krajnjih opterećenja za kombinirane zglobove na temelju postojećih metoda dobivena kao rezultat analize SP „Lira“ s ostvarenim eksperimentalnim podacima prikazana je u članku. Nadalje, u radu je iskazan i odnos dijagrama krajnjeg opterećenja s ekscentričnošću opterećenja i indirektnim pojačanjem.

Ključne riječi: krajnje opterećenje, kombinirani spoj, indirektno pojačanje, prirodno otvrdnuta betonska pjena, zidne ploče.

1. STATE OF THE MATTER

In contemporary civil engineering, the important place is held by cellular concrete, side by side with the heavy aggregate concrete. The physical and thermal properties of foam concrete have the best usage in the building of houses. Basically, this material is in the form of masonry blocks which lead to a longer duration of the building construction due to the need for additional work. The use of wall panels will reduce the construction time.

The existing methods of the analysis of the horizontal joints of wall panels from cellular concrete [1] are empirical and do not fully reflect the physical side of the work of wall panels with support zones.

Currently, the Laboratory of Reinforced Concrete and Masonry Structures of the Kazan State University of Architecture and Engineering is engaged in the study of the stress-strain state of the butt joints of large-panel

buildings. The method of joint strength analysis, which is based on the theory of the compression resistance of anisotropic materials and which reflects the destruction mechanism of supporting the zones of wall panels from heavy concrete, is developed by the authors of [2, 3, 4]. The applicability of this theory for the determination of the ultimate loads for horizontal joints of the wall panels from cellular concrete has not been studied.

The research of the joints' stress-strain state of wall panels from natural hardening foam concrete is provided in the Odessa State Academy of Civil Engineering and Architecture. The method of the numerical study of the joints' stress state, implemented in the SC "LIRA," is described in [5].

The purpose of experimental research is to study the destructive nature of the combined horizontal joints of the wall panels from natural hardening foam concrete and the influence of various factors on the ultimate load for the joints.

2. PLANNING OF EXPERIMENTAL RESEARCH

The two most significant factors: the eccentricity of the load application and the amount of indirect reinforcement grids that may affect the ultimate load for the joint have been isolated. The coded and full-scale values of the factor are shown in Table 1. The scheme of the tests is shown in Figure 1.

Table 1. Characteristics of experimental samples

Sample code	Values of factors			
	The amount of indirect reinforcement grids X_1		The eccentricity of load application X_2	
	Coded	Full-scale, pcs.	Coded	Full-scale, mm
JCP-0-0	-1	0	-1	0
JCP-2-0	0	2	-1	0
JCP-4-0	+1	4	-1	0
JCP-0-20	-1	0	0	20
JCP-2-20(1)	0	2	0	20
JCP-2-20(2)	0	2	0	20
JCP-2-20(3)	0	2	0	20
JCP-4-20	+1	4	0	20
JCP-0-40	-1	0	+1	40
JCP-2-40	0	2	+1	40
JCP-4-40	+1	4	+1	40

The samples that consist of three parts are the overlying panel, the underlying panel and floor slab, and they were prepared for the experiment. The dimensions of the test sample elements were accepted by a geometric similarity as full-scale parameters of panels and their joints. The thickness of wall panels is accepted as 200 mm (100 mm the contact part and 100 mm the platform part). The thickness of the floor slab is accepted as 150 mm. The width of the test samples is accepted as 600 mm with a consideration of the dimensions of the support platform of press.

The supporting areas in the contact and platform parts of the overlying panel are located close to each other, which is why we can assume that the load on the sample is applied to its full width $l_c = 200$ mm. The height of the overlying panel is accepted as $3l_c = 600$ mm. The maximum possible width of the support in the platform part of the underlying panel is 100 mm. The required height of the underlying panel is $3l_c = 300$ mm. The ledge height of the underlying panel is accepted as 160 mm. Finally, the height of the underlying panel with the ledge is accepted as 600 mm with a consideration of the production conditions. The cantilevered ledge of the floor slab fragment is 510 mm.

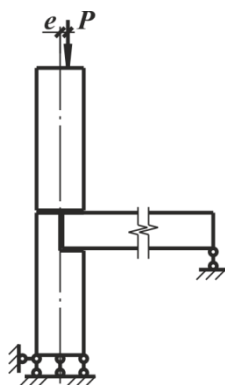


Figure 1. Scheme of tests

The wall panels of test samples are made of natural hardening foam concrete with a density from 700 to 1000 kg/m³. The floor slab is made of a concrete class C20/25. The indirect reinforcement of the wall panels is made of grids from reinforcement wires Ø3 mm, class Bp-I with a characteristic yield strength $f_y = 608$ MPa and modulus of elasticity $E = 20.51 \times 10^5$ MPa.

The model of a test sample with the main dimensions and scheme of the instrumentation layout is presented in Figure 2. The tensoresistors are installed at the levels of the first and fourth grids of indirect reinforcement. The general view of test samples is shown in Figure 3.

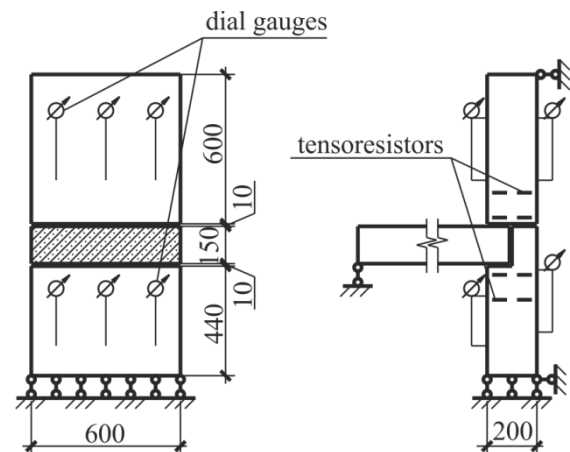


Figure 2. Model of test sample with a scheme of an instrumentation layout



Figure 3. The general view of test sample, which is mounted on a press platform

All samples were exposed to a static load. At each stage, the load on the sample of a combined joint was applied by 0.1 of the expected destructive value.

3. MAIN RESULTS OF THE EXPERIMENT

The characteristic schemes of destruction that were identified on the testing results of the horizontal joints of the wall panels from natural hardening foam concrete are shown in Figure 4.

The destruction of the test samples without indirect reinforcement occurred in accordance with the diagram shown in Figure 4(a). The formation of the first vertical

crack was observed near the cement mortar joint on the boundary between the contact and platform parts of the wall panel. The development of vertical cracks at the height of wall panels took place with the load increasing. The destruction of the samples occurred as a result of the split of panels on the conditional boundary between the contact and platform part.

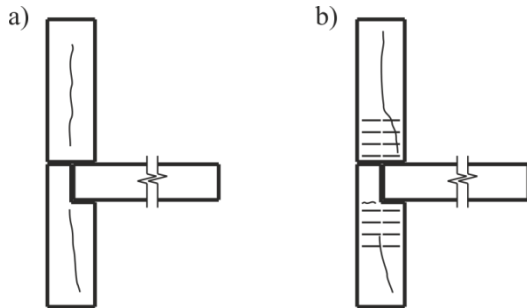


Figure 4. Characteristic scheme of destruction
 a) samples without indirect reinforcement;
 b) samples with indirect reinforcement.

The destruction of test samples with indirect reinforcement occurred in accordance with the diagram shown in Figure 4(b). The character of cracking on the visible surfaces of samples with indirect reinforcement is generally consistent with the cracking of samples without indirect reinforcement. At the same time, the presence of grids had prevented the development of vertical cracks. The destruction of samples occurred as a result of the crushing of the foam concrete of wall panels in the locations of resting on the concrete floor slab and support platform of press. The spalling of the underlying panel ledge occurred in the samples onto which load was applied with the eccentricity.

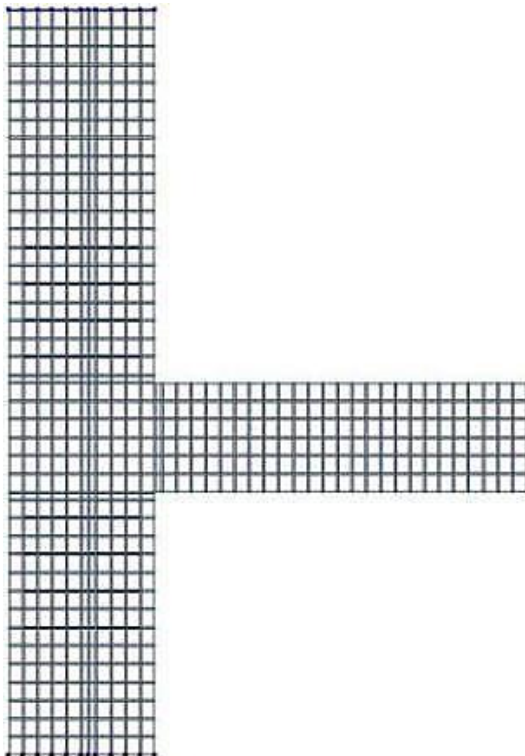


Figure 5. General view of the joint that was built for the analysis in the SC "LIRA"

Moreover, a combined joint was modeled in the software complex "LIRA 9.4" [5] which implements the finite elements method (Figure 5).

The finite elements, which allow for the building of the plane model, were used for modeling:

223 – physically non-linear universal rectangular finite element of a plane problem (beam-wall), which simulates the body of foam concrete and the mortar;

210 – physically non-linear universal spatial rod finite element, which simulates the indirect reinforcement of the joint.

The analysis was performed in the nonlinear formulation with a stepwise increment of the load. The physical and mechanical characteristics of the materials were set according to the results of cubes' and prisms' tests in compression and reinforcing bars in tension. A significant increment of the nodes' displacement of the design scheme at the current stage of load was assumed as a destruction criterion.

The values of the foam concrete cube strength, as well as the values of the joint ultimate load obtained from tests, analysis by the formulas given in the normative literature [1] and studies carried out under the guidance of B.S. Sokolov [2, 3, 4], and numerical studies [5] are given in Table 2.

Charts of ultimate loads for the combined horizontal joints of the wall panels from natural hardening foam concrete depending on the studied factors are shown in Figure 6.

Table 2. Ultimate loads for the combined horizontal joints

Sample code	Cube strength $f_{ed,cube}$, MPa	Ultimate load, kN			
		by test results	by [1]	by [4]	by numerical study results
JCP-0-0	2,39	60,00	141,3	380,9	53,33
JCP-2-0	0,89	33,33	66,3	-	20,00
JCP-4-0	1,99	46,67	192,0	-	53,33
JCP-0-20	1,42	33,33	78,7	147,0	26,67
JCP-2-20(1)	2,95	73,33	198,1	-	66,67
JCP-2-20(2)	2,84	46,67	130,3	-	40,00
JCP-2-20(3)	4,16	86,67	372,3	-	80,00
JCP-4-20	3,26	46,67	163,6	-	53,33
JCP-0-40	2,14	33,33	93,9	427,4	46,67
JCP-2-40	1,66	53,33	89,3	-	40,00
JCP-4-40	4,61	73,33	216,9	-	80,00

Note: The method [4] does not allow taking into account the indirect reinforcement of the wall panel support zones

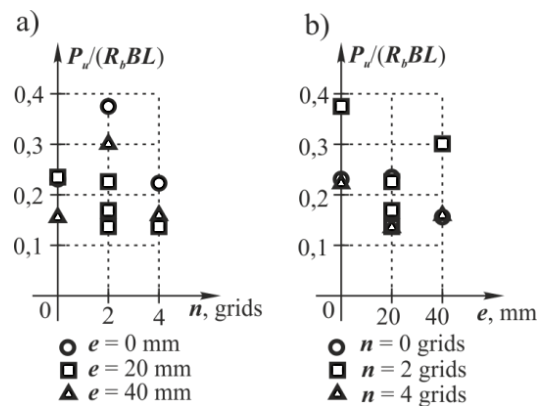


Figure 6. Ultimate load depending on:
 a) the quantity of indirect reinforcement grids;
 b) the eccentricity of loads application

4. CONCLUSION

The next conclusions could be made according to the analysis of the test results:

- the ultimate loads of the horizontal joints of the wall panels from natural hardening foam concrete, that has been calculated according to the normative literature [1] and propositions of the authors [2, 3, 4], is significantly overtaken compared to the results of the numerical and natural experiments;
- an increase in the load application eccentricity leads to the decrease of the ultimate load for the joint;
- an indirect reinforcement of the wall panels that end by two grids leads to the increase of the joint bearing the capacity; indirect reinforcement of the wall panels that end by four grids does not influence on the joint bearing the capacity.

5. REFERENCES

- [1] Guide to design of concrete and reinforced concrete construction from cellular concrete – Moscow: Tzentr. in-t tipovogo proekt., 1986 (rus).
- [2] Nikitin, G. P. Strength of horizontal joints of concrete constructions of buildings and structures: dissertation. ... PhD.: 05.23.01 / Nikitin Georgiy Petrovich – Kazan, 2007. – 173 p.(rus)
- [3] Sedov, A. N. Structural and technological features of combined joints strengthening in reconstruction of large-panel buildings: abstract of dissertation ... PhD / A.N.Sedov – Kazan: KazGASU, 2009. – 20 p. (rus)
- [4] Sokolov, B. S. A new approach to the calculation of concrete elements strength in the local action of loading / B.S. Sokolov // Beton i zhelezobeton. – Moscow, 1992 – No. 10. – pp. 22-25. (rus)
- [5] Kostyuk, A. I. Numerical analysis of the combined joint of foam concrete non-autoclave hardening / A.I. Kostyuk, D.O. Zazulya // Budivelni konstruktсии. Mizhvidomchyy naukovو-tekhnichnyy zbirnyk. – Kiev: SE NIISK, 2011 – No. 74. Vol. 2. – pp. 326-332. (rus).

Contact addresses

Kostyuk Anatoliy, Prof., PhD

Odessa State Academy of Civil Engineering and Architecture
65029, Ukraine, Odessa, Didrikhsona St., 4
Tel.: +380 505 523 855
e-mail: pcb.odaba@mail.ru

Kovtunenکو Dariya

Odessa State Academy of Civil Engineering and Architecture
65029, Ukraine, Odessa, Didrikhsona St., 4
Tel.: +380 673 655 520,
e-mail: dashunya_2805@mail.ru

12pt

12pt

12pt

ARTICLE TITLE IN ENGLISH (Style: Arial Narrow, 14pt, Uppercase, Center)

12pt

ARTICLE TITLE IN CROATIAN (Style: Arial Narrow, 14pt, Bold, Uppercase, Center)

12pt

Ivan Horvat, Thomas Johnson (Style: Times, 12pt, Bold, Italic, Center)

12pt

Article categorization

Abstract: Article abstract contains maximum of 150 words and is written in the language of the article. The abstract should reflect the content of the article as precisely as possible. TECHNICAL JOURNAL is a trade journal that publishes scientific and professional papers from the domain(s) of mechanical engineering, electrical engineering, civil engineering, multimedia, logistics, etc., and their boundary areas. This document must be used as the template for writing articles so that all the articles have the same layout. (Style: Times New Roman, 10 pt, Italic)

10pt

Keywords: keywords in alphabetical order (5-6 key words). Keywords are generally taken from the article title and/or from the abstract. (Style: Times New Roman, 10 pt, Italic)

10pt

Kategorizacija članka

Sažetak: Article abstract in Croatian (Style: Times New Roman, 10 pt, Italic)

10pt

10pt (The authors from abroad leave free space for the text of abstract in Croatian language.)

10pt

10pt

10pt

Ključne riječi: keywords in Croatian (Style: Times New Roman, 10 pt, Italic)

10pt

10pt

1. ARTICLE DESIGN (Style: Arial Narrow, 12pt, Bold, Uppercase, Align Center)

10pt

The article is written in Latin script and Greek symbols can be used for labelling. The length of the article is limited to eight pages of international paper size of A4 (in accordance with the template with all the tables and figures included). When formatting the text the syllabification option is not to be used.

10pt

1.1. General guidelines (Style: Arial Narrow, 12pt, Bold, Align Left)

10pt

(First line indentation 5mm) The document format is A4 with 20 mm margins on all sides. A two column layout is used with the column spacing of 7 mm. The running text is written in Times New Roman with single line spacing, font size 10 pt, alignment justified.

Article title must clearly reflect the issues covered by the article (it should not contain more than 15 words).

Body of the text is divided into chapters and the chapters are divided into subchapters, if needed. Chapters are numbered with Arabic numerals (followed by a period). Subchapters, as a part of a chapter, are marked with two Arabic numerals i.e. 1.1, 1.2, 1.3, etc. Subchapters can be divided into even smaller units that are marked with three Arabic numerals i.e. 1.1.1, 1.1.2, etc. Further divisions are not to be made.

Titles of chapters are written in capital letters (uppercase) and are aligned in the center. The titles of subchapters (and smaller units) are written in small letters (lowercase) and are aligned left. If the text in the title of the subchapter is longer than one line, hanging indent of 0.7 mm is defined.

10pt

Typographical symbols (bullets), which are being used for marking an item in a list or for enumeration, are placed at a beginning of a line. There is a spacing of 10pt following the last item:

- Item 1
- Item 2
- Item 3

10pt

The same rule is valid when items are numbered in a list:

1. Item 1
2. Item 2
3. Item 3

10pt

1.2. Formatting of pictures, tables and equations (Style: Arial Narrow, 12pt, Bold, Align Left)

10pt

Figures (drawings, diagrams, photographs) that are part of the content are embedded into the article and aligned in the center. In order for the figure to always be in the same position in relation to the text, the following

settings should be defined when importing it: text wrapping / inline with text.

Pictures must be formatted for graphic reproduction with minimal resolution of 300dpi. Pictures downloaded from the internet in ratio 1:1 are not suitable for print reproduction because of unsatisfying quality.

10pt

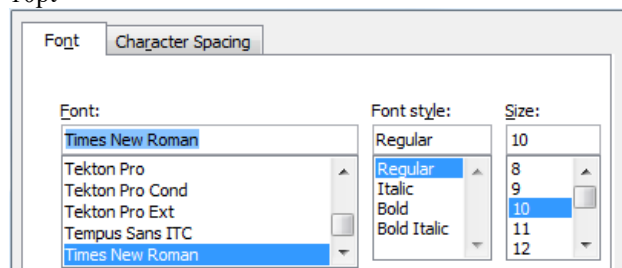


Figure 1. Text under the picture[1]

(Style: Times New Roman, 10pt, Align Center)

10pt

The journal is printed in black ink and the figures have to be prepared accordingly so that bright tones are printed in a satisfactory manner and are readable. Figures are to be in color for the purpose of digital format publishing. Figures in the article are numbered with Arabic numerals (followed by a period).

10pt

Table 1. Table title aligned center
(Style: Times New Roman, 10pt, Align Center)

	1	2	3	4	5	6
ABC	ab	ab	ab	ab	ab	ab
DEF	cd	cd	cd	cd	cd	cd
GHI	ef	ef	ef	ef	ef	ef

10 pt

Text and other data in tables is formatted - Times New Roman, 8pt, Normal, Align Center.

When describing figures and tables, physical units and their factors are written in italics with Latin or Greek letters, while the measuring values and numbers are written upright.

Equations in the text are numbered with Arabic numerals inside the round brackets on the right side of the text. Inside the text they are referred to with equation number inside the round brackets i.e. “... from (5) follows ...” (Create equations with MS Word Equation Editor - some examples are given below).

10pt

$$F_{\text{avg}}(t, t_0) = \frac{1}{t} \int_{t_0}^{t_0+t} F(q(\tau), p(\tau)) d\tau, \quad (1)$$

10pt

$$\cos \alpha + \cos \beta = 2 \cos \frac{\alpha + \beta}{2} \cdot \cos \frac{\alpha - \beta}{2}. \quad (2)$$

10pt

Variables that are used in equations and also in the text or tables of the article are formatted as *italics* in the same font size as the text.

Figures and tables that are a part of the article have to be mentioned inside the text and thus connected to the content i.e. „... as shown in figure 1...” or „data from table 1...” and similar.

10pt

10pt

2. PRELIMINARY ANNOTATION

10pt

Article that is offered for publication cannot be published beforehand, be it in the same or similar form, and it cannot be offered at the same time to a different journal. Author or authors are solely responsible for the content of the article and the authenticity of information and statements written in the article.

Articles that are accepted for publishing are classified into four categories: original scientific papers, preliminary communications, subject reviews and professional papers.

Original scientific papers are articles that according to the reviewer and the editorial board contain original theoretical or practical results of research. These articles need to be written in such a way that based on the information given, the experiment can be repeated and the results described can be achieved together with the author's observations, theoretical statements or measurements.

Preliminary communication contains one or more pieces of new scientific information, but without details that allow recollection as in original scientific papers. Preliminary communication can give results of an experimental research, results of a shorter research or research in progress that are deemed useful for publishing.

Subject review contains a complete depiction of conditions and tendencies of a specific domain of theory, technology or application. Articles in this category have an overview character with a critical review and evaluation. Cited literature must be complete enough to allow a good insight and comprehension of the depicted domain.

Professional paper can contain a description of an original solution to a device, assembly or instrument, depiction of important practical solutions, and similar. The article need not be related to the original research, but it should contain a contribution to an application of known scientific results and their adaptation to practical needs, so it presents a contribution to spreading knowledge, etc.

Outside the mentioned categorization, the Editorial board of the journal will publish articles of interesting content in a special column. These articles provide descriptions of practical implementation and solutions from the area of production, experiences from device application, and similar.

10pt

10pt

3. WRITING AN ARTICLE

10pt

Article is written in the English language and the terminology and the measurement system should be adjusted to legal regulations, standards (ISO 80000 series) and the SI international system of units. The article should be written in third person.

Introduction contains the depiction of the problem and an account of important results that come from the articles that are listed in the cited literature.

Main section of the article can be divided into several parts or chapters. Mathematical statements that obstruct the reading of the article should be avoided. Mathematical statements that cannot be avoided can be written as one or

more addendums, when needed. It is recommended to use an example when an experiment procedure, the use of the work in a concrete situation or an algorithm of the suggested method must be illustrated. In general, an analysis should be experimentally confirmed.

Conclusion is a part of the article where the results are being given and efficiency of the procedure used is emphasized. Possible procedure and domain constraints where the obtained results can be applied should be emphasized.

10pt

10pt

4. RECAPITULATION ANNOTATION

10pt

In order for the articles to be formatted in the same manner as in this template, this document is recommended for use when writing the article. Finished articles written in MS Word for Windows and formatted according to this template must be submitted using our The Paper Submission Tool (PST) (<https://tehnickiglasnik.unin.hr/authors.php>) or eventually sent to the Editorial board of the Technical Journal to the following e-mail address: tehnickiglasnik@unin.hr

The editorial board reserves the right to minor redaction corrections of the article within the framework of prepress procedures. Articles that in any way do not follow these authors' instructions will be returned to the author by the editorial board. Should any questions arise, the editorial board contacts only the first author and accepts only the reflections given by the first author.

10pt

10pt

5. REFERENCES

10pt

The literature is cited in the order it is used in the article. Individual references from the listed literature inside the text are addressed with the corresponding number inside square brackets i.e. "... in [7] is shown ...". If the literature references are web links, the hyperlink is to be removed as shown with the reference number 8. Also, the hyperlinks from the e-mail addresses of the authors are to be removed. In the literature list, each unit is marked with a number and listed according to the following examples (omit the subtitles over the references – they are here only to show possible types of references):

10pt

books:

- [1] Franklin, G. F.; Powel, J. D.; Workman, M. L.: Digital Control of Dynamic System, Addison-Wesley Publishing Company, Massachusetts, 1990
- [2] Kostrenčić, Z.: Teorija elastičnosti, Školska knjiga, Zagreb, 1982.

articles in journals:

- [3] Michel, A. N.; Farrell, J. A.: Associative Memories via Artificial Neural Networks, IEEE Control System Magazine, Vol. 10, No. 3 (1990) 6-17
- [4] Dong, P.; Pan, J.: Elastic-Plastic Analysis of Cracks in Pressure-Sensitive Materials, International Journal of Solids and Structures, Vol. 28, No. 5 (1991) 1113-1127
- [5] Kljajin, M.: Prijedlog poboljšanja proračuna parametara dodira na primjeru evolventnih bokova

zubi, Tehnički vjesnik/Technical Gazette, Vol. 1, No. 1,2 (1994) 49-58

articles published in conference proceedings:

- [6] Albertsen, N. C.; Balling, P.; Laursen, F.: New Low Gain S-Band Satellite Antenna with Suppressed Back Radiation, Proc. 6th European Microwave Conference, Rome, September 1976, 14-17
- [7] Kljajin, M.; Ergić, T.; Ivandić, Ž.: Izbor robota za zavarivanje uvjetovan konstrukcijom proizvoda, Zbornik radova - 3. međunarodno savjetovanje proizvodnoga strojarstva/3rd International Conference on Production Engineering CIM '95, Zagreb, November 1995, C-35 - C-41

links:

- [8] http://www.sciencedaily.com/articles/w/wind_power.htm (Accessed:19.06.2012.)

10pt

10pt

Author contact:

10pt

Full Name, title

Institution, company

Address

Tel./Fax,e-mail

12pt

12pt

12pt

NASLOV NA HRVATSKOM JEZIKU (Stil: Arial Narrow, 14pt, Bold, Verzal, Center)

12pt

NASLOV NA ENGLESKOM JEZIKU (Stil: Arial Narrow, 14pt, Verzal, Center)

12pt

Ivan Horvat, Thomas Johnson (Stil: Times, 12pt, Bold, Italic, Center)

12pt

Kategorizacija članka

Sažetak: Sažetak članka na hrvatskom jeziku sa najviše 150 riječ pisan jezikom članka (obično hrvatski). Sažetak mora što vjernije odražavati sadržaj članka. U njemu se navode upotrijebljene metode i ističu ostvareni rezultati kao i doprinos članka. Časopis *TEHNIČKI GLASNIK / TECHNICAL JOURNAL* objavljuje znanstvene i stručne radove iz područja strojarstva, elektrotehnike, graditeljstva, multimedije, logistike a također i iz njihovih graničnih područja. Ovaj dokument se koristiti kao predložak za pisanje članka kako bi svi članci imali isti način prijeloma (Stil: Times New Roman, 10 pt, Italic)

10pt

Ključne riječi: Abecedni popis ključnih riječi na hrvatskom jeziku (5-6 ključnih riječi). Ključne riječi u pravilu su iz naslova članka, a samo eventualno iz sažetka članka. (Stil: Times New Roman, 10 pt, Italic)

10pt

Categorization article

Abstract: Sažetak članka na engleskom jeziku (Stil: Times New Roman, 10 pt, Italic)

10pt

Key words: ključne riječi na engleskom jeziku (Stil: Times New Roman, 10 pt, Italic)

10pt

10pt

1. OBLIKOVANJE ČLANKA (Stil: Arial Narrow, 12pt, Bold, Verzal, Align Center)

10pt

Članak se piše latiničnim pismom, a za oznake se može koristiti i grčko pismo. Opseg članka u pravilu se ograničava na osam stranica A4 formata (sukladno predlošku s uključenim svim slikovnim priložima). Pri oblikovanju teksta članka ne smije se koristiti postavka za automatsko rastavljanje riječi.

10pt

1.1. Osnovna uputstva (Stil: Arial Narrow, 12pt, Bold, Align Left)

10pt

(Uvlaka prvog reda 5mm) Dokument je formata A4 sa marginama 20 mm sa svake strane. Koristi se prijelom u dvije kolone međusobno udaljene 7 mm. Za tekući tekst se koristi vrsta pisma Times New Roman sa jednostrukim poredom, veličina pisma 10 pt, obostrano poravnanje.

Naslov članka mora jasno odražavati problematiku članka (sadrži ne više od 15 riječi).

Tekst članka dijeli se na poglavlja, a po potrebi poglavlja se dijele na podpoglavlja. Poglavlja se označavaju rednim arapskim brojevima. Podpoglavlja, kao dijelovi poglavlja, označavaju se s dva redna arapska broja kao npr. 1.1, 1.2, 1.3, ... Podpoglavlje se može podijeliti na još manje cjeline koje se označavaju sa tri redna arapska broja, npr. 1.1.1, 1.1.2, ... Daljnja podjela nije poželjna.

Nazivi glavnih poglavlja se pišu velikim slovima (verzalom) i poravnavaju se u centar, a nazivi podpoglavlja (kao i manjih cjelina) pišu se malim

slovima (kurentom) te se poravnavaju u lijevo. Ako tekst naziva podpoglavlja i manjih cjelina prelazi u više redaka tada se definira viseća uvlačka (*Hanging intent*) 0,7 mm.

10pt

Grafičke oznake (*Bullet*) koje se koriste za označavanje stavki u nekoj listi, odnosno za nabrojanje započinju na početku retka, a nakon zadnje stavke dolazi razmak od 10pt:

- Stavka 1
- Stavka 2
- Stavka 3

10pt

Isto pravilo vrijedi prilikom numeriranja stavki u nekoj listi:

1. Stavka 1
2. Stavka 2
3. Stavka 3

10pt

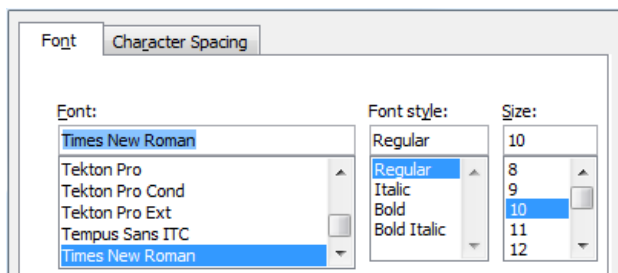
1.2. Oblikovanje slika, tabela i jednadžbi (Stil: Arial Narrow, 12pt, Bold, Align Left)

10pt

Slike (crteži, dijagrami, fotografije) koje čine sadržaj ugrađuju se u članak te poravnavaju se u centar. Kako bi slika uvijek zauzimala isto mjesto u odnosu na tekst prilikom uvoza moraju se definirati postavke *Text wrapping / Inline with text*.

Slike moraju biti pripremljene za grafičku reprodukciju sa minimalnom rezolucijom od 300dpi. Slike skinute s interneta sa 72dpi u veličini 1:1 nisu primjerene za reproduciranje u tisku zbog loše kvalitete.

10pt



Slika 1. Tekst ispod slike [1]

(Stil: Times New Roman, 10pt, Align Center)

10pt

Tisak knjižnog bloka je u crnoj boji stoga treba prilagoditi slike takvom načinu reproduciranja kako se svijetli tonovi (svijetle boje) ne bi izgubili u tisku ili tekst u slikama bio nečitljiv. Slike moraju ostati u koloru zbog objavljivanja u elektronskom obliku. Slike se kroz čitavi članak numeriraju u slijedu arapskim brojkama.

10pt

Tabela 1. Naslov tabele poravnat u centar
(Stil: Times New Roman, 10pt, Align Center)

	1	2	3	4	5	6
ABC	ab	ab	ab	ab	ab	ab
DEF	cd	cd	cd	cd	cd	cd
GHI	ef	ef	ef	ef	ef	ef

10 pt

Tekst i ostali podaci u tabelama oblikuju se kao Times New Roman, 8pt, Normal, Align Center.

Prilikom opisivanja slika i tabela fizikalne veličine i njihovi faktori ispisuju se kosim slovima latinične abecede ili grčkog alfabeta, dok se za mjerne jedinice i brojke upotrebljavaju uspravni znakovi.

Jednadžbe u tekstu numeriraju se arapskim brojevima u okruglim zagradama uz desni rub teksta, a na njih se u tekstu poziva pomoću broja jednadžbe u okruglim zagradama, npr. ".... iz (5) slijedi"

10pt

$$x = \frac{-b \pm \sqrt{b^2 - 4ac}}{2a} \quad (1)$$

10pt

$$\cos \alpha + \cos \beta = 2 \cos \frac{1}{2}(\alpha + \beta) \cos \frac{1}{2}(\alpha - \beta) \quad (2)$$

10pt

Veličine (varijable) koje se koriste u jednadžbama, ali i u tekstu članka ili u tabelama oblikuju se kao *kurziv* u istoj veličini teksta.

Slike i tabele koje su sastavni dio članka moraju se spomenuti u pratećem tekstu i na taj način povezati sa sadržajem, npr. „... prikazano na slici 1 ...“ ili „... podaci iz tabele 1 ...“ i slično.

10pt

10pt

2. UVODNE NAPOMENE

10pt

Ponuđeni članak ne smije biti ranije objavljen, bilo u jednakom ili sličnom obliku, niti smije biti istodobno ponuđen drugom časopisu. Za sadržaj članka, autentičnost podataka i tvrdnji u njemu isključivo i u cijelosti odgovara autor ili autori.

Članci prihvaćeni za objavljivanje svrstavaju se u četiri kategorije: izvorni znanstveni članci (original scientific papers), prethodna priopćenja (preliminary

communications), pregledni članci (subject reviews) i stručni članci (professional papers).

U **izvorne znanstvene članke** svrstavaju se radovi, koji po ocjeni recenzenata i Uredničkog odbora, sadrže originalne teorijske ili praktične rezultate istraživanja. Ovi članci trebaju biti napisani tako da se na osnovi danih informacija može ponoviti eksperiment i postići opisane rezultate, odnosno autorova opažanja, teorijske izvode ili mjerenja.

Prethodno priopćenje sadrži jedan novi znanstveni podatak ili više njih, ali bez dovoljno pojedinosti koje bi omogućavale provjeru kao kod izvornih znanstvenih članaka. U prethodnom se priopćenju mogu dati rezultati eksperimentalnih istraživanja, rezultati kraćih istraživanja ili istraživanja u tijeku, kojih se objavljivanje procijeni korisnim.

Pregledni članak sadrži cjelovit prikaz stanja i tendencija određenog područja teorije, tehnologije ili primjene. Članci ove kategorije su preglednog karaktera s kritičkim osvrtom i ocjenom. Citirana literatura mora biti dovoljno cjelovita tako da omogućiti dobar uvid i uključivanje u prikazano područje.

Stručni članak može sadržavati prikaz originalnog rješenja nekog uređaja, sklopa ili instrumenta, prikaz važnijih praktičnih izvedbi i slično. Rad ne mora biti vezan uz originalna istraživanja, nego sadrži doprinos primjeni poznatih znanstvenih rezultata i njihovoj prilagodbi potrebama prakse, pa je doprinos širenju znanja, itd.

Izvan navedene kategorizacije Urednički odbor časopisa pozdravit će i članke zanimljivog sadržaja za rubriku "Zanimljivosti". U ovim člancima daju se opisi praktičnih izvedbi i rješenja iz proizvodnje, iskustva iz primjene uređaja i slično.

10pt

10pt

3. PISANJE ČLANKA

10pt

Članak se piše hrvatskim jezikom te se metrološki i terminološki valja uskladiti sa zakonskim propisima, normama (ISO 80000 serija) i međunarodnim sustavom jedinica (SI). Materija u članku izlaže se u trećem licu jednine.

Uvod sadrži opis problema i prikaz važnijih rezultata radova opisanih u citiranoj literaturi. Navodi se način rješavanja problema, koji se opisuje u članku, kao i prednosti predloženog postupka.

Središnji dio članka može se sastojati od nekoliko dijelova. Treba izbjegavati matematičke izvode koji opterećuju praćenje izlaganja. Neizbježni matematički izvodi mogu se po potrebi, dati kao cjeline u obliku jednog priloga ili više njih. Preporuča se navođenje primjera kad je potrebno ilustrirati proceduru eksperimenta, postupak primjene rezultata rada u konkretnom slučaju ili algoritam predložene metode. Razmatranje treba u pravilu eksperimentalno potvrditi.

Zaključak u kojem se navode ostvareni rezultati i naglašava efikasnost korištenog postupka. Istaknuti treba eventualna ograničenja postupka kao i područja moguće primjene dobivenih rezultata.

10pt

10pt

4. ZAKLJUČNE NAPOMENE

10pt

Kako bi članci bili pripremljeni istovjetno ovom predlošku preporuča se ubacivanje sadržaja u njega. Gotovi članci pripremljeni u MS Word za Windows i prelomljeni prema ovom predlošku šalju se Uredništvu časopisa Tehnički Glasnik na slijedeću e-mail adresu: zivko.kondic@unin.hr

Urednički odbor zadržava pravo manjeg redakcijskog ispravka članka u okviru pripreme za tisak. Članke, koji u bilo kojem pogledu ne zadovoljavaju naputak autorima, Urednički će odbor vratiti autoru. Radi eventualnih nejasnoća u svezi predloženog članka, Urednički se odbor obraća samo prvom autoru, ako ima nekoliko autora, i uvažava samo stavove koje iznese prvi autor.

10pt

10pt

5. LITERATURA

10pt

Literatura se navodi redosljedom kojim se citira u članku. Pojedine literarne reference iz popisa literature u tekstu pozivaju se odgovarajućim brojem u uglatim zagradama, npr. "... u [7] je pokazano ...". Ako su literarne reference poveznice (linkovi) hiperveza se mora ukloniti kao što je vidljivo kod literarne reference 8. Također se uklanjaju hiperveze sa e-mail adresa kod kontakta autora. U popisu literature svaka se jedinica označava brojem, a navodi se prema sljedećim primjerima (podnaslovi iznad referenci se izostavljaju – navedeni su samo kao primjer izvora):

10pt

knjige:

- [1] Franklin, G. F.; Powel, J. D.; Workman, M. L.: Digital Control of Dynamic System, Addison-Wesley Publishing Company, Massachusetts, 1990
- [2] Kostrenčić, Z.: Teorija elastičnosti, Školska knjiga, Zagreb, 1982.

članci u časopisima:

- [3] Michel, A. N.; Farrell, J. A.: Associative Memories via Artificial Neural Networks, IEEE Control System Magazine, Vol. 10, No. 3 (1990) 6-17
- [4] Dong, P.; Pan, J.: Elastic-Plastic Analysis of Cracks in Pressure-Sensitive Materials, International Journal of Solids and Structures, Vol. 28, No. 5 (1991) 1113-1127
- [5] Kljajin, M.: Prijedlog poboljšanja proračuna parametara dodira na primjeru evolventnih bokova zubi, Tehnički vjesnik/Technical Gazette, Vol. 1, No. 1,2 (1994) 49-58

članci u zbornicima znanstveno-stručnih skupova:

- [6] Albertsen, N. C.; Balling, P.; Laursen, F.: New Low Gain S-Band Satellite Antenna with Suppressed Back Radiation, Proc. 6th European Microwave Conference, Rome, September 1976, 14-17
- [7] Kljajin, M.; Ergić, T.; Ivandić, Ž.: Izbor robota za zavarivanje uvjetovan konstrukcijom proizvoda, Zbornik radova - 3. međunarodno savjetovanje proizvodnoga strojarstva/3rd International Conference on Production Engineering CIM '95, Zagreb, November 1995, C-35 - C-41

poveznice (linkovi):

- [8] http://www.sciencedaily.com/articles/w/wind_power.htm (Dostupno:19.06.2012.)

10pt

10pt

Kontakt autora:

10pt

Ime Prezime, titula

Institucija, tvrtka

Adresa

Tel./Fax,e-mail
